THE FABRICATION AND STUDY OF STIMULI-RESPONSIVE MICROGEL-BASED MODULAR ASSEMBLIES

A Dissertation
Presented to
The Academic Faculty

by

Kimberly Corinne Clarke

In Partial Fulfillment
of the Requirements for the Degree
Doctor of Philosophy in the
School of Chemistry and Biochemistry

Georgia Institute of Technology
August 2015

THE FABRICATION AND STUDY OF STIMULI-RESPONSIVE MICROGEL-BASED MODULAR ASSEMBLIES

Approved by:

Dr. L. Andrew Lyon, Advisor
Schmid College of Science and Technology
Chapman University

Dr. Nick Hud
School of Chemistry and Biochemistry
Georgia Institute of Technology

Dr. David Collard
School of Chemistry and Biochemistry
Georgia Institute of Technology

Dr. Todd Sulchek
Woodruff School of Mechanical Engineering
Georgia Institute of Technology

Dr. Facundo Fernandez
School of Chemistry and Biochemistry
Georgia Institute of Technology

Date Approved: May 4, 2015

To my parents, David and Lisa, and the many others who have helped me along the way.

ACKNOWLEDGEMENTS

There are numerous people who have helped me throughout my time in grad school. My family has always been a wonderful cheering section, and their consistency throughout this process has been most appreciated. A special thank you to my parents, for their love, support, and belief in me. I want to especially thank my dad for teaching me to work hard, but for always reminding me that there is more to life than what you do.

As an undergraduate at Mercyhurst I was fortunate enough to be educated, advised, and mentored by Prof. Clint Jones. He was an integral part in my decision to come to grad school, and I am extremely grateful for each of the lessons he taught me. Also during my time as an undergrad, I had the opportunity to participate in a summer REU program at Georgia Tech, where I worked in the Lyon group. I especially want to thank my student mentor Dr. Toni South for her patience and willingness to teach. As it turned out, I enjoyed my time in the group so much that I decided to come back for grad school. When I first joined the group I was surrounded by several amazing mentors: Dr. Mike Smith, Dr. Jeff Gaulding, Dr. Grant Hendrickson, and Dr. Emily Herman. I can't imagine there being a better set of senior grad students to look up to and learn from. There was never a time when someone wasn't willing to lend a hand or give advice. I want to especially thank Emily for being an amazing friend and lab mate. I owe what remains of my sanity to her support and friendship, and our coffee breaks.

I have also been fortunate enough to work with several wonderful past group members, Dr. Mark Spears, Dr. Hiro Yoshida, Dr. Ling Zhang, Dr. Bob Hu, Dr. Nicole Welsch, and current members, Dr. Ashley Brown, Purva Kodlekere, Caroline Hansen,

Haylee Bachman, and Shalini Saxena. Your research group is an extremely important part of grad school, and I am proud to have been a part this one. A special thank you to Ashley for taking over the day-to-day operations following Andrew's departure. I am looking forward to seeing the exciting work that comes out of her research group in the coming years. In addition, I had the opportunity to mentor two intelligent, promising students, Tanya Su and Trisha Dalapati. I have no doubt that they will do wonderful things in the years to come.

Lastly, I would like to thank Andrew for letting me spend that initial summer in his research group. His willingness to listen to ideas regardless of who they came from was the thing that impressed me the most, and it is an approach I hope to carry with me. I have appreciated his approach to science and research, and I am extremely grateful for his continued support.

TABLE OF CONTENTS

	Page
ACKNOWLEDGEMENTS	iv
LIST OF TABLES	ix
LIST OF FIGURES	x
LIST OF SCHEMES	xii
LIST OF SYMBOLS AND ABBREVIATIONS	xiii
SUMMARY	xv
CHAPTER	
1 Introduction to Hydrogel Materials	1
1.1 Hydrogels	1
1.1.1 Crosslinking in Hydrogel Formation	3
1.1.2 Environmentally Responsive Hydrogels	4
1.1.3 Hydrogels as Biomaterials	6
1.1.3.1 Drug Delivery	6
1.1.3.2 Extracellular Matrix Scaffolding	8
1.2 The Microgel – A Microscopic Hydrogel	10
1.2.1 Microgels as Building Blocks	11
1.2.2 Temperature Responsive Microgels	13
1.3 References	15
2 Surface Modification of Substrates	25
2.1 Surface Assemblies and Coatings	25
2.2 References	35

3 Modulation of the Deswelling Temperatures of Thermoresponsive Microgel Films 43

3.1 Introduction 43

3.2 Experimental 45

3.2.1 Materials 45

3.2.2 Microgel Synthesis 46

3.2.3 Microgel Characterization 46

3.2.4 Microgel Film Fabrication 47

3.2.5 AFM Imaging 48

3.2.6 Light Scattering Curves 48

3.2.7 Differential Scanning Calorimetry 49

3.2.8 Percent Transmittance Curves 49

3.2.9 Confocal Microscopy of Mixed Microgel Films 50

3.3 Results and Discussion 50

3.4 Conclusion 59

3.5 References 60

4 Core/Shell Microgels De-couple the pH and Temperature Responsivities of Microgel Films 64

4.1 Introduction 64

4.2 Experimental 66

4.2.1 Materials 66

4.2.2 Microgel Synthesis 67

4.2.3 Dynamic Light Scattering 67

4.2.4 Microgel Film Fabrication 67

4.2.5 Atomic Force Microscopy 68

4.2.6 Temperature-Dependent Light Scattering Curves 68

4.3 Results and Discussion 69

4.4 Conclusion 78

4.5 References 78

5 Modification of Microgel Surfaces with a Self-Assembling Peptide 81

5.1 Introduction 81

5.2 Experimental 83

5.2.1 Materials 83

5.2.2 Microgel Synthesis 83

5.2.3 Microgel Characterization 84

5.2.4 Preparation of RADA-Coated Microgels 84

5.2.5 Circular Dichroism 85

5.2.6 Atomic Force Microscopy 85

5.2.7 Fluorescence Microscopy 85

5.3 Results and Discussion 86

5.4 Conclusions 94

5.5 References 94

6 Outlook and Future Directions 99

6.1 Controlled Swelling of Microgel Coatings 99

6.2 Peptide-Coated Microgels 100

6.3 References 105

APPENDIX A: Collecting Film Thickness Measurements and Optimization of AFM Imaging Parameters 108

A.1 Collecting Film Thickness Measurements 108

A.2 Impact of AFM Parameters on Calculated Film Thicknesses 109

A.3 References 113

VITA 114

LIST OF TABLES

Page

Table 1.1: Common Polymers Used in the Preparation of Hydrogels 2

Table 3.1: Synthesis Recipes and Hydrodynamic Radii for Microgels 1-6 51

Table 3.2: Comparison of VPTTs Obtained from Light Scattering and Transmittance 55

Table 3.3: VPTTs and DSTs (°C) for Microgels and Microgel Multilayer Films at pH 3 58

Table 4.1: Feed Ratios for Traditional Microgel Syntheses and De-Swelling Temperatures of Traditional Microgel LbL Films at pH 3 69

Table 4.2: Feed Concentrations of Core/Shell Microgels 70

Table 4.3: DLS data (nm) and de-swelling temperatures (°C) for core/shell microgels 72

Table 4.4: Average Film Thicknesses (nm) for Traditional and Core/Shell Microgel Films Calculated from AFM Height Traces 76

Table 4.5: Average Film Thicknesses (nm) for Traditional and Core/Shell Microgel Films Calculated from AFM Height Retraces 76

Table 5.1: Polymer Feed Ratios of Microgel Syntheses 86

Table 5.2: Hydrodynamic Radii (nm) of Microgel 1 (M1) Coated with RADA/RADAC 88

Table 5.3: Average Fluorescence Intensities of RADA-Coated Microgel 1 Images 92

LIST OF FIGURES

Page

Figure 2.1: Structures of (a) PAH, (b) PDADMAC, (c) PAA, and (d) PSS. 32

Figure 3.1: AFM height retrace images: (a-e) monolayers and (f-j) 6-layer LbL films of Microgels 1-5, respectively. 52

Figure 3.2: (a) Temperature dependent light scattering curves for dispersions of Microgels 1-5, and (b) response temperatures for Microgels 1-5 dispersed in buffer or assembled in 6-layer films as a function of mol% NIPMAm. 53

Figure 3.3: Differential scanning calorimetry curves of Microgels 1-5 (a-e, respectively). 54

Figure 3.4: Temperature dependent percent transmittance curves of mixed microgel composite films at pH 3: (a) alternating deposition of Microgels 2 and 5 (6-layers total) and (b) 2-layers each of Microgels 1-5. Dashed lines indicate the deswelling temperatures for films composed of either Microgel 2 or Microgel 5 only. 56

Figure 3.5: (a) Temperature-dependent percent transmittance curves of composite films of Microgels 2 and 5, assembled by three methods at pH 3. Cartoons illustrating the three assembly methods are provided; (b-d) AFM height images of alternating (layer 2), mixed (layer 1), and sectioned composite films (layer 4), respectively. Dashed lines indicate the deswelling temperatures for films composed of either Microgel 2 or Microgel 5 only. 57

Figure 3.6: Cross-sections (yz plane) of mixed microgel films obtained using a confocal microscope: (a) alternating deposition, 8 microgel layers, (b) deposition from microgel mixture, 6 microgel layers, and (c) deposition of Microgels 2 and 6 in separate sections, 19 microgel layers (Scale bar=2 μm). 59

Figure 4.1: Normalized DST curves of 6-layer microgel/PDADMAC films composed of Microgels 1-5 at (a) pH 3 and (b) pH 7.4. 70

Figure 4.2: AFM height images collected in air of (a) Core 1, (b) Core 2, (c) Core 1/Shell 1, and (d) Core 2/Shell 2. 71

Figure 4.3: Normalized DST curve comparison of microgel/PDADMAC films: (a) Microgel 1 and Core 1/Shell 1, (b) Microgel 3 and Core 2/Shell 2 at pH 3 and pH 7.4. 73

Figure 4.4: AFM height trace images of a 10-layer Microgel 3 film at pH 3, ~26 and 50 °C (a, b, respectively) and at pH 7.4, ~26 and 50 °C (d, c, respectively). 74

Figure 4.5: AFM height trace images of a 10-layer Microgel C2/S2 film at pH 3, ~26 and 50 °C (a, b, respectively) and at pH 7.4, ~26 and 50 °C (d, c, respectively). 75

Figure 4.6: Comparison of film thicknesses from AFM measurements and DST curves at pH 3 and pH 7.4: (a) Microgel 1, (b) Core 1/Shell 1, (c) Microgel 3, (d) Core 2/Shell 2. 77

Figure 5.1: AFM amplitude images (a) Microgel 1, (b) Microgel 1+RADA; (c) brightfield and (d) fluorescence microscopy images of Microgel 1+RADA+TMR (scale bar = 2 μm). 87

Figure 5.2: Microscopy images of Microgels 2-4 after coating with RADA+TMR, (a-c, respectively) brightfield and (d-f, respectively) fluorescence (scale bar = 2 μm). 89

Figure 5.3: AFM amplitude images of Microgels 5 (a) and 6 (b) after incubation with RADA. 90

Figure 5.4: (a) AFM amplitude image of Microgel 1+RADAC; (b) brightfield and (c) fluorescence microscopy images of Microgel 1+RADAC after labeling with 5-IAF; (d) brightfield and (e,f) fluorescence microscopy of Microgel 1+RADAC+TMR after labeling with 5-IAF (scale bar=2 μm). 91

Figure 5.5: Microgel 1+RADAC pellets following centrifugation. 92

Figure 5.6: CD spectra in DI water of (a) RADA peptides (20 μ*M*), and (b-d) Microgels 1, 2, 3, respectively, uncoated and after incubation with RADA peptides. 93

Figure 5.7: Microscopy images of Microgel 1 after mixing with Q11: (a) AFM amplitude image; (b) brightfield image (scale bar = 5 μm). 94

Figure A.1: AFM height image of a microgel film across a scratch in the film (left), and a depiction of the cross-section of each line of the AFM images (right). 108

Figure A.2: Calculated film thicknesses as a function of drive amplitude; (a) pH 3, ~26 °C, set point=218 mV; (b) pH 3, 50 °C, set point=200 mV; (c) pH 7.4, ~26 °C, set point=200 mV; (d) pH 7.4, 50 °C, set point=200 mV; Integral gain=10 for all images. The left height (LH) and right height (RH) are presented. 111

Figure A.3: Calculated film thicknesses as a function of set point; (a) pH 3, 50 °C, drive amplitude=3.0 V; (b) pH 7.4, ~26 °C, drive amplitude=2.0 V; (c) pH 7.4, 50 °C; Integral gain=10 for all images. The left height (LH) and right height (RH) are presented. 112

Figure A.4: Calculated film thicknesses at varying integral gain settings; (a) pH 3, 50 °C, set point=200 mV, drive amplitude=1.6 V; (b) pH 7.4, ~26 °C, drive amplitude=2.0 V; (c) pH 7.4, 50 °C, set point=200 mV, drive amplitude=1.6 V. The left height (LH) and right height (RH) are presented. 112

LIST OF SCHEMES

	Page
Scheme 1.1: Comparison of Hydrogels	4
Scheme 1.2: Synthesis of pNIPAm Microgels	14
Scheme 2.1: Examples of Film Deposition Techniques and Types of Assemblies	26
Scheme 3.1: Assembly of Microgel Layer-by-Layer Thin Films	44
Scheme 4.1: Construction of Linear Polyion and Microgel Layer-by-Layer Films	65

LIST OF SYMBOLS AND ABBREVIATIONS

PVA	Poly(vinyl alcohol)
PEG	Poly(ethylene glycol)
pHEMA	Poly(2-Hydroxyethyl methacrylate)
pAM	Poly(Acrylamide)
pAAc	Poly(Acrylic acid)
pPBA	Poly(3-Acrylamidophenyl boronic acid)
ATRP	Atom Transfer Radical Polymerization
RAFT	Reverse Addition Fragment Transfer
ROMP	Ring Opening Metathesis Polymerization
PLGA	Poly(Lactide-co-glycolic acid)
ECM	Extracellular Matrix
MMP	Matrix Metalloproteinases
pNIPAm	Poly(*N*-Isopropylacrylamide)
pNIPMAm	Poly(*N*-Isopropylmethacrylamide)
BIS	*N,N'*-Methylenebisacrylamide
AAc	Acrylic Acid
SDS	Sodium Dodecylsulfate
APS	Ammonium Persulfate
LB	Langmuir-Blodgett
SAM	Self-Assembled Monolayer
PDADMAC	Poly(diallyldimethylammonium chloride)
PEI	Poly(ethyleneimine)

PAH	Poly(allylamine hydrochloride)
PLL	Poly(L-Lysine)
PSS	Poly(sodium 4-styrenesulfonate)
AFM	Atomic Force Microscopy
LbL	Layer-by-Layer
PB	Phosphate Buffer
LCST	Lower Critical Solution Temperature
VPPT	Volume Phase Transition Temperature
DST	De-Swelling Temperature
DLS	Dynamic Light Scattering
R_H	Hydrodynamic Radius
EDC	*N*-(3-Dimethylaminopropyl)-*N*'-ethylcarbodiimide hydrochloride
NHS	*N*-Hydroxysuccinimde
APTMS	3-Aminopropyltrimethoxysilane
MES	2-(*N*-Morpholino)ethanesulfonic acid
HEPES	4-(2-Hydroxyethyl)piperazine-1-ethanesulfonic acid
5-IAF	5-Iodoacetamidofluorescein
MALS	Multi-Angle Light Scattering
R_{RMS}	Root-Mean-Square Radius
ITC	Isothermal Titration Calorimetry
SAP	Self-Assembling Peptide
GFP	Green Fluorescent Protein
CuAAC	Copper Catalyzed Azide Alkyne Cycloaddition

SUMMARY

This dissertation describes the development of temperature and pH-responsive interfaces, where the emphasis is placed on tuning the responsivities within a physiological temperature range. This tuning is achieved through the utilization of polymeric building blocks, where each component is specifically synthesized to have a unique responsivity. The assembly of these components onto surfaces permits the fabrication of stimuli-responsive interfaces. In addition, this dissertation explores the use of a self-assembling peptide as a modular building block to modify the interface of hydrogel microparticles, resulting in the formation of a new biosynthetic construct.

Hydrogels are three-dimensional, crosslinked polymer networks that swell in water. Over the years, hydrogels have been extensively explored as biomaterials due to their high water content, tunable mechanics, and chemical versatility. Two areas where hydrogels have received considerable interest are drug delivery and extracellular matrices. Unfortunately, developing structurally and functionally complex hydrogels from the top down is challenging because many parameters cannot be independently tuned in a bulk material. An alternative route would be to develop a library of building blocks, where each is tailored for a given function, and assemble these components into composite structures. The building block synthesized and utilized in this dissertation is a microgel. Microgels are a colloidal dispersion of hydrogel microparticles, ranging in size from 100 to 1000 nm in diameter. The microgels were prepared from environmentally responsive polymers, sensitive to both temperature and pH.

Microgels have been used in the fabrication of polyelectrolyte layer-by-layer films, where the microgel serves as the polyanion and a linear polycation is used to "stitch" the particles together. In **Chapters 3 and 4**, stimuli-responsive interfaces are prepared from environmentally responsive microgel building blocks. In particular, **Chapter 3** demonstrates tuning of the film response temperature by preparing several different microgels with differing ratios of two thermoresponsive polymers. **Chapter 4** evaluates the influence of the pH environment on the thermoresponsivity of microgel films. While the pH environment was found to substantially affect some films, it is possible to prepare microgel films that behave independently of pH. The swelling/de-swelling of the films was also investigated by atomic force microscopy (AFM) as a function of both pH and temperature. It was determined that the AFM imaging parameters can drastically affect the measured film thicknesses (**Appendix A**) due to the soft, deformable nature of microgel films. The studies in these chapters illustrate the advantages of preparing composite structures from discrete components, where the functionality of the composite is dictated by the constituent particles.

In **Chapter 5**, attention is placed on modifying the surface of microgel particles. Many of the traditional routes used to modify microgels involve the incorporation of co-monomers into the network or the addition of polymer shells. However, a new core/shell construct is presented, where a microgel core is coated with a self-assembling peptide shell. In this scenario, the peptide shell serves as a modular scaffold, where surface-localized functional groups can participate in reactions. Although there are still a number of questions remaining in regard to the assembly process and stability of the construct, initial experiments suggests that this is an interesting and promising structure to study.

Finally, a discussion of future directions and possible experiments is provided in **Chapter 6**. Hopefully, this will serve as a guide for further exploration of the research presented herein. Microgels remain a rich class of materials to study and employ. While their synthesis is rather straightforward, their use often results in complex behavior and interesting phenomena. Understanding their behavior is a crucial step in realizing their full potential.

CHAPTER 1

INTRODUCTION TO HYDROGEL MATERIALS

Portions adapted from

Clarke, K.C.; Douglas, A.M.; Brown, A.C.; Barker, T.H.; Lyon, L.A. Colloid-Matrix Assemblies in Regenerative Medicine *Curr. Op. Colloid Inter. Sci.* **2013**, *18*, 393-405.

1.1 Hydrogels

Hydrogels are crosslinked polymeric networks that swell extensively in aqueous environments due to hydrophilic functional groups on the polymer chains (e.g. hydroxyl, carbonyl, amine, carboxyl). Hydrogels have been considered for a range of applications including drug delivery, cell scaffolding, tissue regeneration, and analytical techniques.[1-10] This broad utility stems from the unique properties of hydrogels (i.e. they have both liquid and solid properties), and the potential to prepare them from a wide range of precursors. **Table 1.1** highlights several polymers frequently used in the preparation of hydrogels.

Hydrogels have been fabricated from a variety of polymers, including natural as well as synthetic polymers, affording versatility in the chemical composition of the bulk material. Synthetic gels are often prepared by free-radical polymerization of small molecule monomers, where an initiator is used as a free-radical source. Initiators are typically small molecules, where cleavage and radical generation is achieved by temperature, light, or redox processes.[1,11,12] Polymeric material can also be obtained from natural sources or through synthetic routes, and then subsequently crosslinked to form the hydrogel network.[13-16] Hydrogels are commonly classified by the type and method of crosslinking because crosslinking is essential in their preparation.

Table 1.1. Common Polymers Used in the Preparation of Hydrogels

Polymer	Abbreviation	Structure	Notes
poly(vinyl alcohol)	PVA	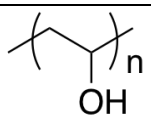	
poly(ethylene glycol)	PEG	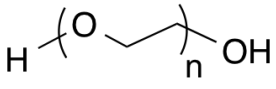	
poly(2-hydroxyethyl methacrylate)	pHEMA	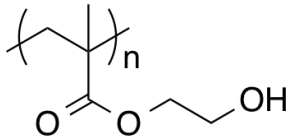	
poly(acrylamide)	pAM	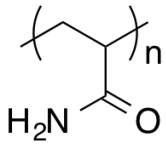	
poly(*N*-isopropylacrylamide)	pNIPAm	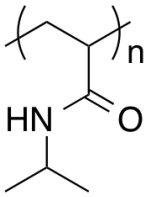	temperature responsive
poly(acrylic acid)	pAAc	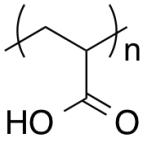	pH responsive
poly(3-acrylamidophenyl boronic acid)	pPBA	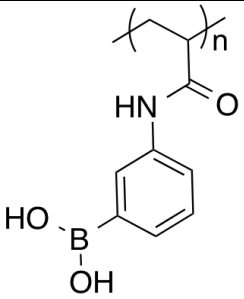	glucose responsive
alginate		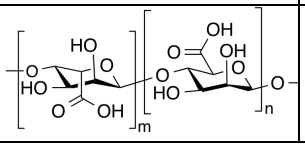	metal ion sensitive

1.1.1 Crosslinking in Hydrogel Formation

Crosslinking lends stability to the network, but also functions as a parameter that can be tuned to alter the mechanics, pore size, and swelling properties of the hydrogel; alterations in the extent of crosslinking often change all three of these properties simultaneously. Network crosslinking can be achieved through physical (i.e. non-covalent) or chemical (i.e. covalent) means.[17] Non-covalent interactions, like hydrogen bonding, electrostatics, and physical entanglement, are commonly used in the formation of hydrogels. Further, the intrinsic self-assembly behavior of biomacromolecules can also be utilized in the preparation of hydrogels. For example, the propensity of peptides to form secondary structures (i.e. β-sheets and α-helices) can be harnessed for macroscopic assembly into hydrogels.[18,19] Moreover, synthetic polymers have been modified with a variety of complementary pairs (e.g. coiled-coil motif, host-guest interactions with cyclodextrin) where the specific interactions become crosslinking points.[20,21] The reversible nature of many physical crosslinks can be used to control network structure, but a drawback to non-covalent crosslinking is network fragility.

Alternatively, covalent crosslinks are employed to yield a permanent, more robust network. Typically, covalent crosslinks are formed as the main monomer is polymerized in the presence of bis-functionalized monomers.[1,22] Alternatively, pre-formed polymers can be crosslinked to form a three-dimensional network. For example, controlled radical polymerization techniques, such as atom transfer radical polymerization (ATRP) and reverse addition fragment transfer polymerization (RAFT), have been used to synthesize polymers which were subsequently crosslinked via terminal reactive groups.[23-25] In a similar manner, naturally sourced polymers have been crosslinked via functional groups extending off the polymer backbone to form covalent crosslinks.[14,16] A general scheme comparing physically and covalently crosslinked hydrogels is presented in **Scheme 1.1**.

Additional strategies have been employed to control the properties of hydrogel networks. One strategy to enhance the functionality of hydrogels is the incorporation of

co-monomers during synthesis.[26,27] For example, functional groups incorporated into the network can be utilized in reactions following hydrogel formation, or for non-covalent interactions with target molecules. Co-monomers can also be used to control the swelling behavior of hydrogels in water. Another tactic is the development of double network hydrogels, where a hydrogel network is imbibed with monomers and a second network is formed *in situ*.[14,28] This strategy enables functionally unique hydrogels to be prepared within the same construct, where the networks can be independently tailored.

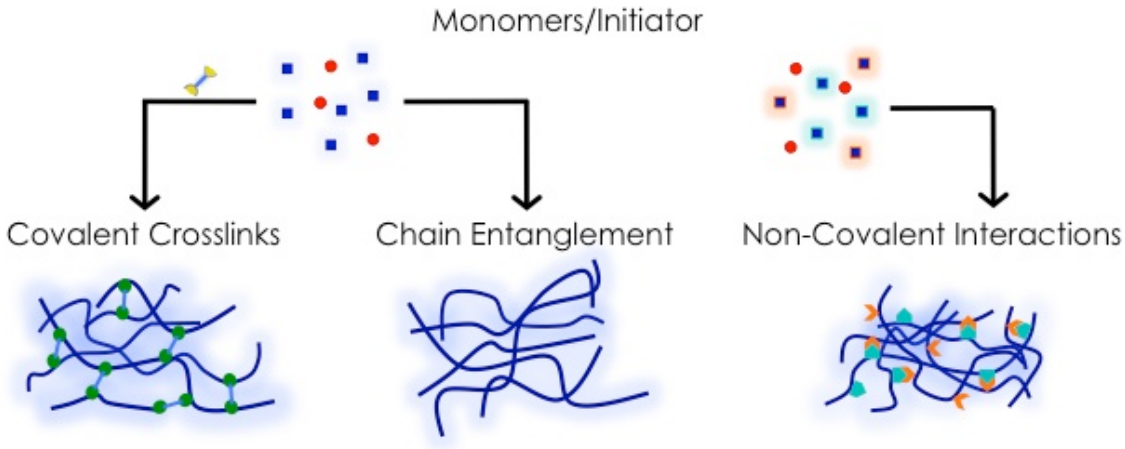

Scheme 1.1. Comparison of Hydrogels

1.1.2 Environmentally Responsive Hydrogels

As the applicability of hydrogels continued to expand, researchers sought new avenues for controlling hydrogel properties, while also developing materials with enhanced functionality. This pursuit led to the investigation of environmentally responsive hydrogels, where changes in the surroundings result in changes in the material itself. Networks synthesized from environmentally responsive polymers exhibit sharp, reversible deswelling/swelling responses as the polymer-solvent interactions transform upon changes in environmental conditions.

Responsive hydrogels have been studied for a number of applications including drug delivery, chemical separations, and actuation.[2,29-31] Temperature, light, and pH-responsive hydrogels have been extensively explored.[32-36] A commonly studied temperature-responsive polymer is poly(*N*-isopropylacrylamide) (pNIPAm).[33] Linear chains of pNIPAm exhibit a reversible coil to globule transition upon an increase in the environmental temperature above 31 °C. This temperature is referred to as the lower critical solution temperature (LCST). A three-dimensional pNIPAm hydrogel network will de-swell in response to temperature increases above 31 °C. The de-swelling of pNIPAm gels is entropically driven, as water molecules are released to the surroundings and polymer-polymer interactions are favored over polymer-solvent interactions.

Beyond these traditional physicochemical stimuli, researchers have developed hydrogels responsive to biological cues.[37] In these systems, the presence of specific biomolecules leads to changes in the polymer-polymer and polymer-solvent interactions. Ideally, responsivity is therefore governed by a specific molecular stimulus rather than a physically induced stimulus. This could be particularly useful in biological applications where external stimuli can be difficult to control with precision. A seminal example is a glucose-responsive hydrogel, where a phenylboronic acid (PBA) co-monomer serves as the functional component. Complexation of glucose with PBA, results in ionization and concomitant swelling of the hydrogel.[37]

In addition to these traditional approaches to responsive hydrogel networks (i.e. bulk swelling/deswelling transitions), a variety of nuanced strategies have been put forth in an effort to wield greater control over hydrogel materials. These very often involve spatial and temporal control over responsivity within the bulk material. Of note, light responsive elements are becoming more regularly investigated because light can be controlled both spatially and temporally. These applications include photopatterning of biomolecules, site-specific degradation, and *in situ* modification of mechanical properties at discrete locations.[26,38-40]

1.1.3 Hydrogels as Biomaterials

Historically, the first use of hydrogels as a biomaterial was for contact lenses.[41] Since the 1960s hydrogel materials have continued to be extensively explored in varying contexts. Generally speaking biomaterials exist as a substitute for damaged or malfunctioning tissue (macroscopic) or to control the local biological environment (molecular or microscopic). Biological tissues exhibit structural and mechanical properties, which can be mimicked, in part, by hydrogels.[42-44] The high water content, porosity, viscoelasticity, and chemical versatility of hydrogels have made them prime candidates for biomedical applications. Specifically, two widely investigated applications for hydrogels will be discussed: drug delivery and extracellular matrix scaffolds. A central theme in the development and realization of biomaterials is the pursuit of ever more complex structures. Because native physiological environments are indeed complex, the materials we implement are continually revised as we seek to recapitulate natural processes and aim to realistically mimic the natural milieu.

1.1.3.1 Drug Delivery

Hydrogels have been extensively explored as drug delivery constructs for the local administration of therapeutics. A simplistic example is the elution of a drug from a hydrogel, where the drug passively diffuses from the matrix into the surrounding environment. Release kinetics are governed by the diffusion coefficient of the therapeutic molecule, the pore size of the hydrogel, and drug-hydrogel interactions.[2] Erodible hydrogels, such as those prepared from poly(lactide-co-glycolic acid) (PLGA), can also be used to release entrapped molecules as the network is hydrolyzed in physiological conditions.[45] However, these simple models lack the ability to turn on and off release, a property necessary in a number of drug release applications. Quite logically, stimuli-responsive hydrogels have been utilized as a platform for gating the release of molecules, where release is governed by a set stimulus, allowing on/off functionality.[29,46]

For example, pNIPAm hydrogels have been employed for temperature-triggered release of molecules. The swelling transitions of the hydrogels, alter the pore size, thereby controlling the release of encapsulated molecules.[47] pH-responsive hydrogels have been employed as well, where a change in pH leads to network swelling through the deprotonation or protonation of carboxylic acid or amine groups, respectively. The increased pore size of the hydrogel permits diffusion of the drug out of the network. Temperature and pH-responsivity can also be used to alter the drug-hydrogel interactions, providing another route to vary the release rate. The glucose-responsive hydrogel described above has been used to deliver entrapped insulin following network swelling in the presence of glucose.[37,46] This particular example more closely mimics feedback mechanisms found in biology.

Release has also been gated using enzyme-responsive hydrogels. The specificity of enzymes and other biomolecules is a supreme advantage over basic physicochemical stimuli, especially under circumstances where direct access or probing of the material *in situ* is not possible. Furthermore, a specific cell signal or disease state serves as the trigger, permitting release only when that biochemical cue is present. Crosslinks bearing protease-cleavable substrates have been used to control the pore size of the hydrogel. As the protease cleaves the crosslinks, larger pores are formed, and release of the encapsulated therapeutic is achieved.[48] Alternatively, the drug can be tethered to the network *via* an enzymatically degradable linker. The drug is therefore released in the presence of the enzyme without altering the network structure and mechanics of the hydrogel.[49,50]

Hydrogels can be synthesized with varying levels of complexity, making them useful as simple drug reservoirs, or with precisely tuned responsive elements. A material that gradually elutes its contents over a designated time frame can be useful for reducing inflammation at the site of biomaterial implantation. For example, drug-eluting stents have been used to reduce the inflammatory response post-implantation and prevent the

growth of tissue around the stent.[51] Degradability can be added to the system as a way to control pharmacokinetics, and to remove the material once it has served its purpose. Responsive hydrogels are used to enhance the user-defined control, by permitting release only when designated by a pre-defined stimulus. Hydrogels with gated release may be most useful for precise spatiotemporal control, such as when the released therapeutic is used to treat only a subset of cells.

1.1.3.2 Extracellular Matrix Scaffolding

The essential non-cellular component of all tissues is the extracellular matrix (ECM), the protein scaffold and microenvironment in which cells reside.[42] The protein composition and structure of the ECM can influence cell adhesion and signaling, as cells bind to specific ligand sites on ECM proteins via cell surface receptors. Cell-ECM interactions are complex and dynamic in nature and can dictate cellular phenotype, influencing cell survival, proliferation, migration, and differentiation. Various ECM proteins also bind and sequester growth factors, which can lead to spatial and temporal control of the dynamics of cellular processes. Additionally, the ECM can determine the mechanical properties of each organ through its compressive modulus, elasticity, and water retention.

The native ECM is an extremely complex, dynamic environment through which many cell fate processes are controlled. The fields of tissue engineering and regenerative medicine have sought to develop biomaterials capable of recapitulating the behavior of the ECM in the context of synthetic or biosynthetic hybrids of reduced complexity, with the ability to regenerate severely damaged tissues either *in vitro* or *in vivo* remaining the primary goal. In addition, such materials can lead to the creation of accurate models to study cell behavior and fate under a multitude of environmental conditions. Hydrogels, both synthetic and natural, have been a main choice for ECM mimics because their mechanical properties and high water content resemble those of many tissues.[52]

Naturally derived polymers, such as collagen, fibrin, hyaluronic acid, and the commercially available Matrigel, have been used as ECM scaffolds.[4,8,9,53,54] These polymers are found in the native ECM, but quite often only one or two are selected as the scaffold material for simplicity. Biopolymer hydrogels have several inherent advantages, including biocompatibility, degradability, and the presence of cell and growth factor binding sites. However, modifications (e.g. chemical, mechanical, structural) to biopolymer-based hydrogels can be challenging. For this reason synthetic polymer hydrogels have been explored as ECM scaffolds.

Synthetic hydrogels serve as a blank scaffold, where bio-interactive components are selectively incorporated into the matrix as needed. For instance, the amino acid sequence RGD is very often covalently bound to promote cell adhesion.[55,56] Growth factors have also been included through covalent or non-covalent means to assist in cell survival and differentiation.[57] Numerous studies have focused on the employment of PEG hydrogels as scaffold mimics because of their biocompatibility and ease of preparation. Synthetic hydrogels typically lack sites for degradation, so this particular attribute has been added in by careful selection and/or preparation of co-monomers and crosslinkers. In the native ECM, cells are known to excrete proteases, such as matrix metalloproteinases (MMPs), to degrade the local ECM and permit migration. Likewise, MMP degradable substrates have been added to PEG hydrogels to allow cells to control the matrix.[58]

Despite the many successes in the fabrication and use of artificial ECMs – reductionist scaffolds based on natural ECM components and purely synthetic systems – drawbacks and challenges remain preventing the full implementation of these scaffolds. Many of these constructs have deepened our knowledge and understanding of the parameters most important to ECMs and cell function. However, most of these scaffolds only incorporate a few of the many possible components, and it is still not well understood what level of complexity is needed for a given task.

Our group, as well as others, has recognized the need for increasing the functionality and complexity within ECM scaffolds in a controlled and predictable manner.[59-61] Further, there is a need to access smaller dimensions in biomaterials, as native ECMs span several orders of magnitude in size. It is, however, particularly challenging to enable precise, localized functionality within a bulk material. Therefore, a particularly enticing tactic is to prepare a population of building blocks, each with a tailored functionality, where the assembly of these modular components provides access to complex constructs. In particular, we have been interested in the use of colloidal components in artificial ECMs as a means of adding the necessary physicochemical complexity as well as to enhance existing properties. Colloids provide a large synthetic and physical playground within which modularity can be imparted to biosynthetic matrices while potentially maintaining the biological properties required for adequate function in biomedical applications. One such colloidal particle with an abundance of promise as a building block will be the focus of the ensuing section.

1.2 The Microgel – A Microscopic Hydrogel

Like hydrogels, microgels are crosslinked, polymeric networks, which swell in water. However, unlike bulk gels, microgels are colloidal particles ranging in size from less than 100 to several thousand nanometers in diameter.[62,63] They are commonly synthesized through emulsion polymerization techniques, but can also be prepared from the self-assembly of block co-polymers into micelles. Additional strategies rely on lithographic techniques to prepare microgel particles.[64,65] Microgels have many analogous properties to bulk hydrogels (e.g. hydrophilicity, tunable mechanics, porosity), making them ideal for biomedical applications, but they allow access to vastly different size scales. The small size has resulted in several unique characteristics, as they share both colloidal particle and polymer properties.[66] Deformability at small length scales has also become an increasingly important attribute of microgels, as the “softness” of the

particles has been implicated in their use as a biomaterial and in 3-dimensional assemblies.[67-69]

The advantageous properties of microgels have resulted in their study for a variety of applications, including drug delivery, diagnostics, analytical analyses, colloidal crystals, and in biomaterial coatings. Rather than describe the numerous microgels which have been studied and utilized, this section will focus first on the utility of microgels as building blocks, and then, more specifically, on thermoresponsive microgels, as these two areas pertain more strongly to the research described in this document.

1.2.1 Microgels as Building Blocks

Due to their size and versatility microgels have been employed as building blocks within bulk and assembled structures. Composite structures can be fabricated, where properties are inherited through the building blocks. This approach has two main advantages. First, building blocks can be independently tailored in regard to specific functionalities. Second, assembly of the constituents is inherently modular (i.e. "plug and play"), permitting more precise tailoring of the final composite. Microgels have been used as functional components within bulk hydrogels, and, these discrete particles have also been used in the build-up of microgel-based architectures.

The potential to impart stimuli-responsiveness into unresponsive hydrogels or to enhance the responsivity of environmentally responsive hydrogels has been demonstrated through the incorporation of responsive microgels.[70-72] Microgels have also been included within macrogels to function as drug delivering modules, providing a means for tuning the release from hydrogel scaffolds, or to release multiple molecules independently.[73] In this way, the chemical nature of the microgel inclusions can be used to add or enhance functionality of a bulk matrix. Moreover, mechanical properties of bulk gels have been strengthened through the incorporation of microgels into the network, either as crosslinking points or as non-covalent additives to the matrix.[74,75] Within these relatively

simple constructs, the ability to tune gel properties or enhance the functionality is provided through the incorporation of microgels.

Alternatively, assemblies of microgel particles can be fabricated. Nano/micro-particulate objects, including microgels, have been pieced together through a variety of methods. Substrate supported assemblies have been prepared through particle surface interactions (covalent or noncovalent). For example, the Lyon group has demonstrated the fabrication of microgel-based thin films on planar surfaces, where electrostatic interactions facilitate assembly. These microgel assemblies have been used to prepare microlenses for sensing, and to modify substrates for non-fouling coatings.[76-78] The assembly of microgels on particulate substrates via covalent bond formation has been shown as well. These heteroaggregates have been fabricated using two different types of microgels demonstrating the modularity of assembling materials from building blocks.[79] The direct synthesis of microgel structures onto a substrate has also been utilized in the development of chip-based analytical approaches.[80,81]

In addition to substrate-supported architectures, freestanding microgel assemblies have been prepared following delamination from a surface.[82] The advantage of preparing freestanding assemblies is the adoption of unique shapes that are challenging to access on 2-dimensional substrates. For example, our group has fabricated microgel films where two different microgels with differing swelling properties are used to control the 3-dimensional shape following delamination from the substrate.[83] More recently, examples of the self-assembly of microgel building blocks and other microgel-like colloids have begun to emerge.[84,85] Here the goal is direct access to a multitude of 3-dimensional arrangements of the constituent soft particle components. Though promising, the often-required inclusion of anisotropy into particle architectures to control self-assembly has limited broad-spectrum fabrication of such structures.

The chemical and functional tailorability of microgels coupled with their size has made them worthwhile for investigation within biomaterial scaffolds or as stand-alone

structures. Specific tasks can be divided among several populations of particles, and then recombined to provide greater control at tangible length scales. The use of modular components for assembly fabrication is a central theme of this dissertation.

1.2.2 Temperature-Responsive Microgels

The Lyon group has worked extensively with temperature-responsive microgels prepared from NIPAm.[63,76,86] PNIPAm microgels are synthesized by aqueous free-radical precipitation polymerization.[87] Reagents commonly used in the preparation of pNIPAm microgels and a schematic of microgel synthesis are provided in **Scheme 1.2**. Monomers, and often a surfactant (e.g. sodium dodecylsulfate), are dissolved in water and heated to 70 °C. Usually a crosslinker (e.g. *N,N'*-methylenebisacrylamide) is added to the monomer solution, but self-crosslinked microgels can be prepared, where crosslinking is the result of chain transfer reactions.[88,89] Free radicals are introduced into the system typically following the thermal decomposition of an initiator (e.g. ammonium persulfate). Growing oligomer chains condense to form a globule since the environmental temperature is above the LCST of pNIPAm. These collapsed precursor particles serve as the substrate for further polymer addition and microgel growth. Work within the group has expanded the use of precipitation polymerization to synthesize a multitude of particle architectures, including core/shell, degradable, and yolk/shell constructs.[90-92]

PNIPAm microgels can be synthesized with a variety of co-monomers to add responsive elements and incorporate functional groups for post-synthetic modification. Commonly acrylic acid is incorporated, lending pH responsivity to the network. Carboxylic acid, amine, and propargyl co-monomers, among others, have been successfully incorporated into pNIPAm microgel networks, and subsequently employed in conjugation reactions.[93-96] Selection of the parent polymer, copolymers, and particle architecture provides a large parameter space with which to tailor microgel populations.

Size is critical when comparing stimuli-responsive macro- and microgels. For example, bulk responsive hydrogels develop a "skin" layer at the periphery as de-swelling occurs, limiting the release of water and solute from the interior. However, the distance water molecules have to travel from the interior of a microgel to the surrounding phase is much less, meaning that microgels have a much faster response time than their bulk counterparts.[97,98] Indeed this has been an important consideration in the realization of stimuli-responsive systems, which often require rapid, predictable responsivities.

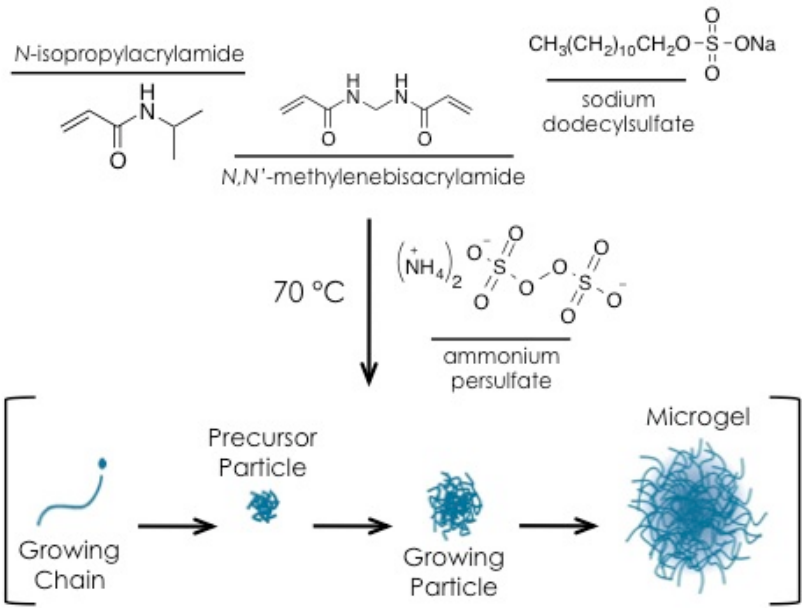

Scheme 1.2. Synthesis of pNIPAm Microgels

The employment of microgels as delivery vehicles has been actively pursued over the years with the main objectives being targeted delivery to the location in need, mitigation of side effects, and protection of sensitive therapeutics.[86] PNIPAm microgels have also been used in the modification of surfaces to bring new functionality to the interface. Using microgels as a film component allows for the build-up of hydrogel layers

on a variety of substrates, while maintaining the applicability of discrete particles. Responsive films can be prepared, where the interfacial properties can be controlled by external stimuli. The modification of surfaces with uniquely tailored materials has become a far-reaching concept, extending from the modification of nanoparticle surfaces to the fabrication of coatings for biomaterial implants.

Microgels have been investigated for a multitude of applications. In particular the use of microgels as a film component is an integral part of this dissertation. The coming chapters will discuss the use of films, in general, to modify surface properties of materials (**Chapter 2**), and, more specifically, the employment of temperature and pH-responsive microgel-based films to controllably alter the interface (**Chapters 3 and 4**). Lastly, the preparation of a new core/shell microgel construct will be described, where the surface of the microgel is modified with a peptide shell (**Chapter 5**).

1.3 References

(1) Buwalda, S.J.; Boere, K.W.M.; Dijkstra, P.J.; Feijen, J.; Vermonden, T.; Hennink, W.E., Hydrogels in a Historical Perspective: From Simple Networks to Smart Materials. *J. Controlled Release* **2014**, *190*, 254-273.

(2) Hoare, T.R.; Kohane, D.S., Hydrogels in Drug Delivery: Progress and Challenges. *Polymer* **2008**, *49*, 1993-2007.

(3) Lin, C-C.; Anseth, K.S., PEG Hydrogels for the Controlled Release of Biomolecules in Regenerative Medicine. *Pharm. Res.* **2009**, *26*, 631-643.

(4) Silva, R.; Fabry, B.; Boccaccini, A.R., Fibrous Protein-Based Hydrogels for Cell Encapsulation. *Biomaterials* **2014**, *35*, 6727-6738.

(5) Drury, J.L.; Mooney, D.J., Hydrogels for Tissue Engineering: Scaffold Design Variables and Applications. *Biomaterials* **2003**, *24*, 4337-4351.

(6) Dash, M.; Chiellini, F.; Ottenbrite, R.M.; Chiellini, E., Chitosan-A Versatile Semi-Synthetic Polymer in Biomedical Applications. *Prog. Polym. Sci.* **2011**, *36*, 981-1014.

(7) Lee, K.Y.; Mooney, D.J., Alginate: Properties and Biomedical Applications. *Prog. Polym. Sci.* **2012**, *37*, 106-126.

(8) Lam, J.; Truong, N.F.; Segura, T., Design of Cell-Matrix Interactions in Hyaluronic Acid Hydrogels. *Acta Biomater.* **2014**, *10*, 1571-1580.

(9) Janmey, P.A.; Winer, J.P.; Weisel, J.W., Fibrin Gels and their Clinical and Bioengineering Applications. *J. R. Soc. Interface* **2009**, *6*, 1-10.

(10) Kiyonaka, S.; Sada, K.; Yoshimura, I.; Shinkai, S.; Kato, N.; Hamachi, I., Semi-Wet Peptide/Protein Array Using Supramolecular Hydrogel. *Nat. Mater.* **2004**, *3*, 58-64.

(11) Bowman, C.N.; Kloxin, C.J., Toward an Enhanced Understanding and Implementation of Photopolymerization Reactions. *AIChE J.* **2008**, *54*, 2775-2795.

(12) Johnson, L.M.; Fairbanks, B.D.; Anseth, K.S.; Bowman, C.N., Enzyme-Mediated Redox Initiation for Hydrogel Generation and Cellular Encapsulation. *Biomacromolecules* **2009**, *10*, 3114-3121.

(13) Jung, J.P.; Sprangers, A.J.; Byce, J.R.; Su, J.; Squirrell, J.M.; Messersmith, P.B.; Eliceiri, K.W.; Ogle, B.M., ECM-Incorporated Hydrogels Cross-Linked via Native Chemical Ligation to Engineer Stem Cell Microenvironments. *Biomacromolecules* **2013**, *14*, 3102-3111.

(14) Truong, V.X.; Ablett, M.P.; Richardson, S.M.; Hoyland, J.A.; Dove, A.P., Simultaneous Orthogonal Dual-Click Approach to Tough, in-Situ-Forming Hydrogels for Cell Encapsulation. *J. Am. Chem. Soc.* **2015**, *137*, 1618-1622.

(15) Crescenzi, V.; Cornelio, L.; Meo, C.D.; Nardecchia, S.; Lamanna, R., Novel Hydrogels via Click Chemistry: Synthesis and Potential Biomedical Applications. *Biomacromolecules* **2007**, *8*, 1844-1850.

(16) Kim, S.H.; Won, C.Y.; Chu, C.C., Synthesis and Characterization of Dextran-Based Hydrogel Prepared by Photocrosslinking. *Carbohydr. Polym.* **1999**, *40*, 183-190.

(17) Hennink, W.E.; van Nostrum, C.F., Novel Crosslinking Methods to Design Hydrogels. *Adv. Drug Delivery Rev.* **2002**, *54*, 13-36.

(18) Lowik, D.W.P.M.; Leunissen, E.H.P.; van den Heuvel, M.; Hansen, M.B.; van Hest, J.C.M., Stimulus Responsive Peptide Based Materials, *Chem. Soc. Rev.* **2010**, *39*, 3394-3412.

(19) Hosseinkhani, H.; Hong, P-D.; Yu, D-S., Self-Assembled Proteins and Peptides for Regenerative Medicine. *Chem. Rev.* **2013**, *113*, 4837-4861.

(20) Jing, P.; Rudra, J.S.; Herr, A.B.; Collier, J.H., Self-Assembling Peptide-Polymer Hydrogels Designed from the Coiled Coil Region of Fibrin. *Biomacromolecules* **2008**, *9*, 2438-2446.

(21) Liu, K.L.; Zhang, Z.; Li, J., Supramolecular Hydrogels Based on Cyclodextrin-Polymer Polypseudorotaxanes: Materials Design and Hydrogel Properties. *Soft Matter* **2011**, *7*, 11290-11297.

(22) Ercole, F.; Thissen, H.; Tsang, K.; Evans, R.A.; Forsythe, J.S., Photodegradable Hydrogels Made via RAFT. *Macromolecules* **2012**, *45*, 8387-8400.

(23) Johnson, J.A.; Finn, M.G.; Koberstein, J.T.; Turro, N.J., Synthesis of Photocleavable Linear Macromonomers by ATRP and Star Macromonomers by a Tandem ATRP-Click Reaction: Precursors to Photodegradable Model Networks, *Macromolecules* **2007**, *49*, 3589-3598.

(24) Telitel, S.; Amamoto, Y.; Poly, J.; Morlet-Savary, F.; Soppera, O.; Lalavee, J.; Matyjaszewski, K., Introduction of Self-Healing Properties into Covalent Polymer Networks via the Photodissociation of Alkoxyamine Junctions. *Polym. Chem.* **2014**, *5*, 921-930.

(25) Zhou, H.; Johnson, J.A., Photo-Controlled Growth of Telechelic Polymers and End-Linked Polymer Gels. *Angew. Chem. Int. Ed.* **2013**, *52*, 2235-2238.

(26) Wylie, R.G.; Ahsan, S.; Aizawa, Y.; Maxwell, K.L.; Morshead, C.M.; Shoichet, M.S., Spatially Controlled Simultaneous Patterning of Multiple Growth Factors in Three-Dimensional Hydrogels. *Nat. Mater.* **2011**, *10*, 799-806.

(27) Andrade-Vivero, P.; Fernandez-Gabriel, E.; Alvarez-Lorenzo, C.; Concheiro, A., pHEMA Hydrogels by Copolymerization with Functionalized Monomers. *J. Pharm. Sci.* **2007**, *96*, 802-813.

(28) Gong, J.P., Why are Double Network Hydrogels so Tough? *Soft Matter* **2010**, *6*, 2583-2590.

(29) Qiu, Y.; Park, K., Environment-Sensitive Hydrogels for Drug Delivery. *Adv. Drug Delivery Rev.* **2012**, *64*, 49-60.

(30) Tokarev, I.; Minko, S., Multiresponsive, Hierachically Structured Membranes: New, Challenging, Biomimetic Materials for Biosensors, Controlled Release, Biochemical Gates, And Nanoreactors. *Adv. Mater.* **2009**, *21*, 241-247.

(31) Kim, P.; Zarzar, L.D.; He, X.; Grinthal, A.; Aizenberg, J., Hydrogel-Actuated Integrated Responsive Systems (HAIRS): Moving Towards Adaptive Materials. *Curr. Opin. Solid State Mater. Sci.* **2011**, *15*, 236-245.

(32) Vancoillie, G.; Frank, D.; Hoogenboom, R., Thermoresponsive Poly(oligo ethylene glycol acrylates). *Prog. Polym. Sci.* **2014**, *39*, 1074-1095.

(33) Schild, H.G., Poly(*N*-isopropylacrylamide): Experiment, Theory and Application. *Prog. Polym. Sci.* **1992**, *17*, 163-249.

(34) Suzuki, A.; Tanaka, T., Phase Transition in Polymer Gels Induced by Visible Light. *Nature* **1990**, *346*, 345-347.

(35) Mamada, A.; Tanaka, T.; Kungwatchakun, D.; Irie, M., Photoinduced Phase Transition in Gels. *Macromolecules* **1990**, *23*, 1517-1519.

(36) Zhang, J.; Xie, R.; Zhang, S-B.; Cheng, C-J.; Ju, X-J.; Chu, L-Y., Rapid pH/Temperature-Responsive Cationic Hydrogels with Dual Stimuli-Responsive Grafted Side Chains. *Polymer* **2009**, *50*, 2516-2515.

(37) Miyata, T.; Uragami, T.; Nakamae, K., Biomolecule-Sensitive Hydrogels. *Adv. Drug Delivery Rev.* **2002**, *54*, 79-98.

(38) Guvendiren, M.; Burdick, J.A., Stiffening Hydrogels to Probe Short- and Long-Term Cellular Responses to Dynamic Mechanics. *Nat. Commun.* **2012**, DOI:10.1038/ncomms1792.

(39) Kloxin, A.M.; Kasko, A.M.; Salinas, C.N.; Anseth, K.S., Photodegradable Hydrogels for Dynamic Tuning of Physical and Chemical Properties. *Science* **2009**, *324*, 59-63.

(40) Tomatsu, I.; Peng, K.; Kros, A., Photoresponsive Hydrogels for Biomedical Applications. *Adv. Drug Delivery Rev.* **2011**, *63*, 1257-1266.

(41) Wichterle, O.; Lím, D., Hydrophilic Gels for Biological Use. *Nature* **1960**, *185*, 117-118.

(42) Frantz, C.; Stewart, K.M.; Weaver, V.W., The Extracellular Matrix at a Glance. *J. Cell Sci.* **2010**, *123*, 4195-4200.

(43) Wegst, U.G.K.; Bai, H.; Saiz, E.; Tomsia, A.P.; Ritchie, R.O., Bioinspired Structural Materials. *Nature Mater.* **2015**, *14*, 23-36.

(44) Levental, I.; Georges, P.C.; Janmey, P.A., Soft Biological Materials and Their Impact on Cell Function. *Soft Matter* **2007**, *3*, 299-306.

(45) Yuen, W.W.; Du, N.R.; Chan, C.H.; Silva, E.A.; Mooney, D.J., Mimicking Nature by Codelivery of Stimulant and Inhibitor to Create Temporally Stable and Spatially Restricted Angiogenic Zones. *Proc. Natl. Acad. Sci.* **2010**, *107*, 17933-17938.

(46) Siegel, R.A., Stimuli Sensitive Polymers and Self Regulated Drug Delivery Systems: A Very Partial Review. *J. Controlled Release* **2014**, *190*, 337-351.

(47) Park, T.G., Temperature Modulated Protein Release from pH/Temperature-Sensitive Hydrogels. *Biomaterials* **1999**, *20*, 517-521.

(48) Burke, M.D.; Park, J.O.; Srinivasarao, M.; Khan, S.A., A Novel Enzymatic Technique for Limiting Drug Mobility in a Hydrogel Matrix. *J. Controlled Release* **2005**, *104*, 141-153.

(49) Lin, C-C.; Anseth, K.S., PEG Hydrogels for the Controlled Release of Biomolecules in Regenerative Medicine. *Pharm. Res.* **2009**, *26*, 631-643.

(50) Zisch, A.H.; Lutolf, M.P.; Ehrbar, M.; Raeber, G.P.; Rizzi, S.C.; Davies, N.; Schmokel, H.; Bezuidenhout, D.; Djonov, V.; Zilla, P.; Hubbell, J.A., Cell-Demanded Release of VEGF from Synthetic, Biointeractive Cell Ingrowth Matrices for Vascularized Tissue Growth. *FASEB J.* **2003**, *17*, 2260-2262.

(51) Serruys, P.W.; Kutryk, M.J.B.; Ong, A.T.L., Coronary-Artery Stents. *N. Engl. J. Med.* **2006**, *354*, 483-495.

(52) Slaughter, B.V.; Khurshid, S.S.; Fisher, O.Z.; Khademhosseini, A.; Peppas, N.A., Hydrogels in Regenerative Medicine. *Adv. Mater.* **2009**, *21*, 3307-3329.

(53) Glowacki, J.; Mizuno, S., Collagen Scaffolds for Tissue Engineering. *Biopolymers* **2007**, *89*, 338-344.

(54) Kleinman, H.K.; Martin, G.R., Matrigel: Basement Membrane Matrix with Biological Activity. *Semin. Cancer Biol.* **2005**, *15*, 378-386.

(55) Gobin, A.S.; West, J.L., Cell Migration through Defined, Synthetic ECM Analogs. *FASEB J.* **2002**, *16*, 751-753.

(56) Lee, S-H.; Moon, J.J.; West, J.L., Three-Dimensional Micropatterning of Bioactive Hydrogels via Two-Photon Laser Scanning Photolithography for Guided 3D Cell Migration. *Biomaterials* **2008**, *29*, 2962-2968.

(57) Mehta, M.; Schmidt-Bleek, K.; Duda, G.N.; Mooney, D.J., Biomaterial Delivery of Morphogens to Mimic the Natural Healing Cascade of Bone. *Adv. Drug Delivery Rev.* **2012**, *64*, 1257-1276.

(58) Lutolf, M.P.; Lauer-Fields, J.L.; Schmoekel, H.G.; Metters, A.T.; Weber, F.E.; Fields, G.B.; Hubbell, J.A., Synthetic Matrix Metalloproteinase-Sensitive Hydrogels for the Conduction of Tissue Regeneration: Engineering Cell-Invasion Characteristics. *Proc. Natl. Acad. Sci.* **2003**, *100*, 5413-5418.

(59) Lau, H.K.; Kiick, K.L., Opportunities for Multicomponent Hybrid Hydrogels in Biomedical Applications. *Biomacromolecules* **2015**, *16*, 28-42.

(60) Burdick, J.A.; Murphy, W.L., Moving from Static to Dynamic Complexity in Hydrogel Design. *Nat. Commun.* **2012** DOI:10.1038/ncomms2271.

(61) Eng, G.; Lee, B.W.; Parsa, H.; Cin, C.D.; Schneider, J.; Linkov, G.; Sia, S.K.; Vunjak-Novakovic, G., Assembly of Complex Cell Microenvironments using Geometrically Docked Hydrogel Shapes. *Proc. Natl. Acad. Sci.* **2013**, *110*, 4551-4556.

(62) Saunders, B.R.; Vincent, B., Microgel Particles as Model Colloids: Theory, Properties and Applications. *Adv. Colloid Inter. Sci.* **1999**, *80*, 1-25.

(63) Nayak, S.; Lyon, L.A., Soft Nanotechnology with Soft Nanoparticles. *Angew. Chem. Int. Ed.* **2005**, *44*, 7686-7708.

(64) Eydelnant, I.A.; Li, B.B.; Wheeler, A.R., Micogels on Demand. *Nat. Commun.* DOI: 10.1038/ncomms4355.

(65) Helgeson, M.E.; Chapin, S.C.; Doyle, P.S., Hydrogel Microparticles from Lithographic Processes: Novel Materials for Fundamental and Applied Colloid Science. *Curr. Op. Colloid Inter. Sci.* **2011**, *16*, 106-117.

(66) Lyon, L.A.; Fernandez-Nieves, A., The Polymer/Colloid Duality of Microgel Suspensions. *Annu. Rev. Phys. Chem.* **2012**, *63*, 25-43.

(67) Saxena, S.; Hansen, C.E.; Lyon, L.A., Microgel Mechanics in Biomaterial Design. *Acc. Chem. Res.* **2014**, *47*, 2426-2434.

(68) Hendrickson, G.R.; Lyon, L.A., Microgel Translocation through Pores Under Confinement. *Angew. Chem. Int. Ed.* **2010**, *49*, 1697-1712.

(69) Merkel, T.J.; Jones, S.W.; Herlihy, K.P.; Kersey, F.R.; Shields, A.R.; Napier, M.; Luft, J.C.; Wu, H.; Zamboni, W.C.; Wang, A.Z.; Bear, J.E.; DeSimone, J.M., Using Mechanobiological Mimicry of Red Blood Cells to Extend Circulation Times of Hydrogel Microparticles. *Proc. Natl. Acad. Sci.* **2011**, *108*, 586-591.

(70) Lynch, I.; Dawson, K.A., Synthesis and Characterization of an Extremely Versatile Structural Motif Called the "Plum-Pudding" Gel. *J. Phys. Chem B* **2003**, *107*, 9629-9637.

(71) Nayak, S.; Debord, S.B.; Lyon, L.A., Investigations into the Deswelling Dynamics and Thermodynamics of Thermoresponsive Microgel Composite Films. *Langmuir* **2003**, *19*, 7374-7379.

(72) Xia, L-W.; Xie, R.; Ju, X-J.; Wang, W.; Chen, Q.; Chu, L-Y., Nano-Structured Smart Hydrogels with Rapid Response and High Elasticity. *Nat. Commun.* **2013,** DOI: 10.1038/ncomms3226.

(73) Lynch, I.; de Gregorio, P.; Dawson, K.A., Simultaneous Release of Hydrophobic and Cationic Solutes from Thin-Film "Plum-Pudding" Gels: A Multifunctional Platform for Surface Drug Delivery? *J. Phys. Chem. B* **2005**, *109*, 6257-6261.

(74) Meid, J.; Dierkes, F.; Cui, J.; Messing, R.; Crosby, A.J.; Schmidt, A.; Richtering, W., Mechanical Properties of Temperature Sensitive Microgel/Polyacrylamide Composite Hydrogels–from Soft to Hard Fillers. *Soft Matter* **2012**, *8*, 4254-4263.

(75) Milani, A.H.; Freemont, A.J.; Hoyland, J.A.; Adlam, D.J.; Saunders, B.R., Injectable Doubly Cross-Linked Microgels for Improving the Mechanical Properties of Degenerated Intervertebral Discs. *Biomacromolecules* **2012**, *13*, 2793-2801.

(76) Hendrickson, G.R.; Smith, M.H.; South, A.B.; Lyon, LA., Design of Multiresponsive Hydrogel Particles and Assemblies. *Adv, Funct. Mater.* **2010**, *20*, 1697-1712.

(77) Kim, J.; Singh, N.; Lyon, L.A., Label-Free Biosensing with Hydrogel Microlenses. *Angew. Chem. Int. Ed.* **2006**, *45*, 1446-1449.

(78) South, A.B.; Whitmire, R.E.; Garcia, A.J.; Lyon, L.A., Centrifugal Deposition of Microgels for the Rapid Assembly of Nonfouling Thin Films. *ACS Appl. Mater. Interface Sci.* **2009**, *1*, 2747-2754.

(79) Gaulding, J.C.; Saxena, S.; Montanari, D.E.; Lyon, L.A., Packed Colloidal Phases Mediate the Synthesis of Raspberry-Structured Microgel Heteroaggregates. *ACS Macro Lett.* **2013**, *2*, 337-340.

(80) Dai, X.; Yang, W.; Firlar, E.; Marras, S.A.E.; Libera, M., Surface-Patterned Microgel-Tethered Molecular Beacons. *Soft Matter* **2012**, *8*, 3067-3076.

(81) Christman, K.L.; Schopf, E.; Broyer, R.M.; Li, R.C.; Chen, Y.; Maynard, H.D., Positioning Multiple Proteins at the Nanoscale with Electron Beam Cross-Linked Functional Polymers. *J. Am. Chem. Soc.* **2009**, *131*, 521-527.

(82) Gao, Y.; Xu, W.; Serpe, M.J., Free-Standing Poly(*N*-Isopropylacrylamide) Microgel-Based Etalons. *J. Mater. Chem. C* **2014**, *2,* 5878-5884.

(83) Zhang, L.; Spears, Jr., M.W.; Lyon, L.A., Tunable Swelling and Rolling of Microgel Membranes. *Langmuir* **2014**, *30*, 7628-7634.

(84) Groschel, A.H.; Walther, A.; Lobling, T.I.; Schacher, F.H.; Schmalz, H.; Muller, A.H.E., Guided Hierarchical Co-Assembly of Soft Patchy Nanoparticles. *Nature* **2013**, *503*, 247-251.

(85) Go D.; Kodger, T.E.; Sprakel, J.; Kuehne, A.J.C., Programmable Co-Assembly of Oppositely Charged Microgels. *Soft Matter* **2014**, *10*, 8060-8065.

(86) Smith, M.H.; Lyon, L.A., Multifunctional Nanogels for siRNA Delivery. *Acc. Chem. Res.* **2012**, *45*, 985-993.

(87) Pelton, R., Temperature-Sensitive Aqueous Microgels. *Adv. Colloid Inter. Sci.* **2000**, *85*, 1-33.

(88) Gao, J.; Frisken, B.J., Cross-Linker-Free *N*-Isopropylacrylamide Gel Nanospheres. *Langmuir* **2003**, *19*, 5212-5216.

(89) Bachman, H.; Brown, A.C; Clarke, K.C.; Dhaha, K.S.; Douglas, A.M.; Hansen, C.E.; Herman, E.S; Hyatt, J.; Kodlekere, P.; Saxena, S.; Spears, Jr. M.W.; Welsch, N.; Lyon, L.A., Ultrasoft, Highly Deformable Microgels. *Soft Matter* **2015**, *11*, 2018-2028.

(90) Jones, C.D.; Lyon, L.A., Synthesis and Characterization of Multiresponsive Core-Shell Microgels. *Macromolecules* **2000**, *33*, 8301-8306.

(91) Smith, M.H.; South, A.B.; Gaulding, J.C.; Lyon, L.A., Monitoring the Erosion of Hydrolytically-Degradable Nanogels via Multiangle Light Scattering Couples to Asymmetric Flow Field-Flow Fractionation. *Anal. Chem.* **2010**, *82*, 523-530.

(92) Hu, X.; Tong, Z.; Lyon, L.A., Multicompartment Core/Shell Microgels. *J. Am. Chem. Soc.* **2010**, *132*, 11470-11472.

(93) Hoare, T.; Pelton, R., Titrametric Characterization of pH-Induced Phase Transitions in Functionalized Microgels. *Langmuir* **2006**, *22*, 7342-7350.

(94) Meng, Z.; Hendrickson, G.R.; Lyon, L.A., Simultaneous Orthogonal Chemoligations on Multiresponsive Microgels. *Macromolecules* **2009**, *42*, 7664-7669.

(95) Singh, N.; Lyon, L.A., Synthesis of Multifunctional Nanogels using a Protected Macromonomer Approach. *Colloid Polym. Sci.* **2008**, *286*, 1061-1069.

(96) Farley, R.; Saunders, B.R., A General Method for Functionalization of Microgel Particles with Primary Amines using Click Chemistry. *Polymer* **2014**, *55*, 471-480.

(97) Li, Y.; Tanaka, T., Kinetics of Swelling and Shrinking of Gels. *J. Chem. Phys.* **1990**, *92*, 1365-1371.

(98) Tanaka, T.; Fillmore, D.J., Kinetics of Swelling of Gels. *J. Chem. Phys.* **1979**, *70*, 1214-1218.

CHAPTER 2

SURFACE MODIFICATION OF SUBSTRATES

2.1 Surface Assemblies and Coatings

Generally speaking films exist to impart one or more new functions to the surface of a material, while maintaining the desired intrinsic properties of the base material. Films can be simple, where their role is to control the surface energy.[1] A common example is the use of coatings to alter the surface wettability.[2,3] Other films are more complex and have more active roles, like the drug eluting coatings applied to stents discussed in **Chapter 1**.[4] Even more complex films exist, such as environmentally responsive films or assemblies with architectural complexity. Films can also be thought of as a way to broaden the applicability of the base material because each film can be tailored for the intended environment. Therefore, it would be ideal to develop coatings and deposition techniques that are as versatile as possible, especially in regard to film components and substrates. Below, several film preparation methods are described, and pictorially represented in **Scheme 2.1**. Films can be prepared from small molecule components or larger macromolecular structures, permitting surface modification with wide variety of building blocks.

Molecular films have been typically formed through two main techniques, Langmuir-Blodgett (LB) deposition and self-assembled monolayers (SAMs). LB films were originally described in the 1930's, and utilize the assembly of amphiphilic molecules at an air-water interface.[5,6] Immersion of substrates through the molecular layer transfers the molecules onto the substrate with a defined thickness. There are several drawbacks to the LB technique, such as limitations in the type of material deposited (must organize at liquid/air interface), the size and contours of substrates, film instability, and the need for special equipment. In addition, the ability to build up films

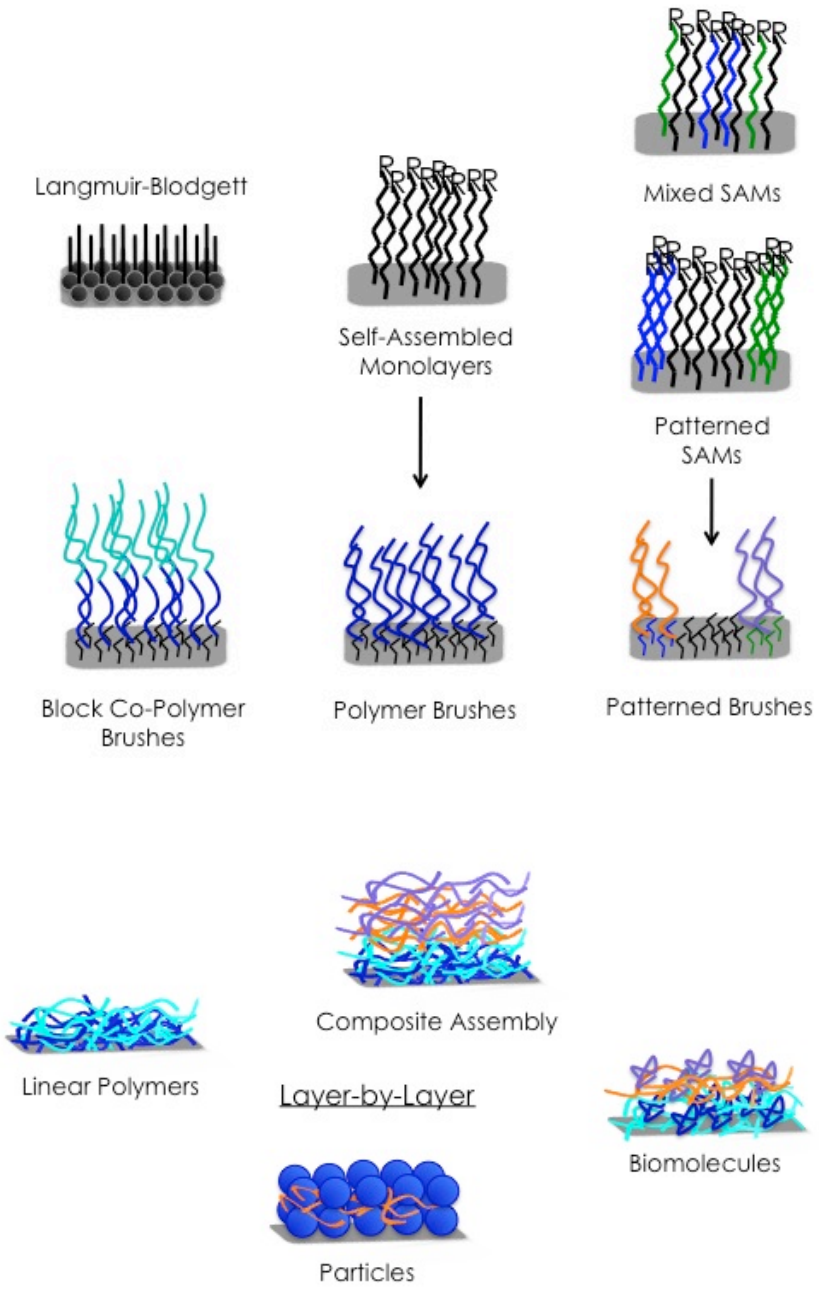

Scheme 2.1. Examples of Film Deposition Techniques and Types of Assemblies

with structural and architectural complexity is limited. SAMs on the other hand permit greater versatility.

SAMs are formed from the spontaneous arrangement of molecules on substrates.[7] Alkanethiols on gold surfaces have been extensively explored as SAMs in numerous applications. Specific interactions between the SAM molecule head group (e.g. thiol) and the substrate (e.g. gold) facilitate adhesion to the surface; for alkanthiols a gold-sulfur bond is formed. Assembly can be accomplished by simply immersing the substrate in a solution of the assembling molecule. SAMs have been assembled with a variety of terminal functional groups, which can be used in post-assembly conjugation reactions.[8] In particular, the modification of SAMs with biomolecules has been used to study the binding of ligands and receptors.[9] SAM deposition has also been expanded to nanoparticle substrates.[10] For example, the surfaces of gold nanoparticles have been modified with a variety of thiol-terminated molecules, including alkane chains and polymers. This has aided in the employment of gold nanoparticles for biological and *in vivo* applications.[11]

Surface patterning techniques, such as soft lithography and scanning probe lithography, have been utilized to spatially arrange functional SAMs on interfaces.[12-14] These high-throughput methods allow the precise localization of molecules on surfaces at the nanoscale. One avenue to explore is the fabrication of protein or nucleic acid arrays for "on chip" screening and diagnostic applications.[15] These surfaces have also been utilized for the presentation of ligands to study cell behavior, where the type, concentration, and spacing of ligands can be independently controlled.[16] The controlled deposition of SAMs has also been used in the fabrication of nano-electronic devices. The metal surface is selectively etched where the SAM has not been patterned, resulting in small metal features of defined shape and dimension.[17]

Switchable interfaces have been developed with SAMs.[18] For example, electric potential has been used to control surface wettability by changing the orientation of an

alkanethiol SAM with a hydrophilic head group.[19] Positive potentials drive the carboxylic acid group to the surface, the bent molecule now presents the hydrophobic alkyl chain at the interface, and a hydrophobic surface results. Negative potentials reverse the orientation, returning the hydrophilic group to the surface, rendering the interface hydrophilic. Electric potential has also been used to release peptides and cells from a SAM interface *via* the electrochemical reduction of an oxime bond.[20] Photopatterning was used in combination to selectively conjugate the integrin-binding peptide RGD to the monolayer through an oxime linkage. Cells selectively adhered to this patterned region, but released from the surface upon reduction of the oxime bond and removal of the peptide. Following release of the peptide, the surface was essentially regenerated with functional groups for more oxime conjugation reactions.

Molecular films, especially those based on SAMs, have been applied in numerous fundamental, technological, and biological applications. Their broad utility stems from the ability to precisely control surface properties in a straightforward manner. Beyond films prepared from the assembly of molecular monolayers, we can also consider the fabrication of polymeric films. Polymers are diverse in chemical functionality, are more mechanically robust than molecular films, and can be prepared in a variety of architectures.

The defined deposition of SAMs has been utilized in the preparation of polymeric brushes.[21,22] A variety of controlled polymerization techniques (e.g. atom transfer radical polymerization (ATRP), reverse fragment transfer polymerization (RAFT), and ring opening metathesis polymerization (ROMP)) have been employed to grow polymer chains off of surfaces; a process known as "grafting from." Substrates are modified with SAMs where the molecules are terminated with an initiator. Controlled polymer growth from the surface is achieved by submerging the film in a solution of monomer and catalyst. Importantly, the polymerization remains confined to the surface. Numerous brush architectures have been described, including block co-polymers, gradient,

branched, and Y-shaped.[22] An alternative method to brush preparation involves first the controlled polymerization of polymers, and, second, their attachment directly to the substrate. This is known as "grafting to." The "grafting from" technique typically allows for higher densities of polymer chains, as well as greater control over the polymer length and, therefore, film thickness. Both planar and colloidal substrates have been modified with polymer brushes, exemplifying the versatility of their use.[23,24]

Films prepared from brush polymers have been used extensively as bio-interfaces.[24] Applications include non-fouling, controlled cell adhesion, and biocidal coatings. Non-fouling coatings have been prepared from poly(ethylene glycol)[25] and hydroxyethylmethacrylate,[26] as well as zwitterionic species.[27] The polymeric chains provide a hydrophilic surface, which helps prevent the adsorption of proteins and adhesion of cells. Cell adhesion can be controlled through the modification of polymer brushes with integrin binding peptides or other extracellular matrix components.[28] Surface patterning of the initiator species controls the location of polymer growth, permitting spatial control over cell adhesion on the interface. Biocidal polymer coatings are typically composed of polymers with a high density of positive charge, such as polymers with quaternary ammonium groups.[29] A combination of non-fouling and biocidal polymer brushes could also be employed, resulting in even greater control over the surface properties.

Polymer brushes have also been useful in the development of stimuli-responsive interfaces.[30] As described in **Chapter 1**, stimuli-responsive polymers translate a specific environmental cue into a change in the polymer-solvent and polymer-polymer interactions. Recall, the temperature-responsive polymer, poly(*N*-isopropylacrylamide) (pNIPAm). PNIPAm transitions from a random coil at low temperatures to a condensed globule above 31 °C. Polymer-polymer interactions are favored at this higher temperature, and polymer-solvent (i.e. water) interactions are at a minimum. When attached to a substrate, pNIPAm chains transition from an extended, hydrated state to a

collapsed, dehydrated state. Because of the switchable surface properties, pNIPAm brushes have been considered for several applications. One specific use of pNIPAm brush layers is for cell-sheet engineering.[31] Cells are cultured on pNIPAm surfaces at a temperature above 31 °C, where the polymer chains are collapsed and the surface is considered to be more hydrophobic. Cells are release from the surface simply by decreasing the environmental temperature below 31 °C resulting in a more hydrophilic interface upon hydration. In this way, cell sheets can be gently removed from the culture substrate circumventing the need for protease treatment. Thermoresponsive brush layers have also been used to control the presentation of RGD from the surface. This is another example of how temperature can be used to control the adhesion of cells to the surface.[32,33]

Controlled polymerization strategies are useful in preparing block co-polymers, where chemically different polymers are connected on the same chain. The synthesis of responsive brush co-polymers permits the fabrication of interfaces where multiple stimuli can be used to tailor the surface properties. This is an extremely useful tactic for the controlled release of therapeutics from films. Zhao and coworkers demonstrate this strategy by preparing multi-responsive films from block co-polymers where temperature, light, and pH were used to control the release of dye molecules.[34] A variety of other responsive brush systems have been explored, including brush gradients and mixed composition films.[30]

The applications of polymer brush architectures described above highlight many of their advantages, including the broad spectrum of chemical functionalities, the potential to post-synthetically add biologically functional elements, and the ability to spatially define their build-up. However, the synthesis of polymer chains from or their attachment to surfaces represents only one type of polymeric film fabrication method. Layer-by-layer (LbL) assembly is an alternative film fabrication technique, which has

expanded the number and type of building blocks that can be used in the preparation of coatings.

An early study of LbL by Iler in 1966, demonstrated the deposition of hard, inorganic cationic (alumina) and anionic (silica) particles.[35] However, LbL rose in popularity when it was introduced as a facile method to prepare polymeric films. Decher and colleagues demonstrated the simplicity of LbL deposition of linear polymers, where linear polyions of opposite charge are sequentially deposited onto a substrate.[36] Charge reversal following each deposition cycle results in self-limiting film growth, permitting the controlled deposition of thin polymeric films of defined thickness.

Perhaps one of the greatest advantages of the LbL technique is substrate versatility. Because of the nature of film build-up, LbL is widely considered to be tolerant of defects both in the substrate and also those that occur throughout the deposition cycles.[37] Deposition of film components is accomplished through dip coating, spin coating, spraying, and mixing.[36,38] Because the coating process takes place in liquid, substrates with varying topological features and curvatures are amenable to the LbL process. For example, LbL assembly can be directed to the surface of colloidal particles. Moreover, the stability of the LbL layers permits core dissolution, resulting in hollow capsules.[39] These capsules have been extensively explored as drug delivery vehicles because of the ability to load a variety of different payloads, and the thickness of the LbL film can be used to tune release rates of encapsulated cargo.[40]

A multitude of linear polyions has been explored as components in the build-up of LbL films. Perhaps two of the most common polycations are poly(allylamine hydrochloride) and poly(diallyldimethylammonium chloride), PAH and PDADMAC, respectively. Two common polyanions are poly(sodium 4-styrenesulfonate) and poly(acrylic acid), PSS and PAAc, respectively (**Figure 2.1**). PAH and PAA are pH

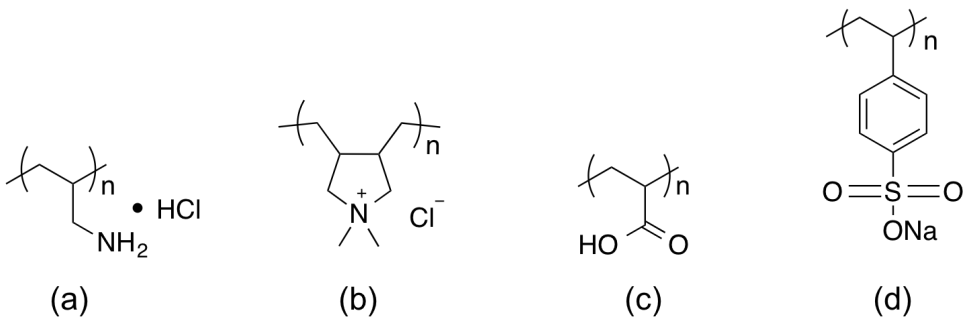

Figure 2.1. Structures of (a) PAH, (b) PDADMAC, (c) PAAc, and (d) PSS.

sensitive polyions, in that the number of charges along the polymer changes depending on the pH environment. In contrast, the charge of the repeat units in PDADMAC and PSS are not as affected by the pH. Interestingly, LbL films composed of polyelectrolytes like PAH and PAA can be prone to film dissolution depending on the pH environment.[41,42] While this may seem counterproductive, it has been utilized in controlled release applications. For instance, biomacromolecules (e.g. proteins, DNA) have been used as building blocks in LbL assembly.[43] Proteins often have charged amino acid residues, which facilitate incorporation, while the backbone of nucleic acids is negatively charged. Hammond and co-workers have demonstrated the controlled release of ovalbumin from LbL films based on the controlled dissolution of the polymer layers as a result of the pH environment.[44] It is also worth noting that by co-assembling functionally different components it is possible to tune the release rate from the films, and also incorporate multiple therapeutics within a single construct.[45,46] This illustrates the modular nature of the LbL assembly process.

Over the years, LbL deposition has expanded beyond electrostatic interactions to include hydrogen bonding and hydrophobic interactions.[47] In addition, covalent LbL films have been pursued for their enhanced stability.[48,49] Importantly, these additional assembly mechanisms have permitted an even greater range of building blocks to be used in thin film fabrication.

LbL assembly has extended the list of possible building blocks to include colloidal particles.[50,51] In this way, many of the advantageous properties of colloidal particles can be brought to the surface of materials. For example, there has been considerable work in the fabrication of block co-polymer micelle LbL films.[52-55] An advantage to using micelles is the ability to encapsulate hydrophobic molecules within the micelle interior for delivery applications. This is a challenging task when working in an aqueous environment, which is common in the preparation of LbL films. The inclusion of degradable particles into LbL films for release applications has also been demonstrated.[56] It should be possible to tune the release rate from the film by controlling the location of the particles within the depth of the film.

An interesting advance is the use of lithographic techniques to pattern LbL assemblies. Utilizing lithographic processes, LbL films can be fabricated with control over the geometric location on a surface. LbL film patterning has been demonstrated with all particle films where traditional photoresist and etching techniques were employed.[51] Another example utilized a photo-initiated crosslinking reaction to locally crosslink an LbL film. Un-crosslinked regions of the film were easily removed by ultrasonication in a surfactant solution.[49] Patterning of LbL films has also been employed to fabricate defined, tailored, cell-adhesive domains to probe the responses of neurons.[57] Because LbL films are assembled one layer at a time, the 3-dimensional location of film components can be more easily controlled. Coupling this with the spatial resolution of lithography is a powerful strategy to precisely control in all dimensions the placement of film components.

Beyond pH-induced film disassembly (described above), additional forms of stimuli-responsivity have been built into LbL assemblies either through the deposition of linear responsive polymers or responsive particles.[58] For example, temperature-responsive LbL films have been prepared from pNIPAm and PAAc polymers assembled *via* hydrogen bonding.[59] The incorporation of stimuli-responsive micelles into an LbL

construct was used for controlled release of encapsulated molecules. A PNIPAm micelle core, when collapsed at 37 °C, impeded the release of the molecule, but decreasing the temperature to 20 °C increased the release rate.[60] Furthermore, light has been used to initiate release from an LbL film through the incorporation of gold nanoparticle/DNA aggregates. Irradiation of the gold nanoparticles resulted in photothermal heating, disrupting the polyelectrolyte LbL film, and releasing encapsulated DNA.[61]

The Lyon group has been particularly interested in the assembly and study of thermoresponsive microgel-based LbL thin films. The incorporation of charged co-monomers into microgel networks facilitates their use as a colloidal polyelectrolyte.[62] Our group has worked primarily with p(NIPAm-co-AAc) microgels, where the microgel is the polyanion, and a linear polycation is employed to build-up microgel layers. PDADMAC, PAH, poly(ethyleneimine), and poly(L-lysine) (PEI, and PLL, respectively) have all been used in film fabrication.[63-65] Films can also be prepared using only microgels by synthesizing polycation particles with an amine co-monomer.[66] Microgels have been deposited onto planar substrates passively *via* diffusion, or actively by spin coating and centrifugal deposition.[62,63,67] Microgel layer deposition by centrifugation was found to yield well-packed microgel films in rapid fashion, and is the current method used within the group.

Initial investigations of thermoresponsive microgel films evaluated their potential as drug delivery coatings.[68,69] Thermal cycling was used to drive imbibed molecules (e.g. doxorubicin and insulin) out of the film network. Microgel films have also been assembled on biomaterial substrates as non-fouling coatings.[63] There is potential to fabricate composite assemblies of microgels where a subset of particles reduce fouling and other particles release therapeutics to the surrounding environment. This two-pronged approach could therefore enhance the integration of materials in biological environments.

Additional experiments with microgel LbL films demonstrated that, when prepared on compliant substrates, such as polydimethylsiloxane, the films have the capacity to self-heal upon hydration following substrate deformation events.[70,71] This has been attributed to the inherent mobility of the film components. Covalent crosslinking of the polycation network or the polycation to the particles abolishes self-healing. The capacity to control mobility has been used to alter the adhesion and spreading of fibroblasts on microgel interfaces.[64]

Although this work has demonstrated the utility of microgel films, the majority of films prepared and studied in the Lyon group thus far contained only one particle type. One of the goals of the research described herein is to prepare and utilize multiple types of microgels in the fabrication of composite microgel films. A key objective is to make these constructs more versatile by understanding the behavior of multiresponsive microgel coatings. **Chapters 3 and 4** will focus on the employment of multiple microgel building blocks to control the temperature-responsivities of thermoresponsive microgel films. The impact of the pH environment on film responsivity will also be examined in **Chapter 4**. **Chapter 5** will instead focus on the microgel building block. We will consider the modification of microgel surfaces, and explore a new route to adding functionality to the microgel surface. In doing so it may be possible to develop new microgel building blocks, growing the existing toolbox and applicability. Moving forward, it is thought that the studies presented here will provide insight into the development of structurally complex materials built from simple components.

2.2 References

(1) Ryu, D.Y.; Shin, K.; Drockenmuller, E.; Hawker, C.J.; Russell, T.P., A Generalized Approach to the Modification of Solid Surfaces. *Science* **2005**, *308*, 236-239.

(2) Russell, T.P., Surface-Responsive Materials. *Science* **2002**, *297*, 964-967.

(3) Thanawala, S.K.; Chaudhury, M.K., Surface Modification of Silicone Elastomer Using Perfluorinated Ether. *Langmuir* **2000,** *16,* 1256-1260.

(4) Serruys, P.W.; Kutryk, M.J.B.; Ong, A.T.L., Coronary-Artery Stents. *N. Engl. J. Med.* **2006**, *354*, 483-495.

(5) Zasadzinski, J.A.; Viswanathan, R.; Madsen, L.; Garnaes, J.; Schwartz, D.K., Langmuir-Blodgett Films. *Science* **1994,** *263,* 1726-1733.

(6) Seufert, M.; Schaub, M.; Wenz, G.; Wegner, G., Topochemical Aspects of the Formation of Networks in Layered Langmuir-Blodgett (LB) Assemblies. *Angew. Chem. Int. Ed.* **1995**, *34*, 340-343.

(7) Ulman, A., Formation and Structure of Self-Assembled Monolayers. *Chem. Rev.* **1996,** *96,* 1533-1554.

(8) Claridge, S.A.; Liao, W-S.; Thomas, J.C.; Zhao, Y.; Cao, H.H.; Cheunkar, S.; Serino, A.C.; Andrews, A.M.; Weiss, P.S., From the Bottom Up: Dimensional Control and Characterization in Molecular Monolayers. *Chem. Soc. Rev.* **2013,** *42,* 2725-2745.

(9) Shuster, M.J.; Vaish, A.; Szapacs, M.E.; Anderson, M.E.; Weiss, P.S.; Andrews, A.M., Biospecific Recognition of Tethered Small Molecules Diluted in Self-Assembled Monolayers. A*dv. Mater.* **2008,** *20,* 164-167.

(10) Love, J.C.; Estroff, L.A.; Kriebel, J.K.; Nuzzo, R.G.; Whitesides, G.M., Self-Assembled Monolayers of Thiolates on Metals as a Form of Nanotechnology. *Chem. Rev.* **2005,** *105,* 1103-1169.

(11) Huang, X.; Neretina, S.; El-Sayed, M.A., Gold Nanorods: From Synthesis and Properties to Biological and Biomedical Applications. *Adv. Mater.* **2009,** *21,* 4880-4910.

(12) Liao, W-S.; Cheunkar, S.; Cao, H.H.; Bednar, H.R.; Weiss, P.S.; Andrews, A.M., Subtractive Patterning via Chemical Lift-Off Lithography. *Science* **2012,** *337,* 1517-1521.

(13) Shuster, M.J.; Vaish, A.; Cao, H.H.; Guttentag, A.I.; McManigle, J.E.; Gibb, A.L.; Martinez, M.M.; Nezarati, R.M.; Hinds, J.M.; Liao, W-S.; Andrews, A.M., Patterning Small-Molecule Biocapture Surfaces: Microcontact Insertion Printing vs. Photolithography. *Chem. Commun.* **2011,** *47,* 10641-10643.

(14) Salaita, K.; Wang, Y.; Mirkin, C.A., Applications of Dip-Pen Nanolithography. *Nature Nanotech.* **2007,** *2,* 145-155.

(15) Zheng, Z.; Daniel, W.L.; Giam, L.R.; Huo, F.; Senesi, A.J.; Zheng, G.; Mirkin, C.A., Multiplexed Protein Arrays Enabled by Polymer Pen Lithography: Addressing the Inking Challenge. *Angew. Chem. Int. Ed.* **2009,** *48,* 7626-7629.

(16) Chen, C.S.; Mrksich, M.; Huang, S.; Whitesides, G.M.; Ingber, D.E., Geometric Control of Cell Life and Death. *Science* **1997,** *276,* 1425-1428.

(17) Salaita, K.; Wang, Y.; Fragala, J.; Vega, R.A.; Liu, C.; Mirkin, C.A., Massively Paralleled Dip-Pen Nanolithography with 55000-Pen Two-Dimensional Arrays. *Angew. Chem. Int. Ed.* **2006,** *45,* 7220-7223.

(18) Nandivada, H.; Ross, A.M.; Lahann, J., Stimuli-Responsive Monolayers for Biotechnology. *Prog. Polym. Sci.* **2010,** *35,* 141-154.

(19) Lahann, J.; Mitragotri, S.; Tran, T-N.; Kaido, H.; Sundaram, J.; Choi, I.S.; Hoffer, S.; Somorjai, G.A.; Langer, R., A Reversibly Switching Surface. *Science* **2003,** *299,* 371-374.

(20) Chan, E.W.L.; Park, S.; Yousaf, M.N., An Electrochemical Catalytic Dynamic Substrate that Immobilizes and Releases Patterned Ligands, Proteins, and Cells. *Angew. Chem. Int. Ed.* **2008,** *47,* 6267-6271.

(21) Edmondson, S.; Osborne, V.L.; Huck, W.T.S., Polymer Brushes via Surface-Initiated Polymerizations. *Chem. Soc. Rev.* **2004,** *33.* 14-22.

(22) Barbey, R.; Lavanant, L.; Paripovic, D.; Schuwer, N.; Sugnaux, C.; Tugulu, S.; Klok, H-A., Polymer Brushes via Surface-Initiated Controlled Radical Polymerization: Synthesis, Characterization, Properties, and Applications. *Chem. Rev.* **2009,** *109,* 5437-5527.

(23) Goh, T.K.; Guntari, S.N.; Ochs, C.J.; Blencowe, A.; Mertz, D.; Connal, L.A.; Such, G.K.; Qiao, G.G.; Caruso, F., Nanoengineered Films via Surface-Confined Continuous Assembly of Polymers. *Small* **2011,** *7,* 2863-2867.

(24) Guntari, S.N.; Wong, E.H.H.; Goh, T.K.; Chandrawati, R.; Blencowe, A.; Caruso, F.; Qiao, G.G., Low-Fouling, Biospecific Films Prepared by the Continuous Assembly of Polymers. *Biomacromolecules* **2013,** *14,* 2477-2483.

(25) Ma, H.; Wells, M.; Beebe Jr., T.P.; Chilkoti, A., Surface-Initiated Atom Transfer Radical Polymerization of Oligo(Ethylene Glycol) Methyl Methacrylate from a Mixed Self-Assembled Monolayer on Gold. *Adv. Funct. Mater.* **2006,** *16,* 640-648.

(26) Mei, Y.; Wu, T.; Xu, C.; Langenbach, K.J.; Elliott, J.T.; Vogt, B.D.; Beers, K.L.; Amis, E.J.; Washburn, N.R., Tuning Cell Adhesion on Gradient Poly(2-Hydroxyethylmethacrylate)-Grafted Surfaces. *Langmuir* **2005,** *21,* 12309-12314.

(27) Feng, W.; Brash, J.L.; Zu, S., Non-Biofouling Materials Prepared by Atom Transfer Radical Polymerization Grafting of 2-Methacryloloxyethyl Phosphorylcholine: Separate Effects of Graft Density and Chain Length on Protein Repulsion. *Biomaterials* **2006,** *27*, 847-855.

(28) Raynor, J.E.; Capadona, J.R.; Collard, D.M.; Petrie, T.A.; Garcia, A.J., Polymer Brushes and Self-Assembled Monolayers: Versatile Platforms to Control Cell Adhesion to Biomaterials. *Biointerphases* **2009**, *4*, FA3-FA16.

(29) Murata, H.; Koepsel, R.R.; Matyjaszewski, K.; Russell, A.J., Permanent, Non-Leaching Antibacterial Surfaces-2: How High Density Cationic Surfaces Kill Baterial Cells. *Biomaterials* **2007,** *28,* 4870-4879.

(30) Luzinov, I.; Minko, S.; Tsukruk, V.V., Responsive Brush Layers: From Tailored Gradients to Reversibly Assembled Nanoparticles. *Soft Matter* **2008,** *4*, 714-725.

(31) Cooperstein, M.A.; Canavan, H.E., Biological Cell Detachment from Poly(*N*-Isopropyl acrylamide) and Its Applications. *Langmuir* **2010,** *26*, 7695-7707.

(32) Ebara, M.; Yamato, M.; Aoyagi, T.; Kikichi, A.; Sakai, K.; Okano, T., Temperature-Responsive Cell Culture Surface Enable "On-Off" Affinity Control between Cell Integrins and RGDS Ligands. *Biomacromolecules* **2004**, 505-510.

(33) Desseaux, S.; Klok, H-A., Temperature-Controlled Masking/Unmasking of Cell-Adhesive Cues with Poly(Ethylene Glycol) Methacrylate Based Brushes. *Biomacromolecules* **2014,** *15,* 3859-3865.

(34) Kumar, S.; Dory, Y.L.; Lepage, M.; Zhao, Y., Surface-Grafted Stimuli-Responsive Block Copolymer Brushed for the Thermo-, Photo-, and pH-Sensitive Release of Dye Molecules. *Macromolecules* **2011,** *44,* 7385-7393.

(35) Iler, R.K., Multilayers of Colloidal Particles. *J. Colloid Inter. Sci.* **1966,** *21,* 569-594.

(36) Decher, G., Fuzzy Nanoassemblies: Toward Layered Polymeric Multicomposites. *Science* **1997**, *277*, 1232-1237.

(37) Ultrathin Polymer Coatings by Complexation of Polyelectrolytes at Interfaces: Suitable Materials, Structure and Properties. *Macromol. Rapid Commun.* **2000,** *21*, 319-348.

(38) Izquierdo, A.; Ono, S.S.; Voegel, J-C.; Scaaf, P.; Decher, G., Dipping Versus Spraying: Exploring the Deposition Conditions for Speeding Up Layer-by-Layer Assembly. *Langmuir* **2005,** *21,* 7558-7567.

(39) Sukhorukov, G.B.; Volodkin, D.V.; Gunther, A.M.; Petrov, A.I.; Shenoy, D.B.; Mohwald, H., Porous Calcium Carbonate Microparticles as Templates for Encapsulation of Bioactive Compounds. *J. Mater. Chem.* **2004,** *14,* 2073-2081.

(40) Becker, A.L.; Johnston, A.P.R.; Caruso, F., Layer-by-Layer-Assembled Capsules and Films for Therapeutic Delivery. *Small*, **2010,** *6,* 1836-1852.

(41) Shiratori, S.S.; Rubner, M.F., pH-Dependent Thickness Behavior of Sequentially Adsorbed Layers of Weak Polyelectrolytes. *Macromolecules* **2000,** *33*, 4213-4219.

(42) Lynn, D.M., Peeling Back the Layers: Controlled Erosion and Triggered Disassembly of Multilayers Polyelectrolyte Thin Films. *Adv. Mater.* **2007,** *19,* 4118-4130.

(43) Lvov, Y.; Ariga, K.; Ichinose, I.; Kunitake, T., Assembly of Multicomponent Protein Films by Means of Electrostatic Layer-by-Layer Adsorption. *J. Am. Chem. Soc.* **1995**, *117*, 6117-6123.

(44) Hong, J.; Kim, B-S.; Char, K.; Hammond, P.T., Inherent Charge-Shifting Polyelectrolyte Multilayer Blends: A Facile Route for Tuning Protein Release from Surfaces.
Biomacromolecules **2011**, *12*, 2975-2981.

(45) Hong, J.; Shah, N.J.; Drake, A.C.; DeMuth, P.C.; Lee J.B.; Chen, J.; Hammond, P.T., Graphene Multilayers as Gates for Multi-Week Sequential Release of Proteins from Surfaces. *ACS Nano* **2012,** *6*, 81-88.

(46) Kim, B-S.; Smith, R.C.; Poon, Z.; Hammond, P.T., MAD(Multiagent Delivery) Nanolayer: Delivering Multiple Therapeutics from Hierarchically Assembled Surface Coatings. *Langmuir* **2009**, *25*, 14086-14092.

(47) Quinn, J.F.; Johnston, A.P.R.; Such, G.K.; Zelikin, A.N.; Caruso, F., Next Generation, Sequentially Assembled Ultrathin Films: Beyond Electrostatics. *Chem. Soc. Rev.* **2007**, *36*, 707-718.

(48) Jierry, L.; Ameur, N.B.; Thomann, J-S.; Frisch, B.; Gonthier, E.; Voegel, J-C.; Senger, B.; Decher, G.; Felix, O.; Schaaf, P.; Mesini, P.; Boulmedais, F., Influence of Cu(I)-Alkyne π-Complex Charge on the Step-by-Step Film Buildup through Sharpless Click Reaction. *Macromolecules* **2010**, *43*, 3994-3997.

(49) Zhang, X.; Jiang, C.; Cheng, M.; Zhou, Y.; Zhu, X.; Nie, J.; Zhang, Y.; An, Q.; Shi, F., Facile Method for the Fabrication of Robust Polyelectrolyte Multilayers by Post-Photo-Cross-Linking of Azido Groups. *Langmuir* **2012,** *28,* 7096-7100.

(50) Lee, D.; Rubner, M.F.; Cohen, R.E., All-Nanoparticle Thin-Film Coatings. *Nano Lett.* **2006**, *6*, 2305-2312.

(51) Hua, F.; Shi, J.; Lvov, Y.; Cui, T., Patterning of Layer-by-Layer Self-Assembled Multiple Types of Nanoparticle Thin Films by Lithographic Technique. *Nano Lett.* **2002,** *2,* 1219-1222.

(52) Pavlukhina, S.; Sukhishvili, S., Polymer Assemblies for Controlled Delivery of Bioactive Molecules from Surfaces. *Adv. Drug Delivery Rev.* **2011**, *63*, 822-836.

(53) Kim, B-S.; Park, S.W.; Hammond, P.T., Hydrogen-Bonding Layer-by-Layer Assembled Biodegradable Polymeric Micelles as Drug Delivery Vehicles from Surfaces. *ACS Nano* **2008,** *2,* 386-392.

(54) Ma, N.; Zhang, H.; Song, B.; Wang, Z.; Zhang, X., Polymer Micelles as Building Blocks for Layer-by-Layer Assembly: An Approach for Incorporation and Controlled Release of Water-Insoluble Dyes. *Chem. Mater.* **2005,** *17,* 5065-5069.

(55) Zhu, Z.; Sukhishvili, S.A., Small Molecule Release with Hydrogen-Bonded Multilayers of Block Copolymer Micelles. *ACS Nano* **2009,** *3,* 3595-3605.

(56) Soike, T.; Streff, A.K.; Guan, C.; Ortega, R.; Tantawy, M.; Pino, C.; Shastri, V.P., Engineering a Material Surface for Drug Delivery and Imaging using Layer-by-Layer Assembly of Functionalized Nanoparticles. *Adv. Mater.* **2010,** *22,* 1392-1397.

(57) Mohammed, J.S.; DeCoster, M.A.; McShane, M.J., Fabrication of Interdigitated Micropatterns of Self-Assembled Polymer Nanofilms Containing Cell-Adhesive Materials. *Langmuir* **2006,** *22,* 2738-2746.

(58) Erel, I.; Zhu, Z.; Zhuk, A.; Sukhishvili, S.A., Hydrogen-Bonded Layer-by-Layer Films of Block Copolymer Micelles with pH-Responsive Cores. *J. Colloid Inter. Sci.* **2011,** *355,* 61-69.

(59) Quinn, J.F.; Caruso, F., Facile Tailoring of Film Morphology and Release Properties Using Layer-by-Layer Assembly of Thermoresponsive Materials. *Langmuir* **2004,** *20,* 20-22.

(60) Tan,W.S.; Cohen, R.E.; Rubner, M.F.; Sukhishvili, S.A., Temperature-Induced, Reversible Swelling Transitions in Multilayers of a Cationic Triblock Copolymer and a Polyacid. *Macromolecules* **2010,** *43,* 1950-1957.

(61) Volodkin, D.V.; Madaboosi, N.; Blacklock, J.; Skirtach, A.G.; Mohwald, H., Surface-Supported Multilayers Decorated with Bio-Active Material Aimed at Light-Triggered Drug Delivery. *Langmuir* **2009,** *25,* 14037-14043.

(62) Serpe, M.J.; Jones, C.D.; Lyon, L.A., Layer-by-Layer Deposition of Thermoresponsive Microgel Thin Films *Langmuir* **2003**, *19*, 8759-8764.

(63) South, A.B.; Whitmire, R.E.; Garcia, A.J.; Lyon, L.A., Centrifugal Deposition of Microgels for the Rapid Assembly of Nonfouling Thin Films. *ACS Appl. Mater. Interfaces* **2009**, *1*, 2747-2754.

(64) Saxena, S.; Spears Jr., M.W.; Yoshida, H.; Gaulding, J.C.; Garcia, A.J.; Lyon, L.A., Microgel Films Dynamics Modulate Cell Adhesion Behavior. *Soft Matter* **2014**, *10*, 1356-1364.

(65) Herman, E.S.; Lyon, L.A., Polyelectrolyte Exchange and Diffusion in Microgel Multilayer Thin Films. *Colloid Polym. Sci.* **2015**, DOI: 10.1007/s00396-015-3547-2.

(66) Hu, X.; Lyon, L.A., Thin Films Constructed by Centrifugal Deposition of Highly Deformable, Charged Microgels. *ACS Macro. Lett.* **2015**, *4*, 302-307.

(67) Sorrell, C.D.; Lyon, L.A., Deformation Controlled Assembly of Binary Microgel Thin Films. *Langmuir* **2008**, *24*, 7216-7222.

(68) Serpe, M.J.; Yarmey, K.A.; Nolan, C.M.; Lyon, L.A., Doxorubicin Uptake and Release from Microgel Thin Films. *Biomacromolecules* **2005**, *6*, 408-413.

(69) Nolan, C.M.; Serpe, M.J.; Lyon, L.A., Thermally Modulated Insulin Release from Microgel Thin Films. *Biomacromolecules* **2004**, *5*, 1940-1946.

(70) South, A.B.; Lyon, L.A., Autonomic Self-Healing of Hydrogel Thin Films. *Angew. Chem. Int. Ed.* **2010**, *49*, 767-771.

(71) Spears, M.W.; Gaulding, J.C.; Lyon, L.A., Plastic Deformation, Wrinkling, and Recovery in Microgel Multilayers. *Poly. Chem.* **2013**, *4*, 4890-4896.

CHAPTER 3

MODULATION OF THE DESWELLING TEMPERATURE OF THERMORESPONSIVE MICROGEL FILMS

Adapted from

Clarke, K.C.; Lyon, L.A. *Langmuir* 2013, 29, 12852-12857

3.1 Introduction

There has been a great deal of interest in the development of responsive interfaces, which are designed to translate a change in the surrounding environment into a change in the properties of the interface.[1,2] For example, self-assembled monolayers have been used to control surface wettability using external cues such as pH,[3] light,[4] and electric potential.[5] A variety of polymer brush layers have been designed from stimulus responsive polymers to control the properties of a material's surface.[6−8] In addition, responsive interfaces have been applied as controlled drug delivery systems[9−13] and to control the adhesion of proteins and cells to surfaces.[14,15] Such approaches can therefore result in new or enhanced properties to a material's interface but remain governed by a specific stimulus, providing the user with specific control.

Further control can be pursued within the bulk system at smaller length scales. The focus then is just on controlling not only macroscopic properties but also the properties of specific regions within the film. For instance, Dawson et al. have demonstrated the utility of their "plum pudding gel", where particulate components are incorporated into a bulk hydrogel matrix. They have been able to independently control the release of several different molecules using this approach.[16,17] In addition, they have developed topographically unique surfaces to probe cell interactions utilizing the

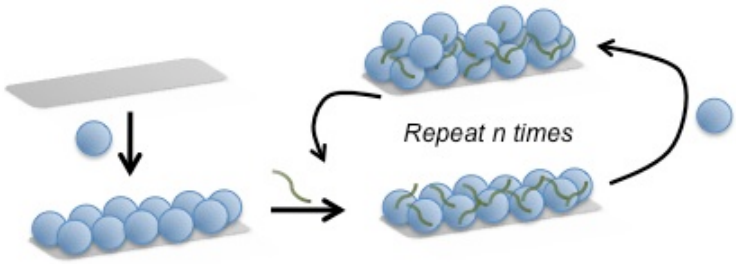

Scheme 3.1 Assembly of microgel layer-by-layer thin films.

demixing of a linear polymer and polymer microparticles.[18] Hoare and co-workers demonstrated the potential to tune the release profile of a charged molecule from a hydrogel by using an oppositely charged particle within the bulk. This allows the release of the drug to be controlled independently from the hydrogel matrix.[19,20] These strategies look to control components within the bulk system, presenting another way in which properties of the surface can be tuned.

Our group has focused on the development of responsive interfaces fabricated using microgels as building blocks for thin films.[21] Microgels are cross-linked, water-swollen polymer networks ranging from 100 to 1000 nm in diameter. Of particular interest to our group are thermoresponsive microgels synthesized from *N*-isopropylacrylamide (NIPAm).[22] Polymers of NIPAm exhibit a coil-to-globule transition at a lower critical solution temperature (LCST) of ~31 °C.[23] When pNIPAm is cross-linked into a microgel network, the thermoresponsive properties are maintained and the microgels exhibit a volume phase transition (VPT). The sharp temperature responsivity of pNIPAm has made it the prototypical responsive polymer, having been utilized widely.

In our group, microgel films are typically assembled using layer-by-layer (LbL) deposition,[24] where p(NIPAm-co-acrylic acid) microgels serve as the polyanion and a linear polycation "stitches" the particles together (**Scheme 3.1**).[25,26] In using this building block approach, it is possible to vary the type of microgel within a given film, permitting the properties of the assembly to be tailored. Herein we focus on designing a variety of microgel-based films capable of responding to temperature changes that span a narrow,

biologically relevant, range (30-40 °C). Our approach was to copolymerize NIPAm with N-isopropylmethacrylamide (NIPMAm); poly(NIPMAm) is a temperature responsive polymer with a LCST of ~44 °C.[27] On the basis of previous studies of linear copolymers,[28] we hypothesized that the microgel copolymer deswelling temperatures would lie between those found for homopolymers of pNIPAm and pNIPMAm, thereby allowing us to tune the microgel volume phase transition temperatures (VPTTs) within our range of interest. By controlling the VPTT of the microgel building block, we were then able to modulate the deswelling temperature(s) (DST) of microgel polyelectrolyte assemblies. Further control of the interface was achieved by fabricating composite films, particle assemblies with two or more microgels possessing different DSTs. In addition, we show that the way in which composite microgel films are assembled does not significantly impact the thermoresponsivities of the films, suggesting that microgels within the film behave independently of their neighboring particles.

3.2 Experimental Section

3.2.1 Materials

All chemicals were purchased from Sigma-Aldrich unless otherwise noted. Monomers NIPAm and NIPMAm were recrystallized from hexanes (BDH Chemicals). *N,N′*-Methylenebisacrylamide (BIS), acrylic acid (AAc, Fluka), sodium dodecyl sulfate (SDS), and ammonium persulfate (APS) were used as received. Covalent coupling reagents, *N*-(3-(dimethylamino)propyl)-N′-ethylcarbodiimide hydrochloride (EDC) and *N*-hydroxysuccinimide (NHS), were used as received. Microgel multilayer films were constructed using poly(diallyldimethylammonium chloride) (PDADMAC, MW 400 000−500 000) diluted in pH 7.4 phosphate buffer (0.01 M), 100 mM ionic strength (PB). Buffer reagents included sodium phosphate mono- hydrate, formic acid (EMD Biosciences), 2-(*N*-morpholino)ethanesulfonic acid (MES), and NaCl (EMD

Biosciences). Acetone and isopropanol were used as received (BDH Chemicals). All water was distilled and deionized to a resistance of 18 MΩ using a Barnstead E-pure system. A 0.2 μm filter was used to further remove particulate matter.

3.2.2 Microgel Synthesis

Microgels were synthesized by free radical precipitation polymerization; **Table 3.1** contains the feed concentrations of monomers used to synthesize each microgel. A typical synthesis is described as follows. NIPAm and/or NIPMAm, BIS, and SDS (0.2 m*M* for Microgel 1 and 1.0 m*M* for Microgels 2−6) were dissolved in 99 mL of water and filtered (0.2 μm) into a three-neck round-bottom flask containing a stir bar. To obtain fluorescent microgels, 4- acrylamidofluorescein (AFA),[25] dissolved in 1.0 mL of DMSO, was added to the monomer solution. The monomer solution was refluxed for 1 h at 70 °C with the stir bar spinning at 450 rpm while purging with N_2. AAc was added approximately 10 min prior to initiation. The reaction was initiated with 1.0 mL of an APS solution (1.0 m*M*) and then continued for 6 h under a blanket of nitrogen. The microgel solution was left to cool overnight under the above conditions. Microgels were filtered through an Acrodisc syringe filter (1.2 μm pore size) and purified by ultracentrifugation. Aliquots of the microgel solution were centrifuged to form a pellet (266000×*g* for Microgel 1 and 136000×*g* for Microgels 2−6). The supernatant was removed, and the pellet was redispersed in DI water. This process was repeated four times. For film fabrication, purified microgels were freeze-dried and redispersed in PB.

3.2.3 Microgel Characterization

Hydrodynamic radii (R_H) were determined by dynamic light scattering. Light scattering data were collected for 20 s per acquisition. A total of 20 acquisitions were collected for each run; five runs were collected for each microgel sample. The average R_H and standard deviation of the 5 runs are presented. R_H values were obtained in formate

buffer (0.01 M, 20 m*M* ionic strength, pH 3) and phosphate buffer (0.01 M, 24 m*M* ionic strength, pH 7.4).

3.2.4 Microgel Film Fabrication

Films were constructed on glass coverslips (VWR), cut to 14 × 22 mm. Film fabrication was carried out according to a previously established procedure.[26] Coverslips were cleaned by sonication in a dilute Alconox solution (30 min), then DI water, acetone, ethanol, and isopropanol (15 min each). The glass surface was rendered cationic by functionalizing the coverslips in a 1% (v/v) aminopropyltrimethoxysilane/absolute ethanol solution on a shaker table for 2 h. The functionalized coverslips were stored in absolute ethanol until used. Coverslips were removed and rinsed with ethanol and DI water, dried with nitrogen, and individually placed in the wells of a six-well plate. The coverslips were then equilibrated in 2.0 mL of PB for 30 min. The buffer was removed, and microgels were centrifugally deposited onto the glass substrate at 2250×*g* using a plate rotor in an Eppendorf centrifuge 5804 R. The resultant monolayer films were rinsed multiple times with DI water, dried with N_2, and stored.

All microgel monolayers were covalently coupled to the glass substrate via EDC coupling. The films were equilibrated in 0.01 *M* MES buffer (100 m*M* ionic strength, pH 5.3) for 30 min. MES buffer was removed, and the coupling reagents were added to each well. The coupling reaction was carried out for 2 h on a shaker table using 2 m*M* EDC and 5 m*M* NHS in MES buffer. The films were rinsed copiously with water, dried with N_2, and stored.

Films fabricated from a mixture of two microgels required the deposition of a bilayer of poly(sodium 4-styrenesulfonate) (PSS, average MW 70 000) and PDADMAC to promote equal adsorption of both particles. Preferential deposition of Microgel 2 was observed when coverslips functionalized with only APTMS were used, thus necessitating the deposition of "primer" layers. Each polyion was adsorbed onto APTMS

functionalized glass coverslips for 30 min on a shaker table, followed by extensive rinsing with water. The polymers were dispersed in PB (1.0 wt % PSS and 1.6 wt % PDADMAC). Microgel monolayers were centrifugally deposited at 650×*g* for 10 min at 25 °C. A solution containing Microgel 2 and either Microgel 5 or Microgel 6 was used for film fabrication. Both of the microgels in the solution were at a concentration of 1.0 mg/mL.

Multilayer buildup was achieved by first equilibrating the films in PB for 30 min. The buffer was removed, and PDADMAC (2.0 mL, 1.6 wt %) was added to each well. The well plate was placed on a shaker table for 30 min, after which the PDADMAC solution was removed. Following extensive rinsing with water another layer of microgels was centrifugally deposited as before. This process was repeated to yield a film with an even number of microgel and PDADMAC layers (PDADMAC is the outermost layer, unless otherwise indicated). Films assembled by alternating between two different microgels were assembled in an analogous fashion.

3.2.5 AFM Imaging

Atomic force microscopy (AFM) was used to image the films throughout the fabrication process. All images presented were acquired in intermittent contact mode in air under ambient conditions using an MFP-3D AFM (Asylum Research). Data were processed using software written in an IgorPro environment (Wavemetrics, Inc.). The force constant of the silicon cantilevers was 42 N/m (Nanoworld).

3.2.6 Light Scattering Curves

A fluorimeter (PTI) was used to acquire temperature-dependent light scattering data of microgel dispersions and films. The dispersions consisted of 5.0 μL of purified microgels in 3.0 mL of formate buffer (pH 3). For scattering measurements of microgel films, the coverslips were placed diagonally in a cuvette with 3.0 mL of formate buffer

such that the coverslip was angled away from the detector and the microgel film faced the incident light, as described previously.[29] The buffer was degassed prior to curve acquisition. The excitation and emission monochromators were set to 600 nm with slit widths set for a bandwidth of 1 nm. Scattered light was detected for 60 s at a set temperature. The temperature was increased and the sample was thermally equilibrated for 6 min before the next 60 s scan was taken. The scattering intensity for each 60 s scan was averaged, and the VPTT (dispersed microgels) or DST (microgel films) was identified as the temperature where the change in scattering intensity was at a maximum.

3.2.7 Differential Scanning Calorimetry

Differential scanning calorimetry (DSC, TA Instruments) was used to characterize the phase transition temperatures of Microgels 1-5. Freeze-dried microgels were resuspended in formate buffer (pH 3) to yield solutions at a final concentration of 30 mg/mL. Aliquots of each microgel solution (20 μL) were pipetted into DSC pans (Tzero) and sealed. The reference pan contained 20 μL of formate buffer. The temperature was increased from 25 to 50 °C at a rate of 1 °C/min.

3.2.8 Percent Transmittance Curves

The temperature responsivity of Microgels 1−5 and mixed microgel films were characterized using a UV-vis spectrophotometer (Shimadzu) in transmittance mode. Particle dispersions consisted of 5 μL of purified microgel in 3.0 mL of formate buffer (pH 3). The films were placed in a cuvette with 3.0 mL of formate buffer, which was subsequently degassed in a vacuum oven. The coverslips were oriented diagonally in the cuvette with the microgel film and coverslip angled toward the incident light (600 nm). Each percent transmittance (%T) measurement was obtained after allowing the temperature to equilibrate for 10 min. VPTTs of microgel dispersions and DSTs of mixed

microgel films were obtained by calculating the temperature at which the change in %T was the greatest in magnitude.

3.2.9 Confocal Microscopy of Mixed Microgel Films

Confocal microscopy was used to visualize microgel arrangement within composite films. Mixed microgel films were assembled using Microgels 2 and 6. Microgel 6 was synthesized with a fluorescent co-monomer and is the visualized component within the films. Films were made analogous to the composite films fabricated with nonfluorescent particles and include the alternating deposition of Microgels 2 and 6 (eight microgel layers), deposition from a mixture of Microgels 2 and 6 (six microgel layers), and separate sections of Microgels 2 and 6 (four layers Microgel 2, five layers Microgel 6, five layers Microgel 2, five layers Microgel 6; 19 total microgel layers). Prior to imaging, a rubber gasket was attached to the surface of the film, filled with pH 3 formate buffer, and allowed to equilibrate for 30 min. Confocal microscopy images were acquired using a Zeiss LSM 700-405 with a 63x oil immersion objective.

3.3 Results and Discussion

In an effort to design microgel films that respond to specific temperature changes within a narrow temperature range (30-40 °C), we synthesized several microgel building blocks in which the ratio of NIPAm to NIPMAm was varied. The hydrodynamic radii (R_H) for each of the microgels are given in **Table 3.1**. The microgels also demonstrate pH-dependent swelling owing to the incorporation of AAc residues within the network. Representative AFM height retraces of a microgel monolayer and a six-layer microgel films assembled from Microgels 1-5 are shown in **Figure 3.1**.

Table 3.1 Synthesis Recipes and Hydrodynamic Radii for Microgels 1-6

Microgel	NIPAm:NIPMAm	BIS	AAc	$[Monomer]_T$ (m*M*)	R_H (nm) pH 3*	R_H (nm) pH 7.4*
1	88:0	2	10	100	264±36	439±69
2	66:22	2	10	100	200±24	286±29
3	44:44	2	10	100	266±41	449±34
4	22:66	2	10	140	260±36	300±36
5	0:88	2	10	140	330±62	443±99
6[†]	0:87.9	2	10	140	399±76	548±90

*DLS data acquired at 25 °C

[†]Co-polymerized with 0.1% AFA

Light scattering was monitored as a function of temperature to determine the VPTTs for each of the microgels synthesized. An increase in scattering intensity is indicative of particle collapse and therefore a volume decrease. As the microgel transitions from a highly solvated network to a collapsed network, where polymer-polymer interactions are favored, the refractive index of the microgel relative to the surrounding aqueous environment greatly increases. The scattering efficiency is mainly dependent on the refractive index.[30] Therefore, the refractive index contrast and heterogeneity results in an increase in the observed scattering intensity. VPTT curves for Microgels 1-5 and VPTTs as a function of mol % NIPMAm are presented in **Figure 3.2a** and **Figure 3.2b**, respectively. Each of the five microgels has a distinct VPTT where increasing the concentration of NIPMAm relative to NIPAm resulted in an elevation of the VPTT. This is likely due to decreased chain flexibility of the microgel network as a result of greater incorporation of NIPMAm.[26] This observation agrees with our original hypothesis that the incorporation of NIPMAm into the network would lead to an increase in the VPTT. Furthermore, only one transition is observed for each microgel, suggesting a uniform distribution of the co-monomers.

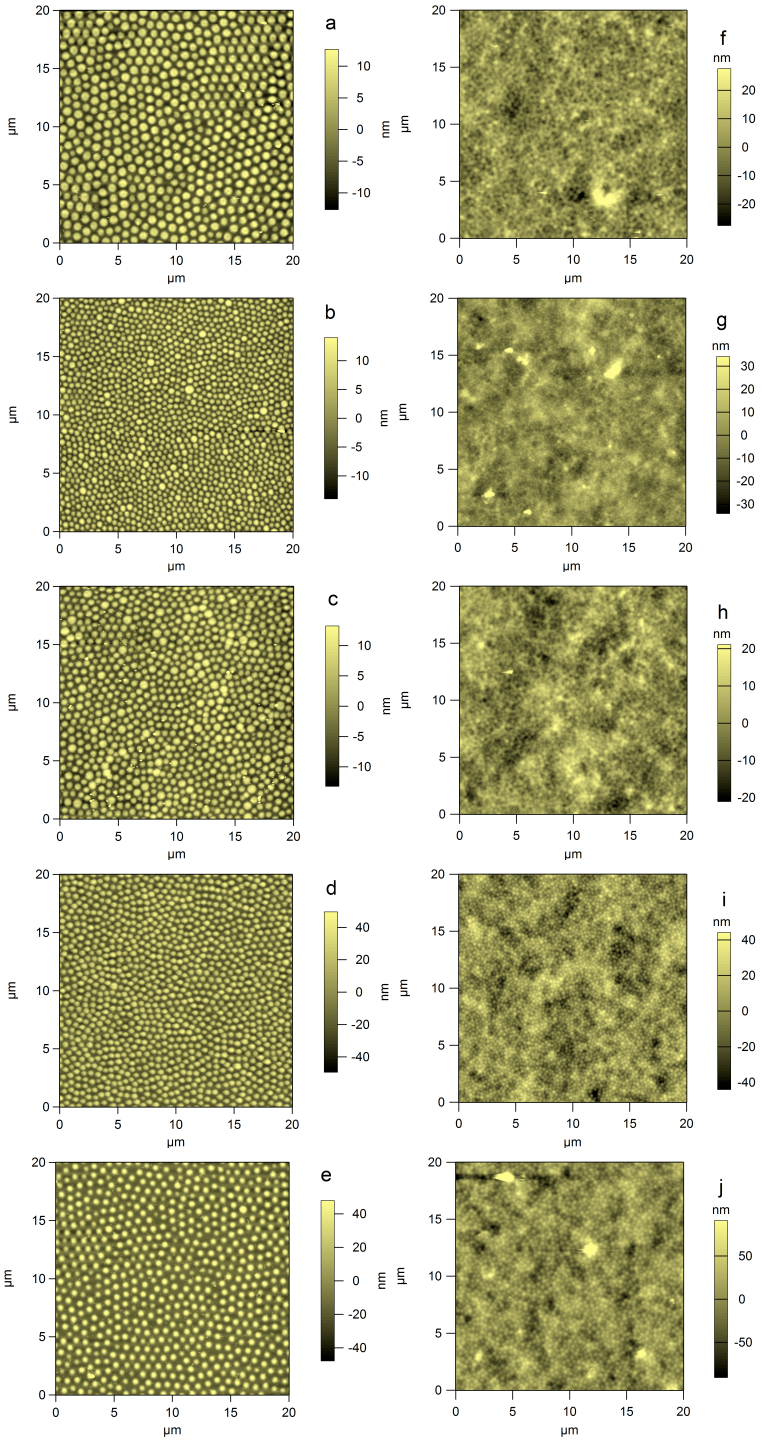

Figure 3.1 AFM height retrace images: (a-e) monolayers and (f-j) 6-layer LbL films of Microgels 1-5, respectively.

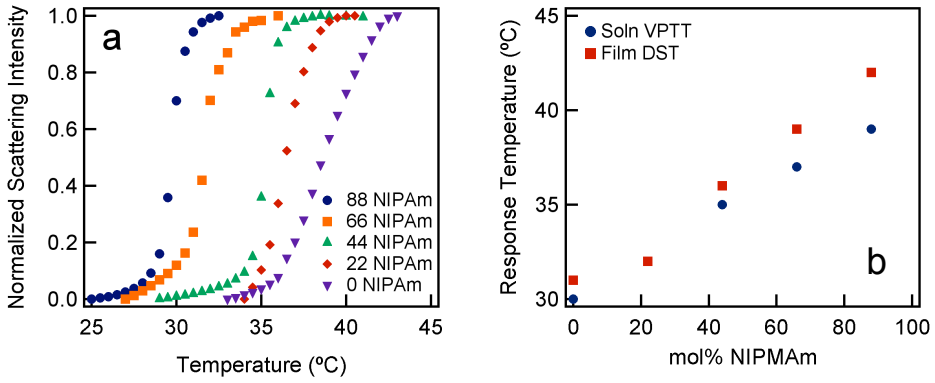

Figure 3.2 (a) Temperature dependent light scattering curves for dispersions of Microgels 1-5, and (b) response temperatures for Microgels 1-5 dispersed in buffer or assembled in 6-layer films as a function of mol% NIPMAm.

Differential scanning calorimetry curves show broadened peaks at higher concentrations of NIPMAm (**Figure 3.3**), indicating a less homogeneous distribution within the microgels than that suggested by light scattering. This observation is in agreement with the report of Richtering and co-workers, where nanophases of pNIPAm were shown to separate before the collapse of p(NIPAm-co-NIPMAm) microgels occurred.[31] These results suggest that DSC measurements are more sensitive to discrete thermodynamic subpopulations in the particles than the simple turbidity or scattering measurements.

Having established that the copolymerization of NIPAm and NIPMAm allowed us to tune the microgel VPTT within our range of interest, we sought to construct microgel films that would recapitulate the same responsivities. Microgel LbL films were assembled, where the microgels serve as the polyanion and PDADMAC is the polycation. Microgels 1−5 were each used to build individual films composed of six microgel layers and six PDADMAC layers. The DSTs of the films as a function of mol % NIPMAm are presented in **Figure 3.2**. The DSTs of the microgel films map on well with those obtained for microgel dispersions, suggesting that the microgels retain their responsivities when confined within the polyelectrolyte assembly. Here we distinguish between VPTT and DST, where VPTTs describe the volume change associated with the collapse of particles

in a dispersion and DSTs describe the deswelling of microgel polyelectrolyte thin films. We propose that DST more correctly describes microgel films because it is not strictly correct to refer to the collapse of the composite film as a "phase transition".

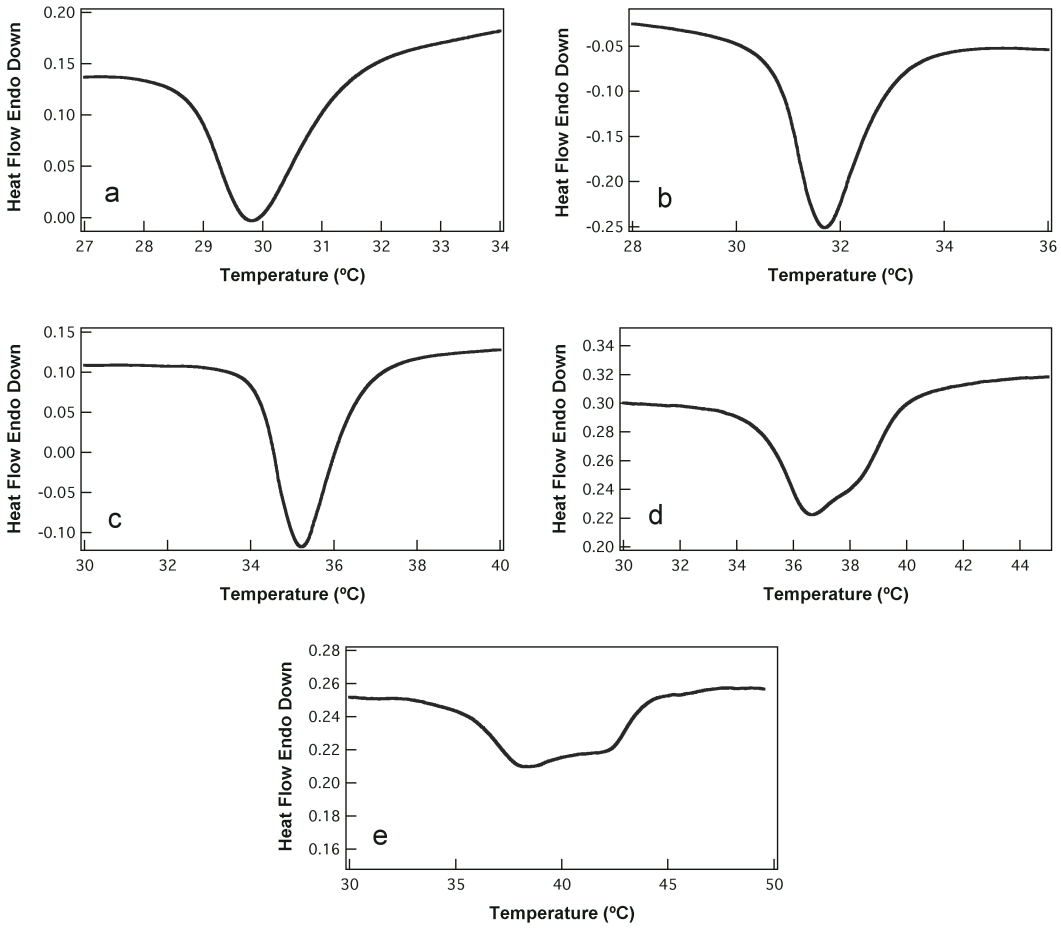

Figure 3.3 Differential scanning calorimetry curves of Microgels 1-5 (a-e, respectively).

This modular approach to film fabrication permits the buildup of microgel assemblies containing more than one type of microgel, providing greater freedom in tuning the responsivities of the interface. Upon demonstrating that microgel-based thin films recapitulate the temperature responsivities of their constituent particles, we next fabricated composite films to investigate multi-temperature responsive films. Mixed

microgel films were built out of two different microgels, each having a unique VPTT. **Figure 3.4a** presents the temperature response of a mixed microgel film composed of alternating layers of Microgels 2 and 5, where Microgel 2 was the initial layer. Decreases in transmitted light indicate that the microgels in the film have collapsed, thereby scattering more light. Two transmittance decreases are observed at approximately 32 and 40 °C. According to **Figure 3.2**, these temperatures correspond well with those obtained for single type particle films of Microgels 2 and 5. Furthermore, assembling a film containing Microgels 1−5 results in a response that spans the entire 10 °C temperature range shown in **Figure 3.1** (**Figure 3.4b**). VPTTs obtained from both light scattering and %T data were found to be in good agreement (**Table 3.2**). From this, we assume that data acquired from %T measurements are analogous to those acquired from measurements of scattering intensity.

Table 3.2 Comparison of VPTTs Obtained from Light Scattering and Transmittance Measurements in pH 3 Formate Buffer

Microgel	Light Scattering (°C)	% Transmittance (°C)
1	30	30
2	32	32
3	36	36
4	37	37
5	39	39

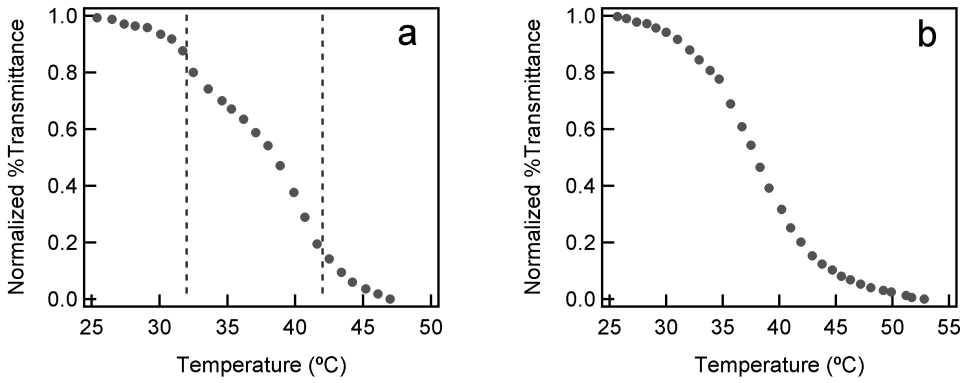

Figure 3.4 Temperature dependent percent transmittance curves of mixed microgel composite films at pH 3: (a) alternating deposition of Microgels 2 and 5 (6-layers total) and (b) 2-layers each of Microgels 1-5. Dashed lines indicate the deswelling temperatures for films composed of either Microgel 2 or Microgel 5 only.

These initial studies demonstrate the ability to control the response of the film by changing both the chemical composition of the building block and by incorporating more than one type of microgel within a film. However, little is known about the behavior of the microgels with respect to each other within the polyelectrolyte assembly. Therefore, we next investigated whether changing the assembly process would influence the response temperatures of the films. In addition to the film assembled by alternating the deposition of Microgels 2 and 5, two more films were fabricated where Microgels 2 and 5 were deposited either in separate sections or from a mixture of the two microgels. The sectioned film was composed of three layers of Microgel 2 followed by three layers of Microgel 5. The mixed film was composed of six microgel layers where each layer contained both Microgels 2 and 5. Representative AFM height images of each mixed composition film are shown in **Figures 3.5b-d**, where the successful deposition of both microgels can be observed. Transmittance data for the sectioned and mixed films are presented in **Figures 3.5a**. DSTs from the %T curves of the composite films can be found in **Table 3.3**. Though there is some slight variability, we find that the assembly process has little effect on the responsivities of the films, suggesting that the microgels behave

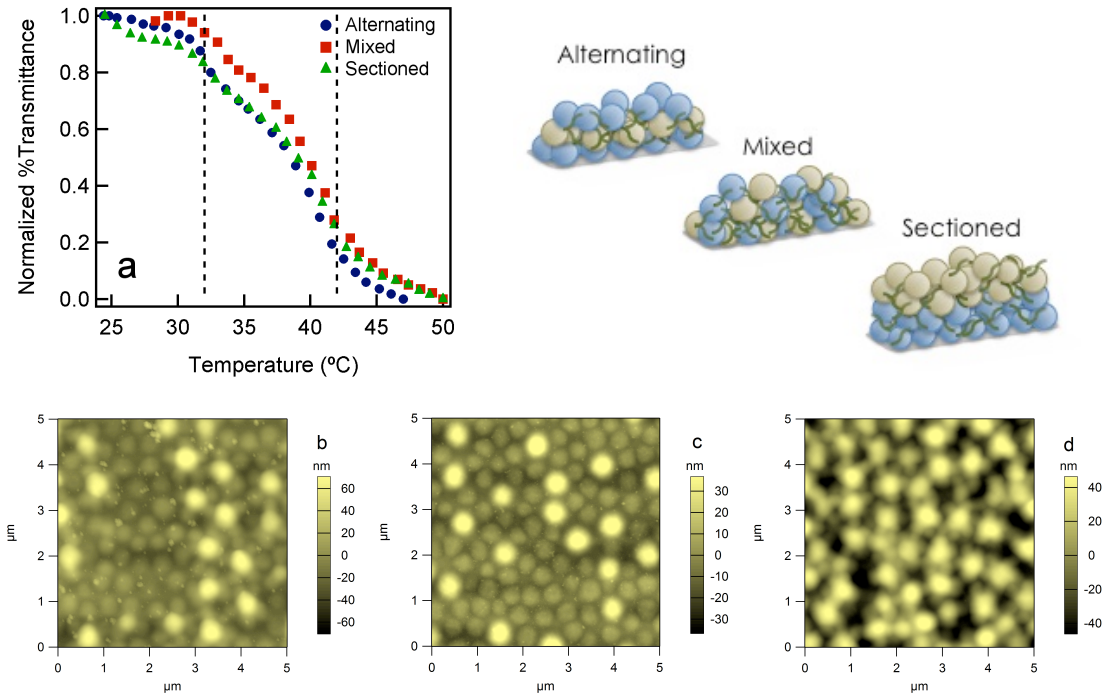

Figure 3.5 (a) Temperature-dependent percent transmittance curves of composite films of Microgels 2 and 5, assembled by three methods at pH 3. Cartoons illustrating the three assembly methods are provided; (b-d) AFM height images of alternating (layer 2), mixed (layer 1), and sectioned composite films (layer 4), respectively. Dashed lines indicate the deswelling temperatures for films composed of either Microgel 2 or Microgel 5 only.

Table 3.3 VPTTs and DSTs (°C) for Microgels and Microgel Multilayer Films at pH 3

	Microgel 2	Microgel 5	Alternated 2/5	Separated 2/5	Mixed 2/5
Solution	32	39	N/A	N/A	N/A
6-layer film	32	42	33/41	33/41	34/42

independently of their neighbors and their proximity to other microgels of the same or different composition was of little importance in the overall deswelling properties.

Confocal microscopy was used to visualize the location of microgels within the various mixed microgel films. Composite films were fabricated using Microgel 2 and Microgel 6, a fluorescent microgel, and were assembled in an analogous fashion to those previously used in transmittance experiments. Cross sections of the films are presented in **Figure 3.6**. Films fabricated by alternating deposition and from a microgel mixture appear to have homogeneously mixed particles; no obvious stratification or demixing is observed. However, the film fabricated with the intention of having a separated architecture does indeed have this separation between layers. These results suggest that the 3-dimensional arrangement of microgels within the assembly can be changed without altering the responsivity of the microgels themselves or the film composed of them. We hypothesize that polycation mobility permits the microgels to respond freely despite penetration of polycation into the microgels[32] because they are not covalently bound to the polyelectrolyte matrix. Indeed, perturbations of microgel thermoresponsivities have been observed when microgels were covalently assembled into a bulk hydrogel[20] or when an interpenetrating network was formed between a bulk hydrogel matrix and the incorporated microgels.[33] Apparently, the LbL assembly process produces films with less particle-particle and particle-"matrix" connectivity than these other examples.

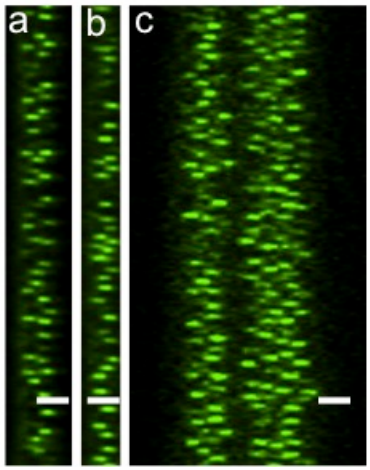

Figure 3.6 Cross-sections (yz plane) of mixed microgel films obtained using a confocal microscope: (a) alternating deposition, 8 microgel layers, (b) deposition from microgel mixture, 6 microgel layers, and (c) deposition of Microgels 2 and 6 in separate sections, 19 microgel layers (Scale bar=2 μm).

In this chapter, we demonstrated the construction of a multicomponent temperature responsive thin film. Using this construct, we gain control of the interface and the nanoscale structure within the film. As described above, there are a number of areas (e.g., drug release, switchable interfaces, actuation) for which such a system could be applied. However, the microgel multilayer approach is a complex one that requires further study before it can be truly utilized.

3.4 Conclusions

We have shown here that the synthesis of p(NIPAm-co-NIPMAm) microgels permits the tuning of the microgel VPTT over ~10 °C temperature range. LbL films assembled from these microgels were shown to have response temperatures very similar to those demonstrated for the microgels in solution. Further tailoring of the film responsivity was achieved when films were assembled from more than one type of microgel. Three different assembly methods were employed to generate composite films, and all three had very similar temperature responses. Overall, these results suggest that the microgel building blocks behave independently of the polyelectrolyte matrix and

neighboring particles, and it is possible that mobile polycation chains enable this behavior. The systems described here could be applied to drug eluting interfaces where release is governed by small temperature fluctuations in the surrounding environment.

3.5 References

(1) Cohen Stuart, M.A.; Huck, W.T.S.; Genzer, J.; Muller, M.; Ober, C.; Stamm, M.; Sukhorukov, G. B.; Szleifer, I.; Tsukruk, V.V.; Urban, M.; Winnik, F.; Zauscher, S.; Luzinov, I.; Minko, S., Emerging Applications of Stimuli-Responsive Polymer Materials. *Nature Mater.* **2010**, *9*, 101-113.

(2) Mendes, P.M., Stimuli-Responsive Surfaces for Bio-Applications. *Chem. Soc. Rev*. **2008**, *37*, 2512-2529.

(3) Yu, X.; Wang, Z.; Jiang, Y.; Shi, F.; Zhang, X., Reversible pH- Responsive Surface: From Superhydrophobicity to Superhydrophilicity. *Adv. Mater.* **2005**, *17*, 1289-1293.

(4) Wan, P.; Jiang, Y.; Wang, Y.; Wang, Z.; Zhang, X., Tuning Surface Wettability through Photocontrolled Reversible Molecular Shuttle. *Chem. Commun*. **2008**, 5710-5712.

(5) Lahann, J.; Mitragotri, S.; Tran, T.; Kaido, H.; Sundaram, J.; Choi, I.S.; Hoffer, S.; Somorjai, G.A.; Langer, R.A., Reversibly Switching Surface. *Science* **2003**, *299*, 371-374.

(6) Luzinov, I.; Minko, S.; Tsukruk, V.V., Responsive Brush Layers: From Tailored Gradients to Reversibly Assembled Nanoparticles. *Soft Matter* **2008**, *4*, 714-725.

(7) Hoy, O.; Zdyrko, B.; Lupiyskyy, R.; Sheparovych, R.; Aulich, D.; Wang, J.; Bittrich, E.; Eichhorn, K.-J.; Uhlmann, P.; Hinrichs, K.; Muller, M.; Stamm, M.; Minko, S.; Luzinov, I., Synthetic Hydrophilic Materials with Tunable Strength and a Range of Hydrophobic Interactions. *Adv. Funct. Mater.* **2010**, *20*, 2240-2247.

(8) Ayers, N.; Cyrus, C. D.; Brittain, W. J., Stimuli-Responsive Surfaces Using Polyampholyte Polymer Brushes Prepared via ATRP. *Langmuir* **2007**, *23*, 3744-3749.

(9) Hong, J.; Kim, B.; Char, K.; Hammond, P.T., Inherent Charge-Shifting Polyelectrolyte Multilayer Blends: A Facile Route for Tunable Protein Release from Surfaces. *Biomacromolecules* **2011**, *12*, 2975-2981.

(10) Kumar, S.; Dory, Y. L.; Lepage, M.; Zhao, Y., Surface-Grafted Stimuli-Responsive Block Copolymer Brushes for the Thermo-, Photo-, and pH-Sensitive Release of Dye Molecules. *Macromolecules* **2011**, *44*, 7385-7393.

(11) Ma, N.; Zhang, H.; Song, B.; Wang, Z.; Zhang, X., Polymer Micelles as Building Blocks for Layer-by-Layer Assembly: An Approach for Incorporation and Controlled Release of Water- Insoluble Dyes. *Chem. Mater.* **2005**, *17*, 5065-5069.

(12) Quinn, J.F.; Caruso, F., Facile Tailoring of Film Morphology and Release Properties Using Layer-by-Layer Assembly of Thermoresponsive Materials. *Langmuir* **2004**, *20*, 20-22.

(13) Serizawa, T.; Matsukuma, D.; Akashi, M., Loading and Release of Charged Dyes Using Ultrathin Hydrogels. *Langmuir* **2005**, *21*, 7739-7742.

(14) Cooperstein, M.A.; Canavan, H.E., Biological Cell Detachment from Poly(N-isopropyl acrylamide) and Its Applications. *Langmuir* **2010**, *26*, 7695-7707.

(15) Cole, M.A.; Voelcker, N.H.; Thissen, H.; Griesser, H.J., Stimuli-Responsive Interfaces and Systems for the Control of Protein-Surface and Cell-Surface Interactions. *Biomaterials* **2009**, *30*, 1827-1850.

(16) Lynch, I.; Dawson, K.A., Synthesis and Characterization of an Extremely Versatile Structural Motif Called the "Plum-Pudding" Gel. *J. Phys. Chem. B* **2003**, *107*, 9629-9637.

(17) Lynch, I.; deGregorio, P.; Dawson, K.A., Simultaneous Release of Hydrophobic and Cationic Solutes from Thin-Film "Plum-Pudding" Gels: A Multifunctional Platform for Surface Drug Delivery. *J. Phys. Chem. B* **2005**, *109*, 6257-6261.

(18) Lynch, I.; Miller, I.; Gallagher, W.M.; Dawson, K.A., Novel Method to Prepare Morphologically Rich Polymeric Surfaces for Biomedical Applications via Phase Separation and Arrest of Microgel Particles. *J. Phys. Chem. B* **2006**, *110*, 14581-14589.

(19) Sivakumaran, D.; Maitland, D.; Hoare, T., Injectable Microgel-Hydrogel Composites for Prolonged Small-Molecule Delivery. *Biomacromolecules* **2011**, *12*, 4112-4120.

(20) Sivakumaran, D.; Maitland, D.; Oszustowicz, T.; Hoare, T., Tuning Drug Release from Smart Microgel-Hydrogel Composites via Cross-Linking. *J. Colloid Interface Sci.* **2013**, *392*, 422-230.

(21) Hendrickson, G. R.; Smith, M. H.; South, A. B.; Lyon, L.A., Design of Multiresponsive Hydrogel Particles and Assemblies. *Adv. Funct. Mater.* **2010**, *20*, 1697-1712.

(22) Nayak, S.; Lyon, L.A., Soft Nanotechnology with Soft Nanoparticles. *Angew. Chem. Int. Ed.* **2005**, *44*, 7686-7708.

(23) Pelton, R., Temperature-Sensitive Aqueous Microgels. *Adv. Colloid Interface Sci.* **2000**, *85*, 1-33.

(24) Decher, G., Fuzzy Nanoassemblies: Toward Layered Polymeric Multicomposites. *Science* **1997**, *277*, 1232-1237.

(25) Serpe, M.J.; Jones, C.D.; Lyon, L.A., Layer-by-Layer Deposition of Thermoresponsive Microgel Thin Films. *Langmuir* **2003**, *19*, 8759-8764.

(26) South, A.B.; Whitmire, R.E.; Garcia, A.J.; Lyon, L.A., Centrifugal Deposition of Microgels for the Rapid Assembly of Nonfouling Thin Films. *ACS Appl. Mater. Interfaces* **2009**, *1*, 2747-2754.

(27) Tang, Y.; Ding, Y.; Zhang, G., Role of Methyl in the Phase Transition of Poly(N-isopropylmethacrylamide). *J. Phys. Chem. B* **2008**, *112*, 8447-8451.

(28) Djokpé E.; Vogt, W., N-Isopropylacrylamide and N- Isopropylmethacrylamide: Cloud Points of Mixtures and Copolymers. *Macromol. Chem. Phys.* **2001**, *202*, 750-757.

(29) Nayak, S.; Debord, S.B.; Lyon, L.A., Investigations into the Deswelling Dynamics and Thermodynamics of Thermoresponsive Microgel Composite Films. *Langmuir* **2003**, *19*, 7374-7379.

(30) Weissman, J.M.; Sunkara, H.B.; Tse, A.S.; Asher, S.A., Thermally Switchable Periodicities and Diffraction from Mesoscopically Ordered Materials. *Science* **1996**, *274*, 959-960.

(31) Keerl, M.; Pedersen, S.; Richtering, W., Temperature Sensitive Copolymer Microgels with Nanophase Separated Structure. *J. Am. Chem. Soc*. **2009**, *131*, 3093-3097.

(32) Kleinen, J.; Klee, A.; Richtering, W., Influence of Architecture on the Interaction of Negatively Charged Multisensitive Poly(N- isopropylacrylamide)-co-Methacrylic Acid Microgels with Oppositely Charged Polyelectrolyte: Absorption vs Adsorption. *Langmuir* **2010**, *26*, 11258-11265.

(33) Lehmann, S.; Sieffert, S.; Richtering, W., Spatially Resolved Tracer Diffusion in Complex Responsive Hydrogels. *J. Am. Chem. Soc.* **2012**, *134*, 15963-15969.

CHAPTER 4

CORE/SHELL MICROGELS DE-COUPLE THE pH AND TEMPERATURE RESPONSIVITIES OF MICROGEL FILMS

Adapted from

Clarke, K.C.; Dunham, S.N.; Lyon, L.A. *Chem. Mater.* **2015**, *27*, 1391-1396.

4.1 Introduction

Layer-by-layer (LbL) film fabrication, as described by Decher and colleagues, is a versatile, facile method for the preparation of thin films.[1,2] Traditionally, substrates are coated by the alternating deposition of oppositely charged polyions (**Scheme 4.1**). Further work in the field expanded fabrication methods to include assembly facilitated by hydrogen bonding,[3,4] the direct incorporation of biomacromolecules,[5,6] and the inclusion of colloidal particles as both a nonplanar substrate[7] and a film building block.[8−10] LbL films held together through non-covalent interactions are often influenced by the pH environment during the assembly process and post-assembly; such films can also be prone to pH-induced deconstruction. Therefore, the impact of pH on the fabrication, integrity, and application of LbL films has been explored extensively.[10−15]

Our group has for a number of years applied the LbL assembly process to fabricate microgel-based thin films. Negatively charged microgels serve as the polyanion, and a (typically) linear polycation is adsorbed to reverse the charge for layer build-up (**Scheme 4.1**).[16,17] Microgels are solvated, cross-linked polymer networks, ranging in size from approximately 100−1000 nm in diameter. We have focused primarily on temperature responsive microgels, synthesized from *N*-isopropylacrylamide (NIPAm).[18,19] Refer to **Section 3.1** for a description of the thermoresponsive behavior of

Scheme 4.1 Construction of Linear Polyion and Microgel Layer-by-Layer Films

pNIPAm and pNIPAm microgels. Through the incorporation of acrylic acid within the network, pNIPAm microgels can be sequentially deposited with a polycation to yield a multilayer film, leading to the assembly of temperature-responsive interfaces. It should be noted that particle-based responsive interfaces have also been demonstrated with block copolymer micelle LbL films.[9,10] Micelles are held together through noncovalent interactions, where the hydrophobic core is segregated from the hydrophilic periphery. This type of compartmentalization may limit the ability of the constructs to respond to environmental stimuli while maintaining structural stability.

In **Chapter 3**, we demonstrated the ability to tune microgel volume phase transition temperatures (VPTTs) by copolymerizing pNIPAm and poly(N-isopropylmethacrylamide) (NIPMAm), a thermoresponsive polymer with a lower critical solution temperature of 41 °C.[20] An elevation in microgel VPTTs was observed as the concentration of NIPMAm increased relative to NIPAm. LbL films assembled from these particles had responsivities similar to those observed for particle dispersions at pH 3. This strategy enabled fine-tuning of the film response temperature, permitting greater control over the behavior of the interface.

While our group has previously shown that changes in pH alter the swelling properties of pNIPAm microgel-polycation films, it is unclear what impact the pH environment has on the thermoresponsivity of these films.[21,22] In this chapter we employ microgels, which should have different response temperatures due to their chemical composition and probe the thermoresponsivities of thin films assembled from these

particles at pH 3 and 7.4. We find that film thermoresponsivity lessens as the environmental pH increases from pH 3 to pH 7.4, resulting in the loss of sharp and predictable response temperatures. In light of this, we synthesized core/shell microgels, to separate the polyelectrolyte component (shell) from the thermoresponsive component (core). Utilizing this construct we prepared films with predictable thermoresponsivities regardless of the pH environment. We further investigated the impact of the pH environment on film swelling/deswelling by measuring film thicknesses via in-liquid AFM. Thickness measurements of the films at pH 3 and 7.4 at ~26 and 50 °C are generally in good agreement with the light scattering data, suggesting that the bulk temperature responses map well with observed internal film scattering properties.

4.2 Experimental

4.2.1 Materials

All chemicals were purchased from Sigma-Aldrich unless otherwise noted. The monomers, NIPAm and NIPMAm, were recrystallized from hexanes (BDH Chemicals). *N,N′*-Methylenebis(acrylamide) (BIS), acrylic acid (AAc, Fluka), sodium dodecyl sulfate (SDS), and ammonium persulfate (APS) were used as received. Covalent coupling reagents, *N*-(3-(dimethylamino)propyl)-N′-ethyl-carbodiimide hydrochloride (EDC) and N-hydroxysuccinimide (NHS), were used as received. Poly(diallyldimethylammonium chloride) (PDADMAC, 20 wt % MW 400 000-500 000) diluted in phosphate buffer (PB, 0.02 M, 0.1 M ionic strength, pH 7.4) was used in the fabrication of microgel multilayer films. Acetone, isopropanol (BDH Chemicals), and ethanol (Koptec) were used as received. Sodium phosphate monohydrate, 2-(*N*-morpholino)ethanesulfonic acid (MES), formic acid (EMD), NaOH, and NaCl were used in the preparation of buffers. All water was distilled and deionized to a resistance of 18 MΩ using a Barnstead E-pure system (DI water). A 0.2 μm filter was used to remove additional particulate matter.

4.2.2 Microgel Synthesis

Microgels were synthesized by aqueous free radical precipitation polymerization as described in **Section 3.2.2**. Refer to **Table 4.1** for monomer feed ratios for Microgels 1-5 (i.e. traditional microgels). Microgel shell addition was achieved by using microgel core particles (Core 1 or 2) as nucleation sites for further growth.[23] Refer to **Table 4.2** for monomer feed ratios for core/shell microgel syntheses. NIPMAm, BIS, and SDS were dissolved in 79 mL of water and filtered (0.2 μm Acrodisc syringe filter) into a round-bottom flask containing 20 mL of core particles. This mixture was heated to 70 °C under the same conditions as above. AAc was added to the reaction mixture approximately 10 min before initiation with APS (1.0 mL). Following initiation, the reaction continued for 6 h under a nitrogen blanket. The core/shell microgels were cooled to room temperature, filtered (1.1 μm Acrodisc syringe filter), and purified as stated above. Purified microgels were lyophilized and resuspended in PB at a concentration of 0.5 mg/mL for film fabrication.

4.2.3 Dynamic Light Scattering

Hydrodynamic radii (R_H) of the microgels were obtained by dynamic light scattering (DLS, Protein Solutions) at 25 °C as described in **Section 3.2.3**.

4.2.4 Microgel Film Fabrication

Microgel polyelectrolyte films were prepared on glass coverslips (VWR) as according to a previously established procedure[17] and as described in **Section 3.2.4**. Films prepared for light scattering experiments were fabricated on coverslips cut to 14 × 22 mm, while films prepared for in-liquid AFM were prepared on 22 × 22 mm glass coverslips.

4.2.5 Atomic Force Microscopy

An Asylum MFP-3D atomic force microscope (AFM) was used throughout the film fabrication process to monitor film build-up. Intermittent contact mode was employed to acquire images in ambient conditions. All imaging in air was performed using silicon cantilevers with a force constant of 42 N/m (Nanoworld). Film thicknesses of traditional and core/shell microgel films (10 layers) were obtained by first scoring the film with a clean razorblade at multiple locations. Images were acquired across a cut in air and in pH 3 formate buffer (FB, 0.02 M, 0.1 M ionic strength) and PB. In-liquid AFM images were acquired using the Asylum iDrive system. An Asylum Bioheater attachment was used in an open configuration to control the buffer temperature within the fluid cell. Images were collected and processed through Asylum MFP-3D software written in the IgorPro (Wavemetrics, Inc.) environment. Film thickness measurements were determined from images collected at four separate locations. Height trace and retrace data were analyzed using Matlab code written in house, where the height value of the substrate was subtracted from the height value of the top of the film for each line of the image. The average thicknesses for the left and right sides were averaged together for both the height trace and retrace for each image. Refer to **Appendix A** for additional information regarding the collection of film thickness data and the optimization of imaging parameters.

4.2.6 Temperature-Dependent Light Scattering Curves

A fluorimeter (PTI) was used to monitor the light scattering of microgels and microgel films.[24] Refer to **Section 3.2.6** for a detailed explanation of sample preparation and data collection.

4.3 Results and Discussion

In **Chapter 3**, we demonstrated the ability to tune VPTTs of temperature responsive microgels within a 10 °C range by copolymerizing NIPAm and NIPMAm in differing ratios. Polyelectrolyte films assembled from p(NIPAm-co-NIPMAm) microgels were shown to have well-defined and sharp response temperatures at pH 3.[20] In this work, we investigate the impact of the pH environment on the DSTs of thermoresponsive microgel films.

Microgel/PDADMAC films (six-layers) were placed in either pH 3 formate buffer or pH 7.4 phosphate buffer, and DST curves were collected by temperature-dependent light scattering. Increases in scattered light intensity are indicative of particle collapse, as the refractive index of the microgels changes during deswelling relative to the surrounding medium.[25] In comparison to results obtained at pH 3, the curves at pH 7.4 broaden, and incremental scattering changes are observed with increasing temperature (**Figure 4.1**). The films lack specific, individual response temperatures as the curves significantly overlap each other. Simply increasing the environmental pH results in less predictable and weaker temperature response behavior.

Table 4.1 Feed Ratios for Traditional Microgel Syntheses and De-Swelling Temperatures of Traditional Microgel LbL Films at pH 3

Microgel	NIPAm:NIPMAm	AAc	BIS	SDS (mM)	APS (mM)	DST (°C), pH3
1	88:0	10	2	0.2	1.0	30
2	66:22	10	2	1.0	1.0	32
3	44:44	10	2	1.0	1.0	35
4	22:66	10	2	1.0	1.0	37
5	0:88	10	2	1.0	1.0	39

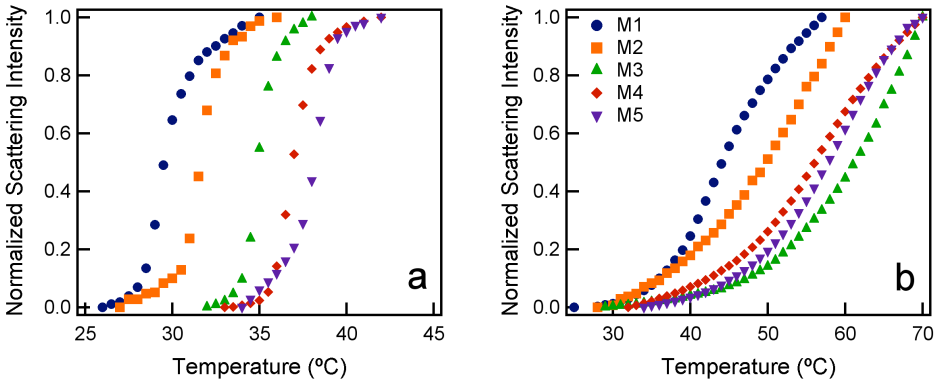

Figure 4.1 Normalized DST curves of 6-layer microgel/PDADMAC films composed of Microgels 1-5 at (a) pH 3 and (b) pH 7.4.

At this higher pH carboxylic acid groups in the network become deprotonated (pKa AAc ~ 4.5). This can result in charge repulsion of AAc groups within the network, increased osmotic pressure due to counterion ingress, and increased interactions between PDADMAC and carboxylate ions; all of which perturb film thermoresponsivity. Previously our group investigated the pH-dependent swelling response of microgel films and found that films are more optically dense at pH 6 versus pH 3.[21,22] This was attributed to enhanced complexation of polycation with AAc groups in the microgel network. It is possible that similar effects are taking place within the films studied here.

Table 4.2 Feed Concentrations of Core/Shell Microgels

	mol% NIPAm	mol% NIPMAm	mol% AAc	mol% BIS	$[Monomer]_T$ (m*M*)	SDS (m*M*)	APS (m*M*)
Core 1	98	--	--	2	100	0.2	1.0
Core 2	49	49	--	2	100	1.0	1.0
C1/Shell 1	--	88	10	2	50	0.5	0.5
C2/Shell 2	--	88	10	2	40	1.0	1.0

In an effort to gain a deeper understanding of the impact of the pH environment on microgel polyelectrolyte films we next implemented core/shell microgels as a film building block. Core/shell microgels consist of two compartments, where the properties of each are segregated.[22] Specifically, the particles were synthesized such that the core is temperature responsive only, and the pH responsive moieties are confined to the shell. In principle, this particular construct will decouple the pH and temperature responsive elements of the microgels, as well as those responses in films assembled from these particles.

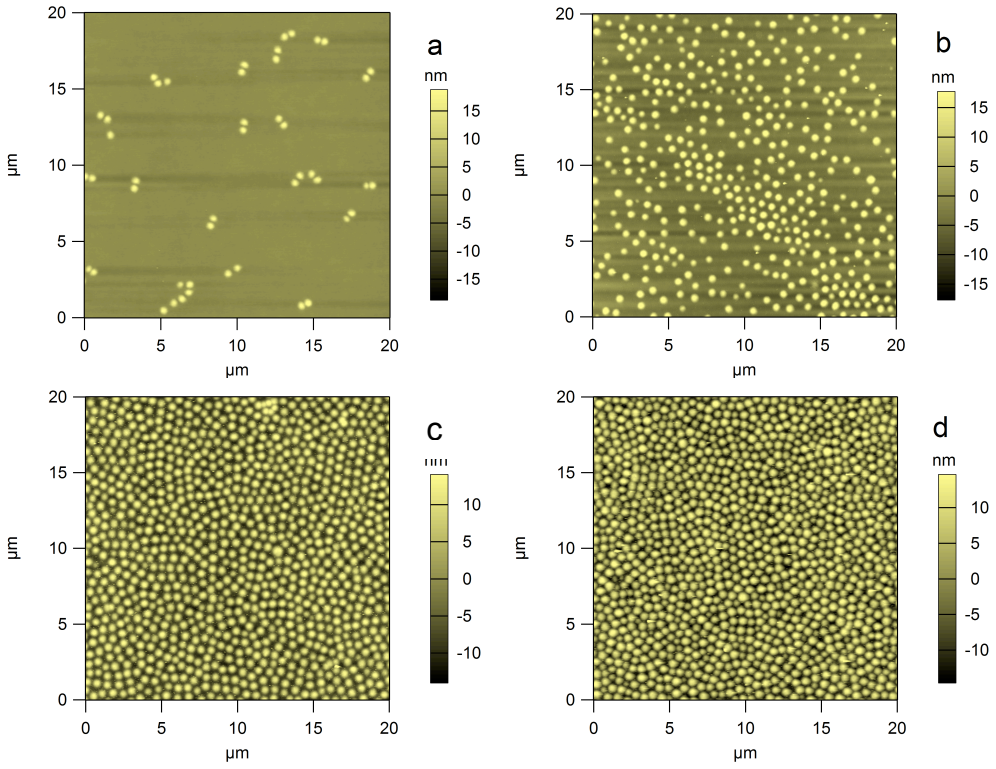

Figure 4.2 AFM height images collected in air of (a) Core 1, (b) Core 2, (c) Core 1/Shell 1, and (d) Core 2/Shell 2.

Table 4.3 DLS data (nm) and de-swelling temperatures (°C) for core/shell microgels

	R_H pH 3	R_H pH 7.4	Dispersion DI Water	Dispersion pH 3	Dispersion pH 7.4	Film pH 3	Film pH 7.4
Core 1	212±28	209±32	32	--	--	--	--
C1/S1	273±38	336±52	--	32	31	31	31
Core 2	228±24	228±33	39	--	--	--	--
C2/S2	258±36	301±46	--	38	38	37	38

Two core particles with differing polymer composition were prepared (**Table 4.2**, and **Figure 4.2**). The thermoresponsivity of Core 1 (C1) comes solely from pNIPAm, while Core 2 (C2) is a copolymer of NIPAm and NIPMAm. The shell added to both cores is composed of pNIPMAm to prevent shell thermoresponsivity from interfering with core deswelling. AFM height images of the core/shell microgels are presented in **Figure 4.2c,d**. Following shell addition the microgels display pH-dependent swelling as observed by the increased hydrodynamic radii at pH 7.4 compared to pH 3 (**Table 4.3**). The response temperatures of the core and core/shell microgels as determined via temperature-dependent light scattering are also presented in **Table 4.3**. Importantly, the core/shell microgels respond at similar temperatures at both pH 3 and 7.4 in dispersions and when assembled into polyelectrolyte films. **Figure 4.3** compares the deswelling curves of core/shell microgel films and analogous traditional microgel films (Microgels 1 and 3) at pH 3 and 7.4. In both systems the core/shell microgel films maintain the ability to respond to temperature as expected given the polymer composition despite the change in pH. Again, it can be seen that the traditional films lack this predictability at pH 7.4. As hypothesized, separating the pH and temperature responsive elements results in microgels and films with pH-independent temperature responsivities.

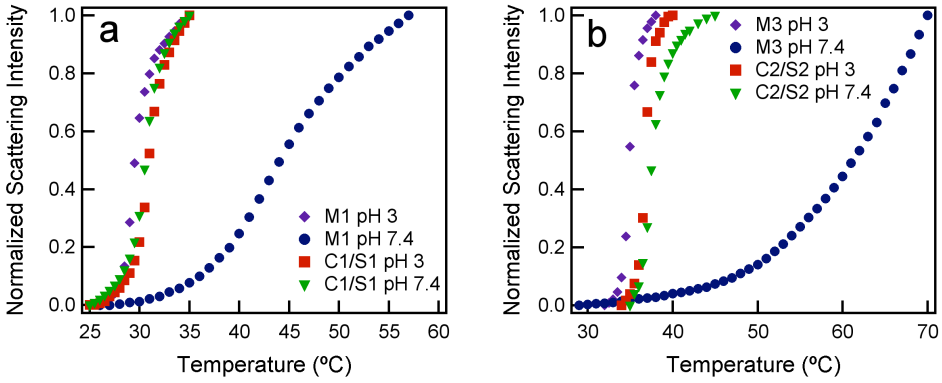

Figure 4.3 Normalized DST curve comparison of microgel/PDADMAC films: (a) Microgel 1 and Core 1/Shell 1, (b) Microgel 3 and Core 2/Shell 2 at pH 3 and pH 7.4.

While increases in scattered light intensity are generally representative of swelling changes occurring within the film, which can result in differences in refractive index heterogeneity, scattering is not a direct measure of film deswelling. Through the use of in-liquid AFM we studied the impact of temperature and pH on the swelling/deswelling of traditional and core/shell films in situ. These experiments provided a means to directly observe the bulk film response to environmental conditions.

Multilayer microgel/PDADMAC films (10 layers each) were prepared on glass substrates. The films were cut multiple times to expose the substrate and imaged across the cut. Imaging was done in buffer at ~26 °C (below DST) and 50 °C (above DST). Representative AFM height images of Microgel 3 and Core 2/Shell 2 films in each imaging environment are presented in **Figures 4.4 and 4.5**. All films are swollen at ~26 °C in both pH environments. For the Microgel 3 film, a change in topography is observed at pH 3 upon increasing the environmental temperature to 50 °C (**Figure 4.4a,b**). However, topographical changes are not observed upon increasing the temperature when the film is immersed in pH 7.4 buffer (**Figure 4.4c,d**). A drastic topographic change can be seen for the Core 2/Shell 2 film at pH 3 after the temperature is raised to 50 °C (**Figure 4.5a,b**). In addition, some slight changes in the topography are also observed at pH 7.4 following an increase in temperature from ~26 °C to 50 °C (**Figure 4.5c,d**). These

in situ observations demonstrate that the topography of the interface can be altered through changes in the environmental conditions.

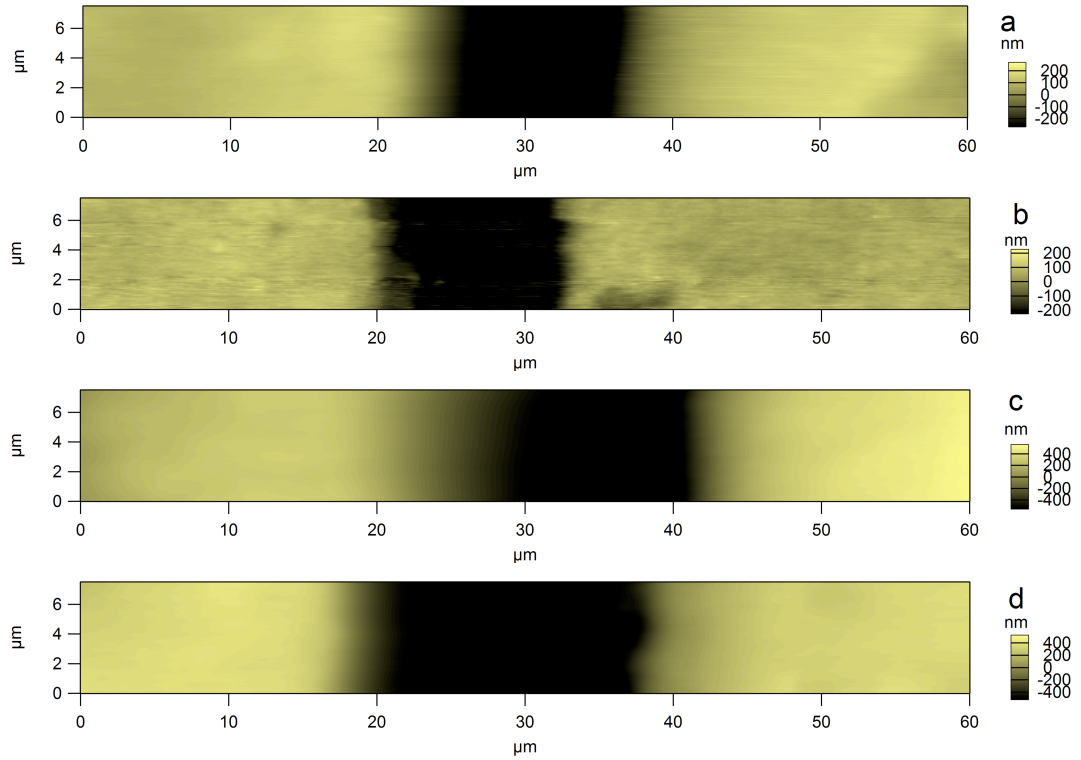

Figure 4.4 AFM height trace images of a 10-layer Microgel 3 film at pH 3, ~26 and 50 °C (a, b, respectively) and at pH 7.4, ~26 and 50 °C (d, c, respectively).

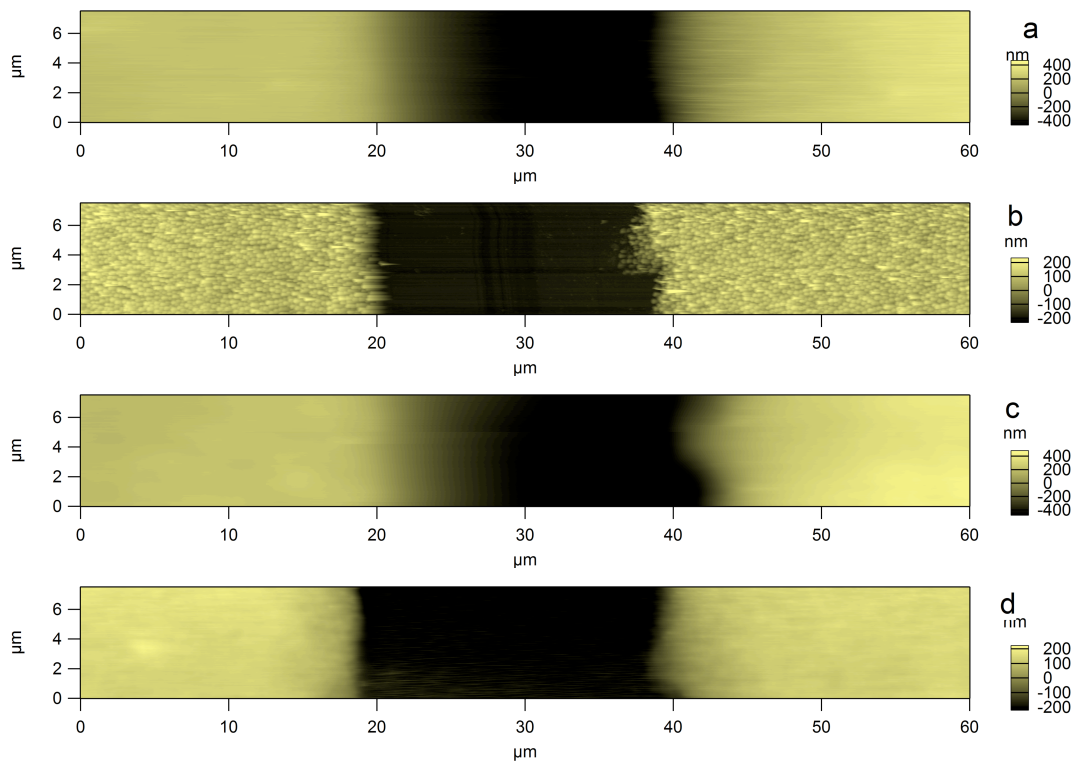

Figure 4.5 AFM height trace images of a 10-layer Microgel Core 2/Shell 2 film at pH 3, ~26 and 50 °C (a, b, respectively) and at pH 7.4, ~26 and 50 °C (d, c, respectively).

The calculated film thickness measurements from height trace and retrace data for each film are presented in **Tables 4.4 and 4.5**, respectively. For clarity only the film thickness measurements from height trace data are presented in **Figure 4.6**. Films composed of core/shell microgels exhibit a decrease in measured thickness at 50 °C in both pH 3 and pH 7.4 buffers (**Figure 4.6b,d**). This agrees with the results of light scattering experiments where the light scattering intensity has increased at temperatures above the DST. Deswelling of films composed of Microgels 1 and 3 is observed at pH 3 upon increasing the temperature from ~26 to 50 °C, but minimal changes in thickness are observed for the traditional films at pH 7.4 after increasing the temperature, in accordance with the light scattering data (**Figure 4.6a,c**). These results suggest that the bulk responses of the films agree with the internal structuring observed by light scattering.

Table 4.4. Average Film Thicknesses (nm) for Traditional and Core/Shell Microgel Films Calculated from AFM Height Traces

Film Type	pH 3 ~26 °C	pH 3 50 °C	% Change	pH 7.4 ~26 °C	pH 7.4 50 °C	% Change
Microgel 1	291±38	249±11	-14%	462±54	463±40	+0.2%
Microgel 3	796±150	309±41	-61%	1012±179	1118±262	+10%
Core 1/Shell 1	707±88	302±18	-57%	662±98	521±66	-21%
Core 2/Shell 2	791±129	336±38	-58%	906±69	424±64	-53%

Table 4.5. Average Film Thicknesses (nm) for Traditional and Core/Shell Microgel Films Calculated from AFM Height Retraces

Film Type	pH 3 ~26 °C	pH 3 50 °C	% Change	pH 7.4 ~26 °C	pH 7.4 50 °C	% Change
Microgel 1	288±45	248±11	-14%	456±54	450±48	-1%
Microgel 3	766±193	309±44	-60%	1003±190	1113±282	+11%
Core 1/Shell 1	695±89	293±22	-58%	686±78	522±75	-24%
Core 2/Shell 2	790±97	331±39	-58%	900±74	425±59	-53%

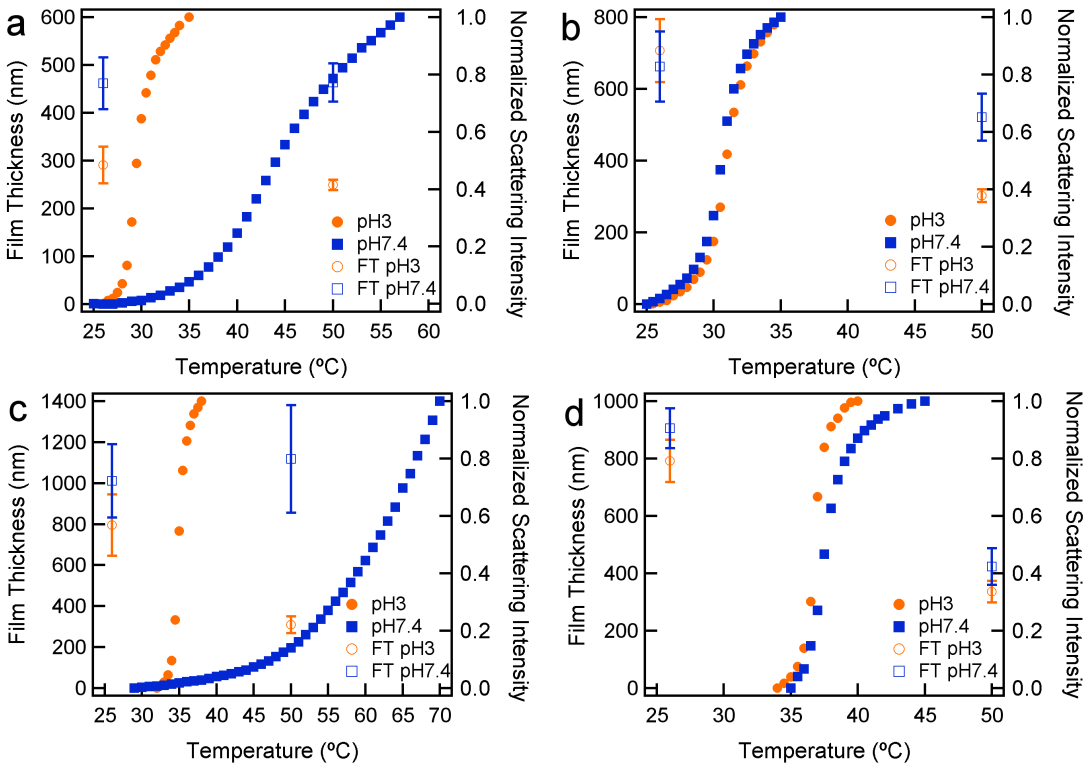

Figure 4.6 Comparison of film thicknesses from AFM measurements and DST curves at pH 3 and pH 7.4: (a) Microgel 1, (b) Core 1/Shell 1, (c) Microgel 3, (d) Core 2/Shell 2.

LbL deposition of temperature responsive microgels is a facile method for preparing thermoresponsive interfaces. In this chapter we demonstrate the versatility of this approach by tailoring the properties of the individual microgel building blocks prior to film assembly. The films were found to swell or deswell in accordance with the polymer composition and architecture of the particles. The resulting control over the swelling and responsivity of the assembly presents new opportunities to modulate the mechanics of the interface or to potentially direct the three-dimensional shape of microgel assemblies[26] using readily available stimuli.

4.4 Conclusion

We demonstrate that the temperature response of pNIPAm, pNIPMAm, and p(NIPAm-co-NIPMAm) microgel LbL films is dependent on the pH environment. When AAc is incorporated throughout the network, deprotonation at pH 7.4 results in inhibited deswelling either due to charge repulsion, counterion ingress, and/or increased complexation with polycation. Localizing the acidic groups to the particle periphery in core/ shell microgels permits pH-independent film thermoresponsivity as observed by light scattering and in-liquid AFM. The modular nature of the film assembly process permits tailoring of the bulk properties through independent evolution of the constituent building blocks. The potential to incorporate multiple microgel types within a single construct is a powerful strategy for designing complex systems from simple components.

4.5 References

(1) Decher, G., Fuzzy Nanoassemblies: Toward Layered Polymeric Multicomposites. *Science* **1997**, *277*, 1232-1237.

(2) Decher, G.; Hong, J.D.; Schmitt, J., Buildup of Ultrathin Multilayer Films by a Self-Assembly Process: III. Consecutively Alternating Adsorption of Anionic and Cationic Polyelectrolytes on Charged Surfaces. *Thin Solid Films* **1992**, *210-211*, 831-835.

(3) Sukhishvilli, S.A.; Granick, S., Layered, Erasable, Ultrathin Polymer Films. *J. Am. Chem. Soc.* **2000**, *122*, 9550-9551.

(4) Such, G.K.; Johnston, A.P.R.; Caruso, F., Engineered Hydrogen-Bonded Polymer Multilayers: From Assembly to Biomedical Applications. *Chem. Soc. Rev.* **2011**, *40*, 19-29.

(5) Hong, J.; Kim, B-S.; Char, K.; Hammond, P.T., Inherent Charge-Shifting Polyelectrolyte Multilayer Blends: A Facile Route for Tunable Release from Surfaces. *Biomacromolecules* **2011**, *12*, 2975-2981.

(6) Saurer, E.M.; Flessner, R.M.; Sullivan, S.P.; Prausnitz, M.R.; Lynn, D.M., Layer-by-Layer Assembly of DNA- and Protein-Containing on Microneedles for Drug Delivery to the Skin. *Biomacromolecules* **2010**, *11*, 3136-3143.

(7) Wang, Y.; Angelatos, A.S.; Caruso, F., Template Synthesis of Nanostructured Materials via Layer-by-Layer Assembly. *Chem. Mater.* **2008**, *20*, 848-858.

(8) Hua, F.; Shi, J.; Lvov, Y.; Cui, T., Patterning of Layer-by-Layer Self-Assembled Multiple Types of Nanparticle Thin Films by Lithographic Technique. *Nano Lett.* **2002**, *2*, 1219-1222.

(9) Tan, W. S.; Cohen, R. E.; Rubner, M. F.; Sukhishvili, S. A., Temperature-Induced, Reversible Swelling Transitions in Multilayers of a Cationic Triblock Copolymer and a Polyacid. *Macromolecules* **2010**, *43*, 1950-1975.

(10) Kim, B-S.; Park, S. W.; Hammond, P. T., Hydrogen-Bonding Layer-by-Layer-Assembled Biodegradable Polymeric Micelles as Drug Delivery Vehicles from Surfaces. *ACS Nano* **2008**, *2*, 386-392.

(11) Yoo, D.; Shiratori, S.S.; Rubner, M.F., Controlling Bilayer Composition and Surface Wettability of Sequentially Adsorbed Multilayers of Weak Polyelectrolytes. *Macromolecules* **1998**, *31*, 4309-4318.

(12) Shiratori, S.S.; Rubner, M.F., pH-Dependent Thickness Behavior of Sequentially Adsorbed Layers of Weak Polyelectrolytes. *Macromolecules* **2000**, *33*, 4213-4219.

(13) Dubas, S.T.; Farhat, T.R.; Schlenoff, J.B., Multiple Membranes from "True" Polyelectrolyte Multilayers. *J. Am. Chem. Soc.* **2001**, *123*, 5368-5369.

(14) Cho, J.; Caruso, F., Polymeric Multilayer Films Comprising Deconstructable Hydrogen Bonded Stacks Confined between Electrostatically Assembled Layers. *Macromolecules* **2003**, *36*, 2845-2851.

(15) Sun, B.; Flessner, R.M.; Saurer, E.M.; Jewell, C.M.; Fredin, N.J.; Lynn, D.M., Characterization of pH-Induced Changes in the Morphology of Polyelectrolyte Multilayers Assembled from Poly(allylamine) and Low Molecular Weight Poly(acrylic acid). *J. Colloid Interface Sci.* **2011**, *355*, 431-441.

(16) Serpe, M.J.; Jones, C.D.; Lyon, L.A., Layer-by-Layer Deposition of Thermoresponsive Microgel Thin Films. *Langmuir* **2003**, *19*, 8759-8764.

(17) South, A.B; Whitmire, R.E.; Garcia, A.J.; Lyon, L.A., Centrifugal Deposition of Microgels for the Rapid Assembly of Nonfouling Thin Films. *ACS Appl. Mater. Interfaces* **2009**, *1*, 2747-2754.

(18) Hendrickson, G.R.; Smith, M.H.; South, A.B.; Lyon, L.A., Design of Multiresponsive Hydrogel Particles and Assemblies. *Adv. Funct. Mater.* **2010**, *20*, 1697-1712.

(19) Pelton, R., Temperature-Sensitive Aqueous Microgels. *Adv. Colloid Interface Sci.* **2000**, *85*, 1-33.

(20) Clarke, K.C.; Lyon, L.A., Modulation of the Deswelling Temperature of Thermoresponsive Microgel Films. *Langmuir* **2013**, *29*, 12852-12857.

(21) Serpe, M.J.; Lyon, L.A., Optical and Acoustic Studies of pH-Dependent Swelling in Microgel Thin Films. *Chem. Mater.* **2004**, *16*, 4373-4380.

(22) Sorrell, C.D.; Lyon, L.A., Bimodal Swelling Responses in Microgel Thin Films. *J. Phys. Chem. B* **2007**, *111*, 4060-4066.

(23) Jones, C.D.; Lyon, L.A., Synthesis and Characterization of Multiresponsive Core-Shell Microgels. *Macromolecules* **2000,** *33*, 8301-8306.

(24) Nayak, S.; Debord, S.B.; Lyon, L.A., Investigations into the Deswelling Dynamics and Thermodynamics of Thermoresponsive Microgel Composite Films. *Langmuir* **2003**, *19*, 7374-7379.

(25) Weissman, J.M.; Sunkara, H.B.; Tse, A.S.; Asher, S.A., Thermally Switchable Periodicities and Diffraction from Mesoscopically Ordered Materials *Science* **1996**, *274*, 959-960.

(26) Zhang, L.; Spears Jr., M.W.; Lyon, L.A., Tunable Swelling and Rolling of Microgel Membranes *Langmuir* **2014**, *30*, 7628-7634.

CHAPTER 5

MICROGEL SURFACE MODIFICATION BY A SELF-ASSEMBLING PEPTIDE

5.1 Introduction

Colloidal particles have found versatile utility in biotechnological applications, including therapeutic delivery, disease targeting, and diagnostics.[1-5] An important contribution to their use is the modification of the particle surface.[6] For example, the direct conjugation of polymers and biomolecules has been routinely used to enhance biocompatibility and site-specific targeting, respectively.[7,8] Additional tactics include layer-by-layer (LbL) assembly onto the particle surface, where linear polymers or biomacromolecules, often of opposite charge, are deposited in alternating fashion onto the colloidal substrate.[9] This allows for the controlled build-up of particle coatings that can be further modified if necessary. By and large, the ability to revise the surface properties of micro and nanomaterials has extended and enhanced their applicability in biotechnology.

Our group, among others, has investigated microgels, polymeric colloidal particles, highly solvated with water, for numerous biotechnological applications.[10-13] Their high water content, facile synthesis, and favorable mechanical properties make microgels a practical and advantageous class of biomaterials. Furthermore, microgel networks can be rendered environmentally responsive (e.g. temperature, pH, light) by synthesizing them from stimuli-responsive polymers.[14] Our group has worked extensively with temperature responsive microgels synthesized from *N*-isopropylacrylamide (NIPAm).[15] Co-monomers, such as acrylic acid (AAc) are commonly incorporated to add pH responsivity and functional groups for post-synthetic modifications. Further, microgel

shells can be added directly to the core particles, and in so doing responsive elements and functional groups can be compartmentalized.[16]

Traditionally target molecules are directly conjugated to microgels using functional groups polymerized into the network.[17-19] However, the ease of co-polymer incorporation can vary, potentially reducing the number and type of chemical handles that can be contained within a single particle.[20,21] Recently, an alternative approach to modify microgel interfaces was demonstrated in which microgels were employed as a substrate for LbL deposition.[22] However, the potential for these constructs in biomedical applications has yet to be fully investigated.

Peptides and proteins serve a wide array of functions in biological systems, making them an important building block in biomaterials.[23-25] Their diversity allows them to serve both biochemical and biophysical roles, helping to create functional materials that more readily recapitulate the chemistry and mechanics of native tissues. Peptides have the ability to span multiple length scales, from the molecular to the macroscopic, because of their propensity to self-assemble into secondary structures (i.e. α-helices and β-sheets).[26-30] This long-range assembly has been of particular interest in the development of cell and tissue scaffolding. Furthermore, the capacity to incorporate non-natural amino acids for selective bioconjugation reactions enhances the versatility of the peptide platform.[23,31]

In this work we demonstrate the modification of microgel surfaces using a self-assembling peptide, RADA. RADA is a 16 amino acid peptide where the sequence, arginine-alanine-aspartic acid-alanine is repeated four times. This peptide self-assembles into β-sheet fibrils, and finally into a macroscopic hydrogel when exposed to physiological ionic strengths.[32,33] Much of the attention RADA has received has focused on the use of RADA gels as cell culture substrates for tissue engineering.[34-36] In the present study, RADA fibrils are observed to assemble on the surface of anionic, thermoresponsive microgels. Appending a cysteine residue to the peptide permits post-

assembly conjugation reactions through the thiol chemoligation site. The modular nature of this biosynthetic construct permits independent tailoring of the interior particle and the exterior peptide shell. This new core/shell structure could have potential as a building block within extracellular matrix mimetic scaffolds.[37]

5.2 Experimental

5.2.1 Materials

Chemicals were purchased from Sigma-Aldrich, unless noted otherwise. RADA peptides were purchased from Anaspec (Ac-$(RADA)_4$-Am) and Genscript (TMR-$(RADA)_4$-Am and Ac-$(RADA)_4$C-Am). Q11 was generously supplied by Tom Barker's group. RADA, RADAC, and Q11 were dissolved in DI water and sonicated for 30 min before use; RADA-TMR was dissolved in DMSO (2.5 mg/mL). NIPAm and NIPMAm were recrystallized from hexanes (BDH Chemical). *N*,*N*'-methylenebisacrylamide (BIS) and acrylic acid (AAc, Fluka) were used as received. The surfactant, sodium dodecylsulfate (SDS), and initiator, ammonium persulfate (APS) were used as received. The following materials were used in the preparation of buffers: HEPES, formic acid, and sodium chloride. All water was distilled and deionized to a resistance of 18 MΩ (Barnstead E-pure).

5.2.2 Microgel Synthesis

Microgels were synthesized via aqueous free-radical precipitation polymerization as described in **Section 3.2.2**. Ultra low crosslinked (ULC) microgels were synthesized in an analogous fashion except the reaction was performed without the addition of BIS to the monomer solution.[38] Refer to **Table 5.1** for feed concentrations of microgels used in these studies. Purified microgels were lyophilized and redispersed in DI water before use.

5.2.3 Microgel Characterization

Dynamic light scattering (DLS, Wyatt Protein Solutions) was used to determine the hydrodynamic radius (R_H) of the microgels as previously described in **Section 3.2.3**. Purified microgels were dispersed in pH 3 formate buffer (0.1 *M*, 5 m*M* ionic strength) and pH 7.4 HEPES buffer (0.1 *M*, 5 m*M* ionic strength).

5.2.4 Preparation of Peptide-Coated Microgels

Microgels were redispersed in DI water and diluted to 0.75 mg/mL. RADA, RADAC, and Q11 were dissolved in DI water, sonicated for 30 min, and diluted to 0.5 mg/mL. TMR-RADA in DMSO was added to RADA or RADAC solutions to make up 0.5 wt% of the total RADA, and the mixture was sonicated for 5 min. Microgel and RADA/RADAC/Q11 solutions were cooled to 4 °C. RADA/RADAC was added to the microgel solution, and mixed at 4 °C for 1 hr. The microgel solution volume was always double the peptide solution volume. The resulting mixture was dialyzed against DI water at 4 °C in cellulose ester membranes (MWCO 1000 kDa). Flocculation resulted upon addition of Q11 to the microgel solution, so this mixture was not mixed for the full hour or dialyzed. For post-assembly conjugation of 5-iodoacetamidofluorescein (5-IAF) to RADAC on the microgel surface, 5-IAF (1.0 m*M* stock solution in DMF) was added to RADAC-coated Microgel 1 at room temperature for 2 hrs. 5-IAF was conjugated at 10 fold molar excess to 1.0 wt% of the theoretical quantity of RADAC added during the coating process. As a control, RADA-coated Microgel 1 and uncoated Microgel 1 were also mixed with 5-IAF for 2 hrs to confirm labeling *via* reaction with the cysteine. The mixtures were dialyzed against DI water in the dark at 4 °C in cellulose ester membranes (MWCO 1000 kDa).

5.2.5 Circular Dichroism

A JASCO-J810 spectropolarimeter was used to determine the conformation of the RADA peptides and RADA-coated microgels. RADA stock solutions were diluted with DI water to a final concentration of 12.5 μ*M*. RADA-TMR was added to a solution of plain RADA to have a final concentration of 0.5 wt% of the total mass of RADA. Microgel 1 before and after coating was diluted to 0.17 mg/mL. Microgels 2 and 3 (0.5 mg/mL in DI water) before and after peptide coating were used as prepared. Aliquots of microgels samples were centrifuged to form a pellet and the supernatant was collected and analyzed by CD. Images of fluorescently labeled pellets were collected following centrifugation. All samples were placed in a quartz cuvette (1 mm pathlength) and scanned from 250-190 nm. Data presented is the average of 4 scans.

5.2.6 Atomic Force Microscopy

Microgel aliquots (1 μL diluted with 25 μL DI) before and after peptide coating were dried on a glass coverslip and imaged using an Asylum MFP-3D atomic force microscope (AFM). Imaging was performed in air operating in intermittent contact mode using silicon nitride cantilevers (k=42 N/m, Nanoworld). Data was processed through software written in the IgorPro environment (Wavemetrics).

5.2.7 Optical Microscopy

The presence of fluorescently labeled RADA or RADAC localized on microgels was visualized using fluorescence microscopy (Olympus IX-71). Microgel aliquots (1 μL) were diluted with 25 μL DI, dried on glass coverslips, and imaged with a 100x oil immersion objective. The exposure was set to 250 ms for all fluorescence images. For fluorescence intensity analysis of Microgel 1 coated with RADA/TMR-RADA and RADAC/5-IAF, aliquots of as-prepared coated-microgels (5 μL) were diluted with DI water (10 μL) and dried on glass coverslips. For plain Microgel 1, a stock solution of 0.5

mg/mL in DI water was used. Five images were collected for each sample, and ImageJ was used to calculate the average fluorescence intensities of each image. The final average and standard deviation of the five images is provided. Brightfield microscopy was also used to image microgels incubated with peptides. Images were acquired using a 100x oil immersion objective.

5.3 Results and Discussion

Microgels are soft, polymeric particles. Typical modifications to microgels are achieved synthetically through the incorporation of co-monomers or the addition of a polymer shell. Functional groups incorporated into the network can subsequently be employed for post-synthetic conjugation reactions. In the present study we explore the utility of self-assembling peptides for the modification of microgel surfaces. One such peptide is RADA, which assembles into β-sheet fibrils due to the alternating hydrophobic and hydrophilic residues. A RADA peptide shell assembles onto the surface of Microgel 1 by simply mixing the two solutions. AFM amplitude images reveal fibrils on the surface of the particles after incubation with RADA (**Figure 5.1b**). For reference, an image of unmodified microgels is presented in **Figure 5.1a**.

Table 5.1 Polymer Feed Ratios of Microgel Syntheses

Microgel	mol% NIPAm	mol% NIPMAm	mol% AAc	mol% BIS
1	22	66	10	2
2	93	0	5	2
3	78	0	20	2
4	90	0	10	0
5	98	0	0	2
6	49	49	0	2

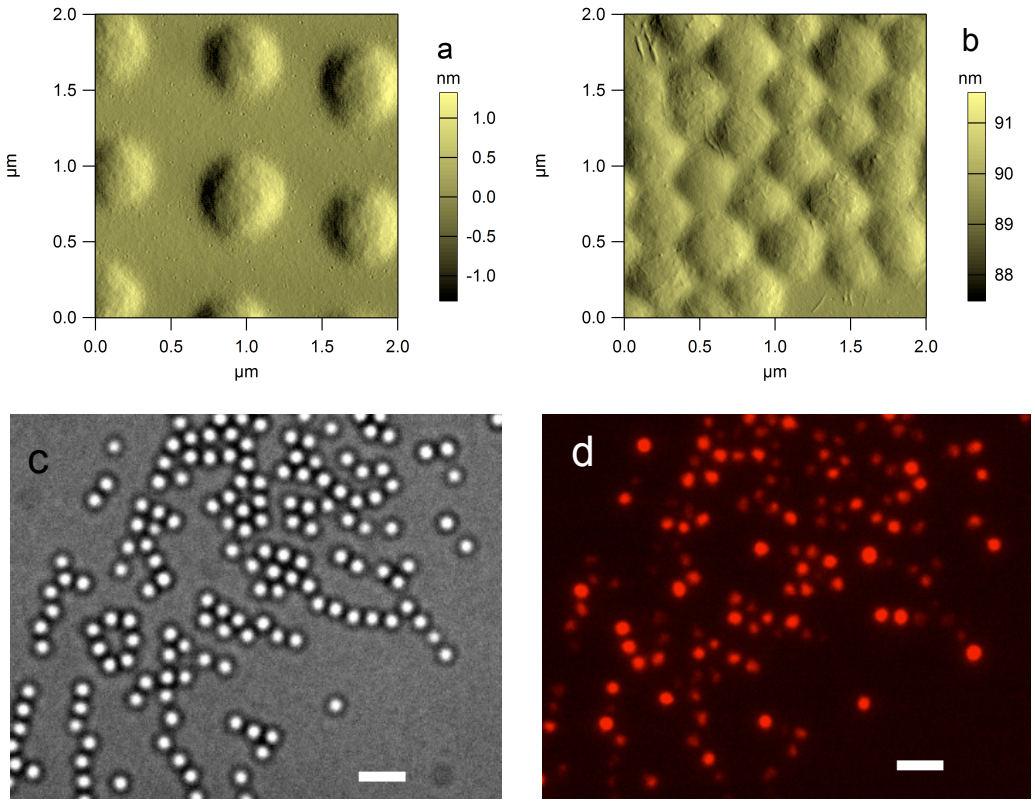

Figure 5.1. AFM amplitude images (a) Microgel 1, (b) Microgel 1+RADA; (c) brightfield and (d) fluorescence microscopy images of Microgel 1+RADA+TMR (scale bar = 2 µm).

Numerous studies with RADA gels have utilized co-assemblies where plain RADA is doped with modified RADA peptides before gelation.[33,35,39] In essence this would permit the inclusion of a variety of functional ligands to be co-assembled into a single construct. As a proof of concept we co-assembled RADA with a rhodamine-labeled RADA peptide (TMR) onto the surface of Microgel 1. Particles present in the brightfield image (**Figure 5.1c**) also appear red in the fluorescence image (**Figure 5.1d**), indicating successful assembly onto the particles. DLS data show good agreement in hydrodynamic radii before and after coating at pH 3 and 7, suggesting that the peptide shell is quite thin.

Table 5.2. Hydrodynamic Radii (nm) of Microgel 1 (M1) Coated with RADA/RADAC

	R_H pH 3	R_H pH 7
M1	261±36	352±63
M1+RADA+TMR	282±56	365±92
M1+RADAC	259±37	344±66
M1+RADAC+TMR	267±46	355±63
M1+RADAC+5IAF	258±37	345±64

Microgel 1 was initially selected because it has a response temperature of 38 °C, close to physiological temperature.[39] After the initial observation of the peptide coating, we explored the use of different microgel polymer compositions in the assembly. Microgels 2 and 3 (synthesized with 5 and 20% AAc, respectively) demonstrated successful coatings with RADA (**Figure 5.2a-d**). Ultra-low, self-crosslinked microgels (Microgel 4) co-polymerized with AAc also show evidence of a RADA peptide shell (**Figure 5.2e,f**). However, microgels lacking AAc resulted in flocculation when the peptide and microgel solutions were mixed (**Figure 5.3**). This suggests that the anionic microgel network is important in stabilizing the colloidal dispersion.

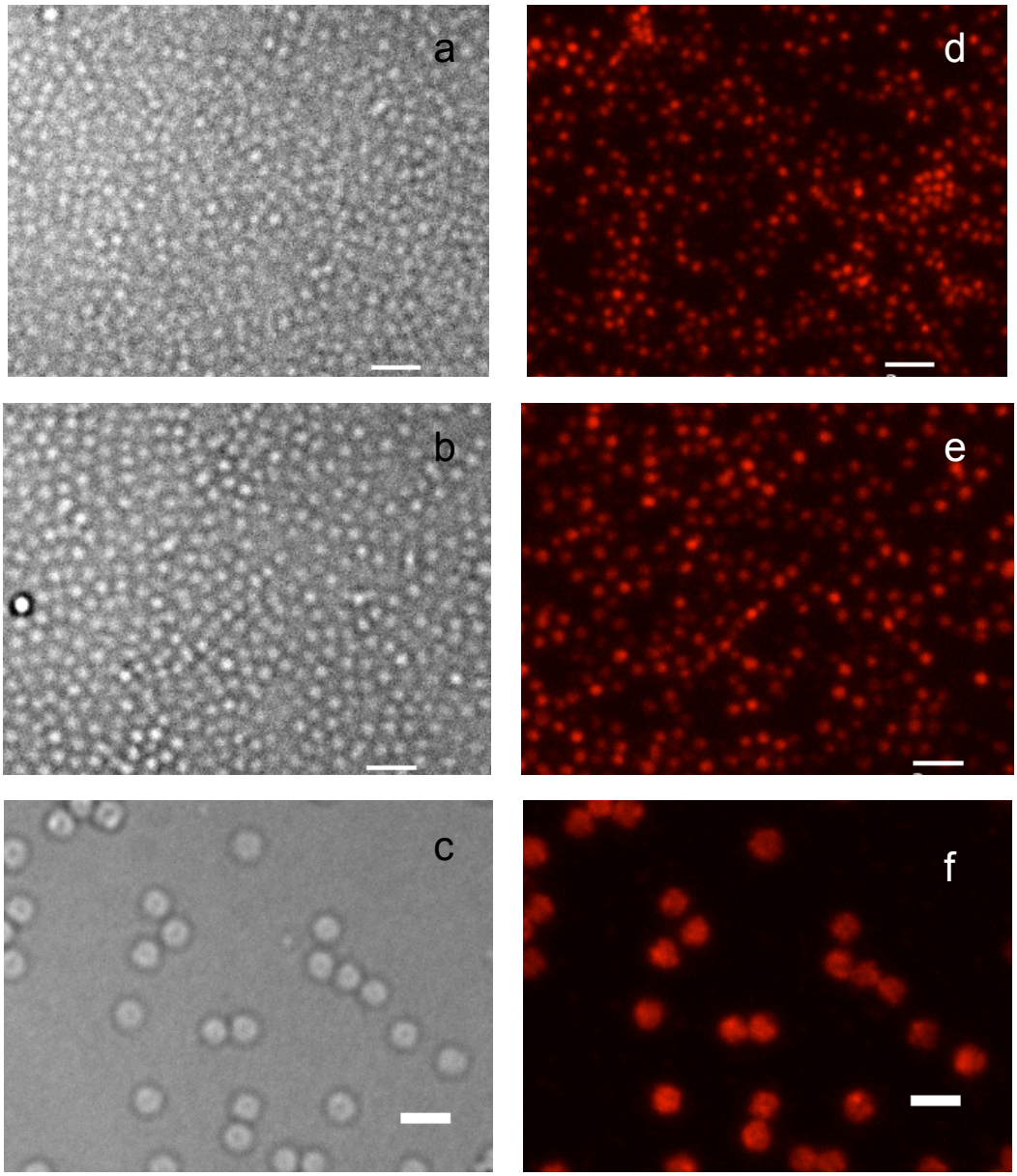

Figure 5.2. Microscopy images of Microgels 2-4 after coating with RADA+TMR, (a-c, respectively) brightfield and (d-f, respectively) fluorescence (scale bar = 2 μm).

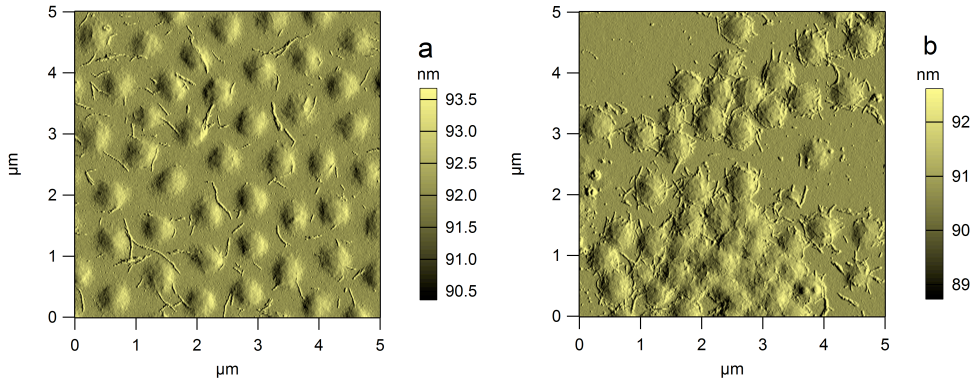

Figure 5.3. AFM amplitude images of Microgels 5 (a) and 6 (b) after incubation with RADA.

We next considered the possibility of post-assembly conjugation to the RADA shell. A cysteine residue was added to the C-terminus of a RADA peptide, to provide a thiol for the conjugation of 5-IAF. RADAC and Microgel 1 were mixed, dialyzed, and then reacted with 5-IAF. Following a second round of dialysis, the particles were analyzed by fluorescence microscopy. As expected, the particles fluoresce green, indicating successful conjugation of the fluorophore (**Figure 5.4b**). Mixtures of Microgel 1 and plain RADA-coated Microgel 1 with 5-IAF did not result in significant labeling (**Table 5.3**). The RADAC coating can be observed in AFM amplitude images (**Figure 5.4a**). Next, RADAC and TMR were mixed and co-assembled on the surface of Microgel 1. Subsequent labeling with 5-IAF demonstrated the potential to incorporate functionality both during and after surface assembly (**Figure 5.4d-f** and **Table 5.3**). Aliquots of each solution were centrifuged to form a pellet. Each pellet is colored in accord with the fluorophores either co-assembled or conjugated to the RADAC shell: unlabeled is colorless, TMR labeled is pink, 5-IAF labeled is yellow, and TMR/5IAF is orange (**Figure 5.5**).

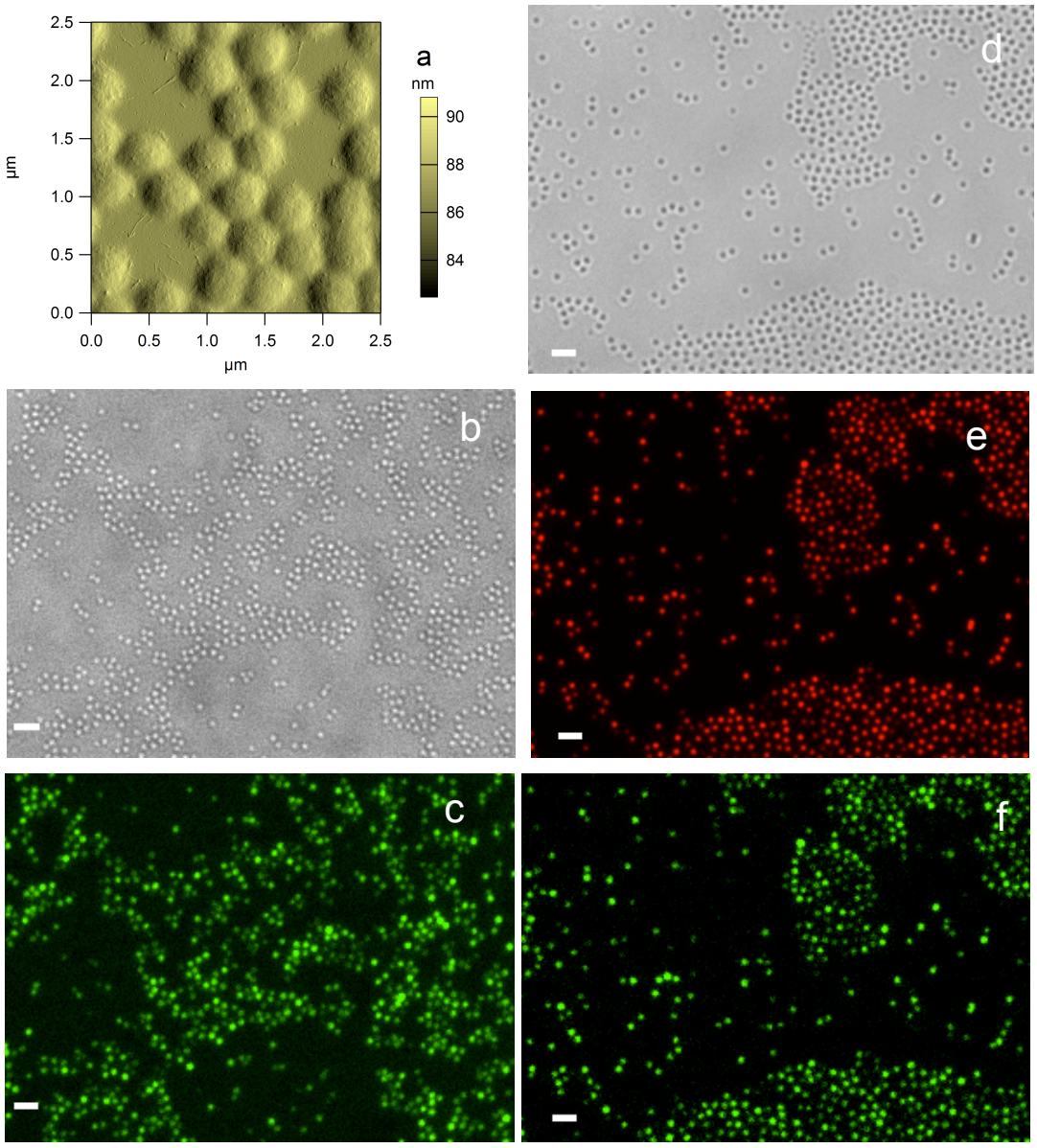

Figure 5.4. (a) AFM amplitude image of Microgel 1+RADAC; (b) brightfield and (c) fluorescence microscopy images of Microgel 1+RADAC after labeling with 5-IAF; (d) brightfield and (e,f) fluorescence microscopy of Microgel 1+RADAC+TMR after labeling with 5-IAF (scale bar=2 µm).

Table 5.3. Average Fluorescence Intensities of RADA-Coated Microgel 1 Images

	Microgel 1	+5IAF	+RADA +TMR	+RADA +TMR +5IAF	+RADAC +TMR	+RADAC +5IAF	+RADAC +TMR +5IAF
Green Ex	103±0	104±0	193±15	194±48	412±52	108±3	471±42
Blue Ex	103±0	106±1	104±0	103±0	105±1	169±18	146±14

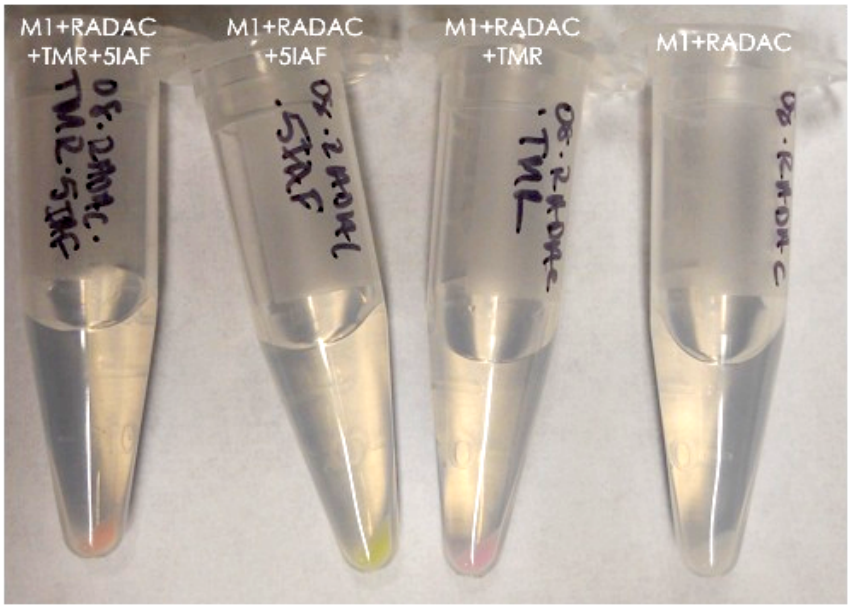

Figure 5.5. Microgel 1+RADAC pellets following centrifugation.

RADA is known to assemble into β-sheets. However, it was unknown whether the secondary structure would be maintained on the microgel surface. CD spectroscopy was used to analyze RADA-coated microgels for β-sheet secondary structure. CD spectra of RADA and RADAC in DI water present typical bands for β-sheets (**Figure 5.6a**). Microgel 1 coated with RADA and RADAC display similar bands suggesting that the peptide fibrils retain the β-sheet structure on the surface of the particles (**Figure 5.6b**). CD spectra of microgels alone and supernatants collected after centrifuging the particles do not show any bands indicative of secondary structure. Furthermore, the spectra of Microgels 2 and 3 also have bands indicative of β-sheets (**Figure 5.6c,d**, respectively).

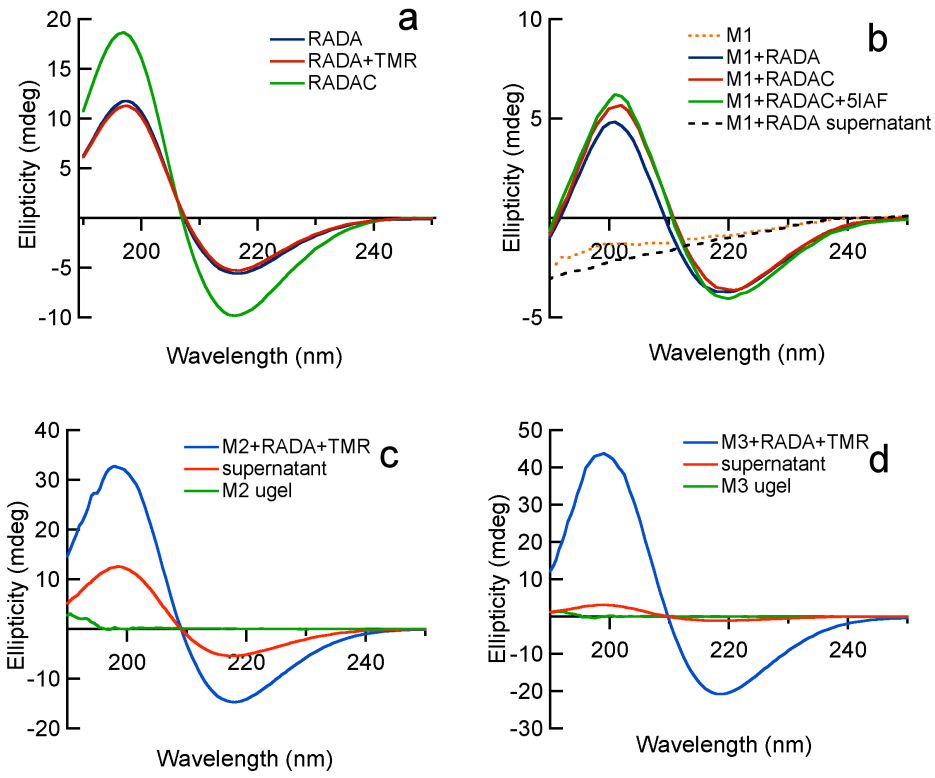

Figure 5.6. CD spectra in DI water of (a) RADA peptides (20 μ*M*), and (b-d) Microgels 1, 2, 3, respectively, uncoated and after incubation with RADA peptides.

The supernatants from Microgels 2 and 3 show the presence of β-sheets, likely due to some RADA disassembling from the particle surface.

In addition to RADA, we were curious whether additional self-assembling peptides were capable of coating microgels. We focused on Q11, a β-sheet forming peptide with the sequence Ac-QQKFQFQFEQQ-Am.[40,41] The residues alternate between hydrophobic (phenylalanine) and hydrophilic (glutamine), but unlike RADA, Q11 has fewer charged residues. When Q11 was mixed with Microgel 1, flocculation was immediately observed. When a sample was dried on a coverslip, large aggregates and entanglements are present (**Figure 5.7**). Additionally, all microgels added to Q11 resulted in aggregation (data not shown).

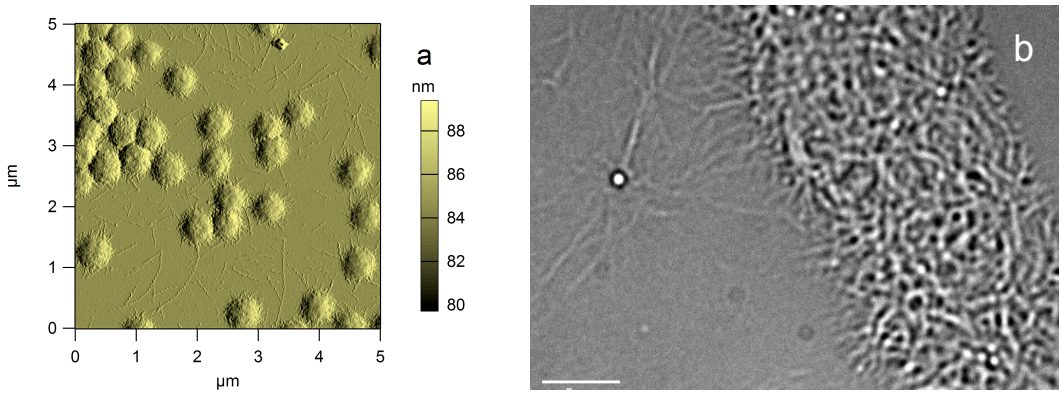

Figure 5.7. Microscopy images of Microgel 1 after mixing with Q11: (a) AFM amplitude image; (b) brightfield image (scale bar = 5 µm).

5.4 Conclusions

In this work we demonstrated the facile assembly of a RADA-based shell onto the surface of microgels. Incorporation of acrylic acid into the microgel network was found to be an important factor in the formation of a stable colloidal solution of coated particles. Two routes were explored for functionalizing the peptide coating: co-assembly of modified peptides and post-assembly functionalization. Both methods permit tailoring of the peptide shell. The surface localized fibrils have a β-sheet secondary structure as confirmed by CD, indicating that the microgels do not interfere with the peptide self-assembly. An alternative β-sheet assembling peptide, Q11, was utilized to investigate the generality of the assembly, but a stable dispersion of Q11-coated particles was not obtained. The microgel core/peptide shell is a modular composite, where each component can be independently modified. In this way a variety of functional constructs can be tailor-made for applications. We are currently interested in the pursuit of new building blocks to modify and enhance extracellular matrix scaffolds for tissue engineering.

5.5 References

(1) Loomis, K.; McNeeley, K.; Bellamkonda, R.V., Nanoparticles with Targeting, Triggered Release, and Imaging Functionality for Cancer Applications. *Soft Matter* **2011**, *7*, 839-856.

(2) Louie, A., Multimodality Imaging Probes: Design and Challenges. *Chem*. *Rev.* **2010**, *110*, 3146-3195.

(3) von Maltzahn, G.; Park, J-H.; Lin, K.Y.; Singh, N.; Schwoppe, C.; Mesters, R.; Berel, W.E.; Ruoslahti, E.; Sailor, M.J.; Bhatia, S.N., Nanoparticles that Communicate In Vivo to Amplify Tumour Targeting. *Nature Mater.* **2011**, *10*, 545-552.

(4) Scheinberg, D.A.; Villa, C.H.; Escorcia, F.E.; McDevitt, M.R., Conscripts of the Infinite Armada: Systemic Cancer Therapy Using Nanomaterials. *Nat. Rev. Clin. Oncol.* **2010**, *7*, 266-276.

(5) Ghosh, P.; Han, G.; De, M.; Kim, C.K.; Rotello, V.M., Gold Nanoparticles in Delivery Applications. *Adv. Drug. Delivery Rev.* **2008**, *60*, 1307-1315.

(6) Algar, W.R.; Prasuhn, D.E.; Stewart, M.H.; Jennings, T.L.; Blanco-Canosa, J.B.; Dawson, P.E.; Medintz, I.L., The Controlled Display of Biomolecules on Nanoparticles: A Challenge Suited to Bioorthogonal Chemistry. *Bioconjugate Chem.* **2011**, *22*, 825-858.

(7) Otsuka, H.; Nagasaki, Y.; Kataoka, K., PEGylated Nanoparticles for Biological and Pharmaceutical Applications. *Adv. Drug. Delivery Rev.* **2003**, *55*, 403-419.

(8) Ruoslahti, E., Peptides as Targeting Elements and Tissue Penetration Devices for Nanoparticles. *Adv. Mater.* **2012**, *24*, 3747-3756.

(9) Becker, A.L; Johnston, A.P.R.; Caruso, F., Layer-by-Layer-Assembled Capsules and Films for Therapeutic Delivery. *Small*, **2010**, *6*, 1836-1852.

(10) Smith, M.H.; Lyon, L.A., Multifunctional Nanogels for siRNA Delivery. *Acc. Chem. Res.* **2012**, *45*, 985-993.

(11) Brown, A.C.; Stabenfeldt, S.E.; Ahn, B.; Hannan, R.T.; Dhada, K.S.; Herman, E.S.; Stefanelli, V.; Guzzetta, N.; Alexeev, A.; Lam, W.A.; Lyon, L.A.; Barker, T.H., Ultrasoft Microgels Displaying Emergent Platelet-Like Behaviours. *Nature Mater.* **2014**, *13*, 1108-1114.

(12) Saxena, S.; Hansen, C.E.; Lyon, L.A., Microgel Mechanics in Biomaterial Design. *Acc. Chem. Res.* **2014**, *47*, 2426-2434.

(13) Milani, A.H.; Freemont, A.J.; Hoyland, J.A.; Adlam, D.J.; Saunders, B.R., Injectable Doubly Cross-Linked Microgels for Improving the Mechanical Properties of Degenerated Intervertebral Discs. *Biomacromolecules* **2012,** *13*, 2793-2801.

(14) Bradley, M., Chemistry at the Polymer-Particle Interface for the Design of Innovative Materials. *Soft Matter* **2012**, *8*, 1268-1274.

(15) Hendrickson, G.R.; Smith, M.H.; South, A.B.; Lyon, L.A., Design of Multiresponsive Hydrogel Particles and Assemblies. *Adv. Funct. Mater.* **2010**, *20*, 1697-1712.

(16) Jones, C.D.; Lyon, L.A., Synthesis and Characterization of Multiresponsive Core-Shell Microgels. *Macromolecules* **2000**, *33*, 8301-8306.

(17) Blackburn, W.H.; Dickerson, E.B.; Smith, M.H.; McDonald, J.F.; Lyon, L.A., Peptide-Functionalized Nanogels for Targeted siRNA Delivery. *Bioconj. Chem.* **2009**, *20*, 960-968.

(18) Nayak, S.; Lee, H.; Chmielewski, J.; Lyon, L.A., Folate-Mediated Cell Targeting and Cytotoxicity Using Thermoresponsive Microgels. *J. Am. Chem. Soc.* **2004**, *126*, 10258-10259.

(19) Meng, Z.Y.; Hendrickson, G.R.; Lyon, L.A., Simultaneous Orthogonal Chemoligations on Multiresponsive Microgels. *Macromolecules* **2009**, *42*, 7664-7669.

(20) Farley, R.; Saunders, B.R., A General Method for Functionalisation of Microgel Particles with Primary Amines Using Click Chemistry. *Polymer* **2014**, *55*, 471-480.

(21) Singh, N.; Lyon, L.A., Synthesis of Multifunctional Nanogels Using a Protected Macromonomer Approach. *Colloid Poly. Sci.* **2008**, *286*, 1060-1069.

(22) Wong, E.W.; Richtering, W., Layer-by-Layer Assembly on Stimuli-Responsive Microgels. *Curr. Opin. Colloid Interface Sci.* **2008**, *13*, 403-412.

(23) Tang, W.; Becker, M.L., "Click" Reactions: A Versatile Toolbox for the Synthesis of Peptide-Conjugates. *Chem. Soc. Rev.* **2014,** *43*, 7013-1039.

(24) Woolfson, D.N.; Mahmoud, Z.N., More than Just Bare Scaffolds: Towards Multi-Component and Decorated Fibrous Biomaterials. *Chem. Soc. Rev.* **2010**, *39*, 3464-3479.

(25) Boekhoven, J.; Stupp, S.I., 25th Anniversary Article: Supramolecular Materials for Regenerative Medicine. *Adv. Mater.* **2014**, *26*, 1642-1659.

(26) Fichman, G.; Gazit, E., Self-Assembly of Short Peptides to Form Hydrogels: Design of Building Blocks, Physical Properties, and Technical Applications. *Acta Biomaterialia* **2014**, *10*, 1671-1682.

(27) Maude, S.; Ingham, E.; Aggeli, A., Biomimetic Self-Assembling Peptides as Scaffolds for Soft Tissue Engineering. *Nanomedicine* **2013**, *8*, 823-847.

(28) Frederix, P.W.J.M.; Scott, G.C.; Abul-Haija, Y.M.; Kalafatovic, D.; Pappas, C.G.; Javid, N.; Hunt, N.T.; Ulijn, R.V.; Tuttle, T., Exploring the Sequence Space for (Tri-)Peptide Self-Assembly to Design and Discover New Hydrogels. *Nature Chem.* **2014**, *7*, 30-37.

(29) Hudalla, G.A.; Sun, T.; Gasiorowski, J.Z.; Han, H.; Tian, Y.F.; Chong, A.S.; Collier, J.H., Gradated Assembly of Multiple Proteins into Supramolecular Materials. *Nature Mater.* **2014**, *13*, 829-836.

(30) Rozkiewicz, D.I.; Meyers, B.D.; Stupp, S.I., Interfacial Self-Assembly of Cell-Like Filamentous Microcapsules. *Angew. Chem. Int. Ed.* **2011**, *50*, 6324-6327.

(31) Dieterich, D.C.; Link, A.J.; Graumann, J.; Tirrell, D.A.; Schuman, E.M., Selective Identification of Newly Synthesized Proteins in Mammalian Cells using Bioorthogonal Noncanonical Amino Acid Tagging (BONCAT). *Proc. Natl. Acad. Sci. USA* **2006**, *103*, 9482-9487.

(32) Zhang, S.; Holmes, T.C.; DiPersio, C.M.; Hynes, R.O.; Su, X.; Rich, A., Self-Complementary Oligopeptide Matrices Support Mammalian Cell Attachment. *Biomaterials* **1995**, *16*, 1385-1393.

(33) Yokoi, H.; Kinoshita, T.; Zhang, S., Dynamic Reassembly of Peptide RADA16 Nanofiber Scaffold. *Proc. Natl. Acad. Sci. USA* **2005**, *102*, 8414-8419.

(34) Wang, X.; Horii, A.; Zhang, S., Designer Functionalized Self-Assembling Peptide Nanofiber Scaffolds for Growth, Migration, and Tubulogenesis of Human Umbilical Vein Endothelial Cells. *Soft Matter* **2008**, *4*, 2388-2395.

(35) Koutsopoulos, S.; Unsworth, L.D.; Nagai, Y.; Zhang, S., Controlled Release of Functional Proteins through Designer Self-Assembling Peptide Nanofiber Hydrogel Scaffold. *Proc. Natl. Acad. Sci. USA* **2009,** *106,* 4623-4628.

(36) Chau, Y.; Luo, Y.; Cheung, A.C.Y.; Nagai, Y.; Zhang, S.; Kobler, J.B.; Zeitels, S.M.; Langer, R., Incorporation of a Matrix Metalloproteinase-Sensitive Substrate into Self-Assembling Peptides – A Model for Biofunctional Scaffolds. *Biomaterials* **2008,** *29,* 1713-1719.

(37) Clarke, K.C.; Douglas, A.M.; Brown, A.C.; Barker, T.H.; Lyon, L.A., Colloid-Matrix Assemblies in Regenerative Medicine. *Curr. Opin. Coll. Interface Sci.* **2013**, *18*, 393-405.

(38) Bachman, H.; Brown, A.C; Clarke, K.C.; Dhaha, K.S.; Douglas, A.M.; Hansen, C.E.; Herman, E.S; Hyatt, J.; Kodlekere, P.; Saxena, S.; Spears, Jr. M.W.; Welsch, N.; Lyon, L.A., Ultrasoft, Highly Deformable Microgels. *Soft Matter* **2015**, *11*, 2018-2028.

(39) Clarke, K.C.; Lyon, L.A., Modulation of the Deswelling Temperature of Thermoresponsive Microgel Films. *Langmuir* **2013**, *29,* 12852-12857.

(40) Jung, J.P.; Gasiorowski, J.Z.; Collier, J.H., Fibrillar Peptide Gels in Biotechnology and Biomedicine. *Biopolymers* **2010,** *94*, 49-59.

(41) Tian, Y.F.; Devgun, J.M.; Collier, J.H., Fibrillized Peptide Microgels for Cell Encapsulation and 3D Cell Culture. *Soft Matter* **2011**, *7,* 6005-6011.

CHAPTER 6

OUTLOOK AND FUTURE DIRECTIONS

6.1 Controlled Swelling of Microgel Coatings

The research discussed in **Chapters 2 and 3** centered on the use of microgel building blocks in thin film assemblies. The films were capable of using both pH and temperature as stimuli to change the surface properties of the substrate. These studies demonstrated that a library of building blocks could be prepared and utilized to fabricate assemblies with predictable responsivities. However, there are still some potential avenues for exploration, specifically in regard to the application of these films as biointerfaces.

Temperature-responsive microgel monolayer films have been employed as cell culture substrates, where temperature-induced switching of the surface from collapsed to swollen was used to delaminate cell sheets.[1] Our group has utilized pNIPAm-based microgel films in a different context. Initial studies elucidated the non-fouling behavior of microgel thin films.[2] More recently, we have explored film mobility to control cell phenotype as opposed to temperature responsivity. When film mobility was reduced by chemically crosslinking the film components (microgels and polycation), increased cell spreading was observed compared to un-crosslinked films.[3]

One possible path moving forward is to employ films with predictable responsivities to control cell behavior as opposed to chemical crosslinking. These studies would, in essence, rely on the ability to modulate both the swelling and mechanics of the film. The impact of the mechanical environment on cell fate has become an increasing explored topic.[4] For example, it has been shown that increasing the elastic modulus of a cell culture substrate, significantly influences cell morphology and differentiation pathway.[5] However, it would be interesting to investigate a mobile surface, where the

mechanical properties can be controlled by the incorporation of building blocks with known responsivities. The hypothesis is that the swelling of microgel films can modulate film mechanics. It has been shown that microgels in the collapsed state have a higher elastic modulus compared to swollen microgels.[6] The extent to which the elastic modulus of a microgel assembly can be tuned is not known.

AFM nanoindentation studies have been used to map the elastic moduli of microgels and microgel films.[3] An AFM tip is pressed into the substrate, and an array of force curves can be generated across the sample. This technique relates the force applied by the tip and the deflection of the tip as it presses into the surface to the elastic modulus using one of several models, the most common being the Hertz model.[7,8] AFM nanoindentation could be employed to investigate the mechanical properties of microgel LbL films at specific temperatures and pH's. Traditional microgel or core/shell microgel assemblies could be employed to control both the swelling and elastic modulus of the interface. Since the films are not chemically crosslinked, they would presumably still be mobile, permitting interactions between cells and the surface to be studied where the modulus is tuned independently from mobility. Ideally, controlled fluctuations in temperature or pH could be employed to alter film properties *in situ*. Overall, these experiments would provide insight into the impact of substrate mobility on cell phenotype. The knowledge obtained could be used in the development of non-fouling films or cell-scaffolding materials.

6.2 Peptide-Coated Microgels

A new core/shell construct was introduced in **Chapter 5**, where a peptide shell assembles onto a core microgel particle. Though this has potential to serve as a new microgel building block there are still aspects about the assembly that have not been investigated. Specifically, the exact parameters guiding the assembly of RADA on microgel surfaces is not known. In addition, post-assembly conjugation of a fluorophore

to RADAC was demonstrated, but the ability to conjugate larger macromolecules has not been determined. Future work should seek to understand the assembly behavior and use this knowledge to create and utilize peptide-coated microgels.

Many fundamental questions remain regarding the coating of microgels with RADA. Observations of particles following incubation with RADA or RADAC show fibrils at the periphery (AFM images) or red fluorescence localized at the periphery. It is not clear whether there is any penetration of RADA into the particle, or if all RADA/RADAC remains surface bound. In addition, it has proven challenging to quantify the amount of RADA/RADAC on the particles. Attempts made to quantify the amount of cysteine *via* the Ellman assay have been unsuccessful. Regardless, this assay would only work for RADAC-coated microgels. Furthermore, DLS data (**Table 5.2**) showed that the size of the microgels does not change appreciably following RADA adsorption.

It was previously demonstrated that cytochrome c (cyt c), a small, globular protein with a patch of lysine residues, could be loaded into anionic microgels. Multiangle light scattering (MALS) was used to investigate cyt c encapsulation within the network.[9] MALS can detect molecular weight changes as well as changes in particle size and weight distribution. Therefore, MALS might be a useful technique for analyzing peptide-coated microgels. Information regarding any changes to the root-mean-square radius (R_{rms}) or the molecular weight would provide insight into the localization of the peptides, and the amount of peptide associated with the particles.

For microgels containing AAc, stable dispersions of RADA-coated microgels were prepared. However, microgels without AAc were not stably coated, and attempts to coat microgels with Q11 failed. These findings suggest that the identity of the peptide and the polymer network both impact the assembly process. Q11, in its monomeric form, is of similar length to RADA (11 amino acids in Q11, 16 amino acids in RADA) and is also a β-sheet fibrillizing peptide. It is likely that the identity of the amino acids in Q11 results in more drastic interactions with microgels. There has been recent interest in

understanding how the identity and order of amino acids affects the assembly behavior.[10] However, this work has only focused on self-association of the peptides. It would be interesting to explore the parameters governing peptide assembly and how this relates to particle interactions. Specifically, the role of hydrogen bonding, electrostatics, and hydrophobic interactions between the peptide and particles would be worth investigating. In addition, the molecular weight and length of the assembled fibrils are likely to also play a role in coating and stability. Some amino acid sequences are stronger assemblers, which may then influence the physical characteristics of the assembled structures in solution.[10]

Overall, the parameter space to explore is extensive. Both the microgel and peptide compositions can be varied. Computational modeling of particle-fibril interactions could therefore assist in narrowing down the most important parameters. Interactions between polymers (uncharged polymers and polyelectrolytes) and colloidal particles have been studied, experimentally and theoretically.[11-16] The goal here would be to model peptide self-assembly behavior in combination with the interactions between the assembled structures and soft particles. The insight gained from these studies could enhance our ability to predictably select favorably interacting particles and peptides. Further down the road, the fundamental understanding of these constructs could be used in the guided 3-dimensional assembly of colloidal particles.

Consideration must also be paid to the colloidal particles. The incorporation of acrylic acid within the microgel network is clearly an important parameter in the assembly with RADA. It is not clear whether charge repulsion simply stabilizes the particles in the presence of an interacting polymer species, or if it controls the behavior of peptides with the microgel surface. The location (i.e. core versus surface localized) of the charged functional groups within the network could provide insight into peptide-microgel interactions. Hoare and Pelton demonstrated the preferential localization of three acidic co-monomers in pNIPAm microgels.[17] Microgels synthesized with these co-monomers

could be used to probe the impact of charge location on RADA-microgel interactions. Changes in the main polymer identity could also be explored, where potential interactions, like hydrogen bonding between the peptide and the polymer, can be altered.

For the preparation of RADA-coated microgels only one concentration of peptide and microgel was used. It is certainly possible that the relative concentrations of microgels and peptide influence the assembly. Further, peptide assembly is known to be concentration dependent, so altering the peptide concentration could be one method to control fibril length. These should be relatively straightforward studies where the concentrations of both the peptide and microgel can be varied.

Thus far, microscopy and circular dichroism have been utilized to confirm the assembly of RADA fibrils on microgel surfaces. However, isothermal titration calorimetry (ITC) could be utilized to gain a deeper understanding of the assembly process, and it might also allow the interactions to be better quantified and compared. ITC measures the amount of heat absorbed or released due to molecular interactions. A typical ITC set-up consists of a sample cell and reference cell maintained at constant temperature. Interactions between molecules added to the sample cell result in temperature differences between the two cells. To keep the temperature constant the energy supplied to the reference cell must be adjusted, and this change is translated into a heat change. This heat change is then used to determine the enthalpic change of the system. ITC has been used to study biomolecular interactions, including peptide self-assembly, and the interaction of biomolecules with particle surfaces.[19,20] Therefore, it may be possible to employ ITC to elucidate how changes in particle and peptide composition alter the interactions.

An advantage to employing self-assembling peptides (SAP) is the potential to use modified peptides and prepare co-assemblies.[21-23] This has been demonstrated on numerous occasions in the preparation of SAP gels. In analogous fashion, the inclusion of a fluorescently tagged RADA was co-assembled with unlabeled RADA on the surface of

microgels. In addition, RADAC was modified with a fluorophore post-assembly on the microgel surface. While these are important proof-of-concept experiments, the co-assembly or conjugation of larger molecules (e.g. peptides, proteins, polymers) remains to be demonstrated. However, the application of these core/shell particles will likely rely on the ability to conjugate (bio)macromolecules to the particle surface. Future work with this construct should evaluate the potential to conjugate larger macromolecules to the RADA shell. Initial experiments could focus on using PEG oligomers or peptides with different chemical handles. Green fluorescent protein (GFP) could also be used to explore the conjugation of proteins to the surface.

Furthermore, peptides provide the unique opportunity to utilize orthogonal chemoligations through the incorporation of non-traditional chemical handles[24] (e.g. alkyne, aldehyde, hydrazide), and experiments can be done to evaluate non-traditional ligation chemistries localized on the peptide shell. Of particular interest is the copper catalyzed azide alkyne cycloaddition (CuAAC) because of its selectivity, efficiency, stability of the triazole, and tolerance in aqueous environments. The Finn group has demonstrated the reaction of an azidocoumarin dye, which becomes fluorescent only after formation of the triazole product.[25] RADA synthesized with a non-natural amino acid carrying a propargyl group could be assembled on the surface of a microgel, and subsequently reacted with the azidocoumarin dye. Successful conjugation will result in a fluorescence signal.

It is certainly important to mention that RADA is a challenging peptide to synthesize and purify.[26] While there are likely approaches to take on the synthetic side to reduce the time and cost of making RADA, it might instead be useful to consider whether fewer RADA repeats could still result in co-assembly. For instance, plain full-length RADA could be used, but a shorter, modified RADA could be co-assembled. This could at least reduce the overall difficulty in preparing multiple types of RADA, and should be considered in the future.

While the initial work with RADA-coated microgels has presented some interesting observations, there is still a substantial amount of work to be done to understand and control the assembly process, and then utilize these constructs. There appear to be few analogous constructs in the literature, especially for soft particles, making this a unique and potentially valuable construct to explore.

6.3 References

(1) Schmidt, S.; Zeiser, M.; Hellweg, T.; Duschl, C.; Fery, A.; Mohwald, H., Adhesion and Mechanical Properties of PNIPAM Microgel Films and Their Potential Use as Switchable Cell Culture Substrates. *Adv. Funct. Mater.* **2010,** *20*, 3235-3243.

(2) South, A.B.; Whitmire, R.E.; Garcia, A.J.; Lyon, L.A., Centrifugal Deposition of Microgels for the Rapid Assembly of Nonfouling Thin Films. *ACS Appl. Mater. Interfaces* **2009**, *1*, 2747-2754.

(3) Saxena, S.; Spears Jr., M.W.; Yoshida, H.; Gaulding, J.C.; Garcia, A.J.; Lyon, L.A., Microgel Films Dynamics Modulate Cell Adhesion Behavior. *Soft Matter* **2014**, *10*, 1356-1364.

(4) Nemir, S.; West, J.L., Synthetic Materials in the Study of Cell Response to Substrate Rigidity. *Ann. Biomed. Eng.* **2010,** *38,* 2-20.

(5) Engler, A.J.; Sen, S.; Sweeney, H.L.; Discher, D.E., Matrix Elasticity Directs Stem Cell Lineage Specification. *Cell* **2006,** *126,* 677-689.

(6) Hashmi, S.M.; Dufresne, E.R., Mechanical Properties of Individual Microgel Particles through the Deswelling Transition. *Soft Matter* **2009,** *5,* 3682-3688.

(7) Oyen, M.L.; Cook, R.F., A Practical Guide for Analysis of Nanoindentation Data. *J. Mech. Behav. Biomed. Mater.* **2009**, *2,* 396-407.

(8) Domke, J.; Radmacher, M., Measuring the Elastic Properties of Thin Polymer Films with the Atomic Force Microscope. *Langmuir* **1998**, *14*, 3320-3325.

(9) Smith, M.H.; Lyon, L.A., Tunable Encapsulation of Proteins within Charged Microgels. *Macromolecules* **2011,** *44,* 8154-8160.

(10) Frederix, P.W.J.M.; Scott, G.C.; Abul-Haija, Y.M.; Kalafatovic, D.; Pappas, C.G.; Javid, N.; Hunt, N.T.; Ulijn, R.V.; Tuttle, T., Exploring the Sequence Space for (Tri-)Peptide Self-Assembly to Design and Discover New Hydrogels. *Nature Chem.* **2014**, *7*, 30-37.

(11) Netz, R.R.; Joanny, J-F., Complexation between a Semiflexible Polyelectrolyte and an Oppositely Charged Sphere. *Macromolecules* **1999,** *32,* 9026-9040.

(12) Kampmann, T.a.; Boltz, H-H.; Kierfeld, J., Controlling Adsorption of Semiflexible Polymers on Planar and Curved Substrates. *J. Chem. Phys.* **2013**, *139*, 034903; DOI: 10.1063/1.4813021.

(13) Messina, R., Electrostatics in Soft Matter. *J. Phys. Condens. Matter* **2009,** *21*, 113102.

(14) Wang, Y.; Wei, G.; Wen, F.; Zhang, X.; Zhang, W.; Shi, L., Adsorption of Poly(N-Isopropylacrylamide-*co*-4-Vinylpyridine) onto Core-Shell Poly(Styrene-*co*-Methacrylic Acid) Microspheres. *Eur. Poly. J.* **2008,** *44,* 1175-1182.

(15) Schneider, G.; Decher, G., Functional Core/Shell Nanoparticles via Layer-by-Layer Assembly. Investigation of the Experimental Parameters for Controlling Particle Aggregation and for Enhancing Dispersion Stability. *Langmuir* **2008,** *24,* 1778-1789.

(16) Kleshchanok, D.; Tuinier, R.; Lang, P.R., Direct Measurements of Polymer Induced Forces. *J. Phys. Condens. Matter* **2008,** *20,* 073101.

(17) Hoare, T.; Pelton, R., Titrametric Characterization of pH-Induced Phase Transitions in Functionalized Microgels. *Langmuir* **2006**, *22*, 7342-7350.

(18) Aggeli, A.; Nyrkova, I.A.; Bell, M.; Harding, R.; Carrick, L.; McLeish, T.C.; Semenov, A.N.; Boden, N., Hierarchical Aelf-Assembly of Chiral Rod-Like Molecules as a Model for Peptide Beta-Sheet Tapes, Ribbons, Fibrils, and Fibers. *Proc. Natl. Acad. Sci. USA* **2001,** *98,* 11857-11862.

(19) Kabiri, M.; Unsworth, L.D., Application of Isothermal Titration Calorimetry for Characterizing Thermodynamic Parameters of Biomolecular Interactions: p\Peptide Self-Assembly and Protein Adsorption Case Studies. *Biomacromolecules* **2014**, *15*, 3463-3473.

(20) Kabiri, M.; Bushnak, I.; McDermot, M.T.; Unsworth, L.D., Toward a Mechanistic Understanding of Ionic Self-Complimentary Peptide Self-Assembly: Role of Water Molecules and Ions. *Biomacromolecules* **2013**, *14,* 3943-3950.

(21) Hudalla, G.A.; Sun, T.; Gasiorowski, J.Z.; Han, H.; Tian, Y.F.; Chong, A.S.; Collier, J.H., Gradated Assembly of Multiple Proteins into Supramolecular Materials. *Nature Mater.* **2014**, *13*, 829-836.

(22) Woolfson, D.N.; Mahmoud, Z.N., More than Just Bare Scaffolds: Towards Multi-Component and Decorated Fibrous Biomaterials. *Chem. Soc. Rev.* **2010**, *39*, 3464-3479.

(23) Taraballi, F.; Campione, M.; Sassella, A.; Vescovi, A.; Paleari, A.; Hwang, W.; Gelain, F., Effect of Functionalization on the Self-Assembling Propensity of β-Sheet Forming Peptides. *Soft Matter* **2009**, *5,* 660-668.

(24) Tang, W.; Becker, M.L., "Click" Reactions: A Versatile Toolbox for the Synthesis of Peptide-Conjugates. *Chem. Soc. Rev.* **2014,** *43*, 7013-1039.

(25) Kislukhin, A.A.; Hong, V.P.; Breitenkamp, .E.; Finn, M.G., Relative Performance of Alkynes in Copper-Catalyzed Azide-Alkyne Cycloaddition. *Bioconjugate Chem.* **2013,** *24,* 684-689.

(26) Paradis-Bas, M.; Tulla-Puche, J.; Zompra, A.A.; Albericio, F., RADA-16: A Tough Peptide-Strategies for Synthesis and Purification. *Eur. J. Org. Chem.* **2013,** 5871-5878.

APPENDIX A

COLLECTING FILM THICKNESS MEASUREMENTS AND OPTIMIZATION OF AFM IMAGING PARAMETERS

A.1 Collecting Film Thickness Measurements

The film thicknesses of the traditional and core/shell films (**Chapter 4**) were calculated from height images acquired via atomic force microscopy (AFM). Microgel multilayer films (10 layers) were assembled *via* layer-by-layer deposition of microgels and a linear polycation. The films were cut with a razorblade to reveal the substrate. Height images were obtained across the scratches. A representative height image of a scratched film imaged under ambient conditions is presented in **Figure A.1**. Height images provide information in the z-dimension, as depicted in **Figure A.1**. These images therefore provide a cross-section of the films, where the thickness of the film is the height value of the substrate subtracted from the height value of the film surface.

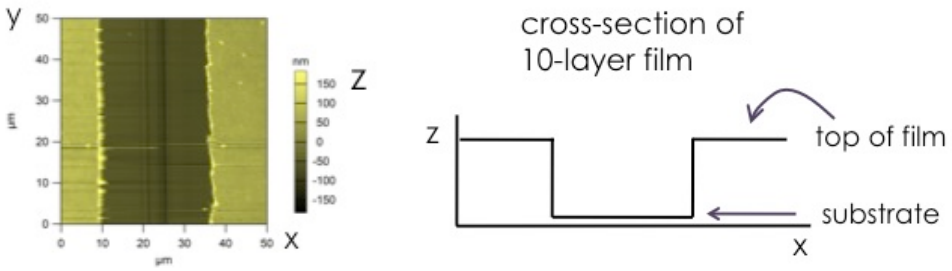

Figure A.1. AFM height image of a microgel film across a scratch in the film (left), and a depiction of the cross-section of each line of the AFM images (right).

The height data of each image was analyzed using Matlab code written in house. In essence, the Matlab code averages the height values from the left of the scratch to the left edge (left height) and from the right of the scratch to the right edge (right height) for

each line of the image. The lowest height value for each line (found within the scratch) is then subtracted from the left and right heights. A total of 256 lines (along the y-dimension) were collected for each image (x=60 μm, y=8 μm). Therefore, 256 thickness measurements for both the left and right sides of the scratch are calculated for each image and averaged. For each film, four different locations were imaged, and the average left and right heights were calculated using the Matlab code. The final thickness values presented in the paper are the average and standard deviation of these four measurements. In addition, both the height trace and retrace data were analyzed in the exact same manner to ensure the imaging conditions were appropriate and the data was consistent.

It should be noted that topographically heterogeneous surfaces (e.g. large pile-up regions, large pieces of foreign material) can alter approximations made by the code. Therefore, the values presented by the code were investigated to verify that outliers are not affecting the calculated values. Within the code, the images can be cropped (in the x and y dimensions) or offset (to move the point on the left or right side of the scratch further out) to permit the exclusion of regions where excess material significantly alters the values.

A.2 Impact of AFM Parameters on Calculated Film Thicknesses

Microgels are soft, deformable polymeric particles.[1,2] For this reason, AFM imaging of microgels and microgel films is performed in intermittent contact mode. However, the extent to which the AFM cantilever contacts the sample as it scans the surface can lead to compression through energy dissipation.[3] Such effects have been demonstrated for carbon nanotubes,[4,5] and a variety of soft materials.[6,7] Three AFM imaging parameters were screened for their potential impact on the measured film thickness: drive amplitude, set point, and integral gain. The drive amplitude and set point control the extent of force applied to the sample by the tip, while the integral gain is related to the response of the system to topographical changes.

AFM images were acquired for a single film assembled from Microgel 3 (44% NIPAm, 44% NIPMAm, 10% AAc, 2% BIS) in four different environments: pH 3, ~26 °C and 50 °C and pH 7.4, ~26 °C and 50 °C. Height trace and retrace data were analyzed using Matlab code, written in house, to calculate the film thicknesses in each environment as a function of the imaging parameters. The drive amplitude and set point were found to have the largest impact on the calculated film thicknesses. The left height and right height (LH and RH, respectively) from height images are presented in **Figures A.2-4**.

The impact of the drive amplitude on the measured thickness is presented in **Figure A.2**. At low drive amplitudes, it appears that the films are very thin. This is a result of poor interaction with the sample. As the drive amplitude is increased, contact with the sample (the top of the film and the exposed substrate) is enhanced, resulting in a more accurate measure of the film thickness. Further increasing the drive amplitude compresses the film, decreasing the thickness of the film. However, when a film has de-swollen (pH 3, 50 °C, **Figure A.2b**) higher drive amplitudes do not appear to greatly impact the measured thickness. The dependence of film thickness on the set point can be seen in **Figure A.3**. Lower set points coupled with higher drive amplitudes result in decreased film thicknesses. When the set point is increased, but the drive amplitude is held constant, the measured thickness is larger. The final parameter investigated was the integral gain (**Figure A.4**). The film thicknesses were not greatly impacted by changes in this parameter.

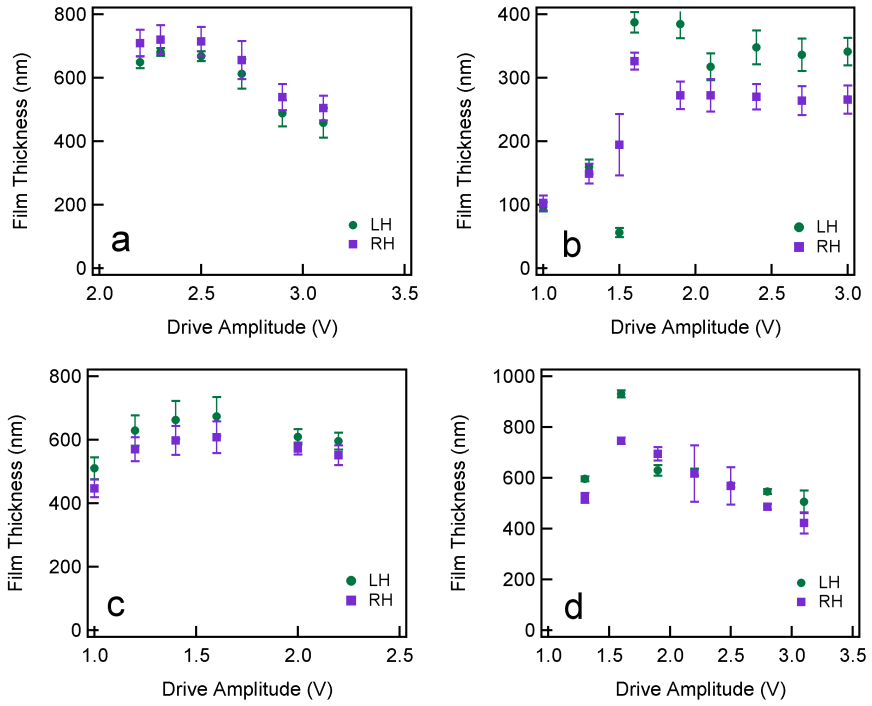

Figure A.2. Calculated film thicknesses as a function of drive amplitude; (a) pH 3, ~26 °C, set point=218 mV; (b) pH 3, 50 °C, set point=200 mV; (c) pH 7.4, ~26 °C, set point=200 mV; (d) pH 7.4, 50 °C, set point=200 mV; Integral gain=10 for all images. The left height (LH) and right height (RH) are presented.

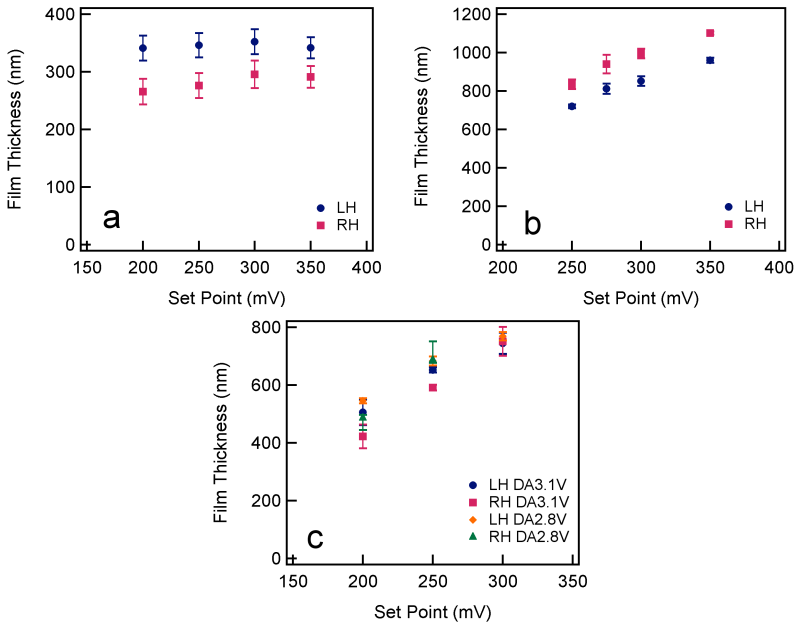

Figure A.3. Calculated film thicknesses as a function of set point; (a) pH 3, 50 °C, drive amplitude=3.0 V; (b) pH 7.4, ~26 °C, drive amplitude=2.0 V; (c) pH 7.4, 50 °C; Integral gain=10 for all images. The left height (LH) and right height (RH) are presented.

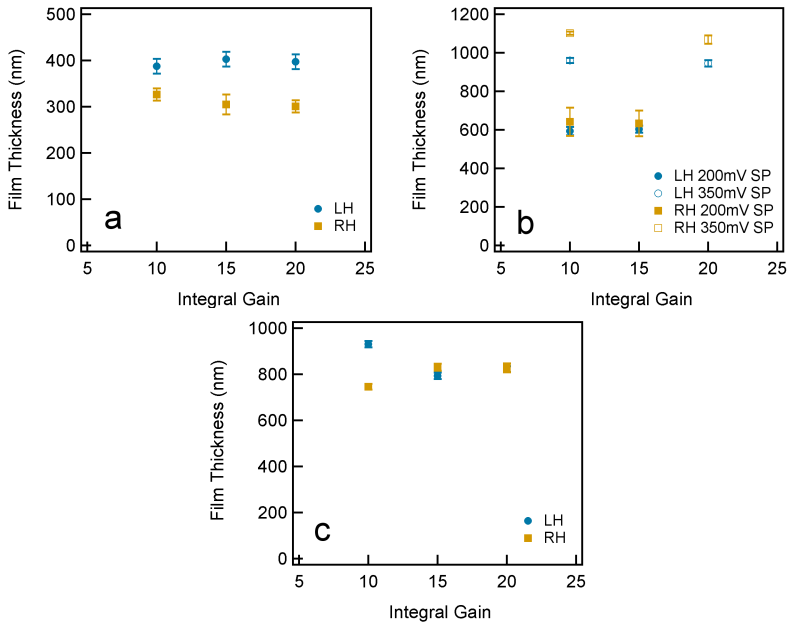

Figure A.4. Calculated film thicknesses at varying integral gain settings; (a) pH 3, 50 °C, set point=200 mV, drive amplitude=1.6 V; (b) pH 7.4, ~26 °C, drive amplitude=2.0 V; (c) pH 7.4, 50 °C, set point=200 mV, drive amplitude=1.6 V. The left height (LH) and right height (RH) are presented.

A.3 References

(1) Hendrickson, G.H.; Lyon, L.A., Translocation through Pores Under Confinement. *Angew. Chem. Int. Ed.* **2010**, *49*, 2193-2197.

(2) Holden, D.A.; Hendrickson, G.H.; Lan, W-J.; Lyon, L.A.; White, H.S., Electrical Signature of the Deformation and Dehydration of Microgels During Translocation through Nanopores. *Soft Matter* **2011**, *7*, 8035-8040.

(3) Cleveland, J.P.; Anczykowski, B.; Schmid, A.E.; Elings, V.B., Energy Dissipation in Tapping-Mode Atomic Force Microscopy. *Appl. Phys. Lett.* **1998**, *72*, 2613-2615.

(4) DeBorde, T.; Joiner, J.C.; Leyden, M.R.; Minot, E.D., Identifying Individual Single-Walled and Double-Walled Carbon Nanotubes by Atomic Force Microscopy. *Nano Lett.* **2008**, *8*, 3568-3571.

(5) Postma, H.W.C.; Sellmeijer, A.; Dekker, C., Manipulation and Imaging of Individual Single-Walled Carbon Nanotubes with an Atomic Force Microscope. *Adv. Mater.* **2000**, *12*, 1299-1302.

(6) Weisenhorn, A.L.; Khorsandi, M.; Kasas, S.; Gotzos, V.; Butt, H-J., Deformation and Height Anomaly of Soft Surfaces Studied with an AFM. *Nanotechnology* **1993**, *4,* 106-113.

(7) Yacoot, A.; Koenders, L., Aspects of Scanning Force Microscope Probes and Their Effects on Dimensional Measurements. *J. Phys. D: Appl. Phys.* **2008**, *41*, 103001.

VITA

Kimberly Corinne Clarke was born in Marion, OH on February 12, 1988. She earned her high school diploma from Pleasant High School in Marion, OH 2006. She subsequently attended Mercyhurst College in Erie, PA, where she earned a B.S. in Biochemistry and a B.S. in Applied Forensic Science in 2010. Chemistry won her heart, and she next attended the Georgia Institute of Technology to pursue her PhD in chemistry.